

**NASA TECHNICAL NOTE**



**NASA TN D-5573**

*C. 1*

NASA TN D-5573



TECH LIBRARY KAFB, NM

LOAN COPY: RETURN TO  
AFWL (WLOL)  
KIRTLAND AFB, N MEX

**ANALYTICAL STUDY OF EFFECTS  
OF SEVERE TURBULENCE ON  
FLIGHT MOTIONS OF A TYPICAL  
SUBSONIC JET-TRANSPORT AIRPLANE**

*by William D. Grantham and Mary S. Adams*

*Langley Research Center*

*Langley Station, Hampton, Va.*



0132364

1. Report No. NASA TN D-5573	2. Government Accession No.	3. Recipient's Catalog No.	
4. Title and Subtitle ANALYTICAL STUDY OF EFFECTS OF SEVERE TURBULENCE ON FLIGHT MOTIONS OF A TYPICAL SUBSONIC JET-TRANSPORT AIRPLANE		5. Report Date December 1969	
		6. Performing Organization Code	
7. Author(s) William D. Grantham and Mary S. Adams		8. Performing Organization Report No. L-5990	
		10. Work Unit No. 126-61-13-02-23	
9. Performing Organization Name and Address NASA Langley Research Center Hampton, Va. 23365		11. Contract or Grant No.	
		13. Type of Report and Period Covered  Technical Note	
12. Sponsoring Agency Name and Address National Aeronautics and Space Administration Washington, D.C. 20546		14. Sponsoring Agency Code	
		15. Supplementary Notes	
16. Abstract  An analytical investigation has been made to determine whether the inherent rigid-body, uncontrolled stability and response characteristics of subsonic jet-transport airplanes could result in a gross upset when the airplane was flying in severe turbulence; and, if so, what techniques might aid in the prevention of possible upsets from this cause. The investigation consisted mainly of calculations of the motions of an airplane when flown through a number of different samples of severe turbulence.			
17. Key Words Suggested by Author(s) Subsonic jet transport Severe atmospheric turbulence Autopilot		18. Distribution Statement  Unclassified - Unlimited	
19. Security Classif. (of this report) Unclassified	20. Security Classif. (of this page) Unclassified	21. No. of Pages 70	22. Price* \$3.00

ANALYTICAL STUDY OF EFFECTS OF  
SEVERE TURBULENCE ON FLIGHT MOTIONS OF A  
TYPICAL SUBSONIC JET-TRANSPORT AIRPLANE

By William D. Grantham and Mary S. Adams  
Langley Research Center

SUMMARY

An analytical investigation has been made to determine whether the inherent rigid-body, uncontrolled stability and response characteristics of subsonic jet-transport airplanes could result in a gross upset when the airplane was flying in severe turbulence; and, if so, what techniques might aid in the prevention of possible upsets from this cause. The investigation consisted mainly of calculations of the motions of an airplane when flown through a number of different samples of severe turbulence.

The results indicated that when the airplane was trimmed at the cruise condition and flown through severe turbulence with no pilot inputs, the airplane could become grossly upset. The cause of the gross upset encountered in this study was the loss in effective dihedral with increase in speed above that for high-speed cruise. The apparent sequence of events was that turbulence would sometimes cause a minor upset, generally lateral, which caused the Mach number to increase to the point that the effective dihedral decreased sufficiently so that the airplane would not raise its low wing (this is the case when spiral stability becomes neutral or negative). In the banked attitude, with the cockpit controls remaining fixed in the original position, the airplane would not have enough vertical component of lift to support its weight and would therefore continue to lose altitude and increase airspeed. Several procedures, any one of which could prevent the airplane from being upset in this manner, were identified as follows:

- (a) Decrease altitude and airspeed for turbulence penetration.
- (b) Keep the wings level with loose attitude roll control or with the roll autopilot.
- (c) Use a yaw damper or roll damper.

The effects of the factors under (b) and (c) are not cumulative, but the use of more than one of these does no harm. Control of pitch attitude alone was not adequate for preventing the airplane from becoming upset, but it was better than allowing the airplane to fly hands off. Since the airplane did not in any case experience a gross upset when the wings were kept relatively level, the uncontrolled rigid-body longitudinal response characteristics did not seem to be a cause of gross upset for the particular configuration and turbulence time histories studied.

## INTRODUCTION

In the past few years, a number of accidents or near accidents involving subsonic jet-transport airplanes have occurred that appear to be related to encountering severe turbulence under instrument flight conditions. Such incidents have occurred with several different makes and models of subsonic jet-transport airplanes – both commercial and military. Some of these incidents occurred when turbulence was encountered at high altitudes and relatively high airspeeds, while others have occurred at much lower altitudes and airspeeds. Typically, the aforementioned incidents were characterized as follows:

- (1) Severe turbulence was encountered while the airplane was being flown on instruments.
- (2) The airplane experienced normal accelerations as high as  $\pm 3g$  units (29.5 meters/second<sup>2</sup>), generated by turbulence or by the piloting technique, or by both.
- (3) The cockpit instrument readings became unreliable as a result of rapid fluctuations of attitude, airspeed, rate of climb, and altitude.
- (4) Airframe structural modes were excited and interfered with the pilot's normal scan of the instruments.
- (5) The pilot's orientation was disrupted.
- (6) The airplane entered a steep dive.

Practically all incidents reported were encountered during instrument flight conditions, and only in those cases where the airplane came out of the overcast and the pilots were able to orient themselves visually were recoveries effected and crashes averted.

Various studies of the turbulence problem have been conducted in the past. In addition to the usual investigative studies of the various incidents experienced during turbulent flight, other investigations have included computer simulation studies, human centrifuge tests, and flight tests. For example, see references 1 and 2. These previous studies, as well as the analyses of flight in turbulence presented in reference 3, have led to a better understanding of the problems of operating jet-transport airplanes in areas of severe turbulence and have particularly highlighted such factors as attitude indicator readability and interpretation, turbulence penetration speeds, and control problems such as high stick forces and the lack of elevator control power associated with the stalling of the horizontal stabilizer drive.

The present investigation was made to determine whether the inherent rigid-body, uncontrolled stability and response characteristics of subsonic jet-transport airplanes could result in a gross upset when the airplane was flying in severe turbulence; and, if so, what techniques might aid in the prevention of possible upsets from this cause. The investigation consisted mainly of calculations of the motions of an airplane when flown

through a number of different samples of severe turbulence. The aerodynamic input data used in the calculations were based on wind-tunnel tests of a model which was representative in general configuration of the class of swept-wing subsonic jet transports. The analysis was made by digital computing techniques and included the nonlinearities of aerodynamic characteristics and atmospheric properties.

### SYMBOLS

The units for the physical quantities used herein are presented in both the U.S. Customary System of Units and the International System of Units.

$a_n$	normal acceleration, g units (meters/second <sup>2</sup> )
$a_y$	lateral acceleration, g units (meters/second <sup>2</sup> )
$b$	wing span, feet (meters)
$\bar{c}$	mean aerodynamic chord, feet (meters)
$C_{1/2}$	cycles required to damp to one-half amplitude
$C_l$	rolling-moment coefficient
$C_m$	pitching-moment coefficient
$C_n$	yawing-moment coefficient
$C_X$	longitudinal-force coefficient
$C_Y$	side-force coefficient
$C_Z$	vertical-force coefficient
$g$	acceleration due to gravity, feet/second <sup>2</sup> (meters/second <sup>2</sup> )
$h$	altitude, feet (kilometers)
$I_X, I_Y, I_Z$	moments of inertia about X, Y, and Z body axes, respectively, slug-feet <sup>2</sup> (kilograms-meters <sup>2</sup> )

K	speed of sound at computed altitude, feet/second (meters/second)
M	Mach number
$M_{MO}$	maximum operational Mach number
m	mass of airplane, slugs (kilograms)
p,q,r	rolling, pitching, and yawing angular velocities, respectively, radians/second
P	period, seconds
S	wing area, feet <sup>2</sup> (meters <sup>2</sup> )
$t_R$	roll time constant, seconds
$t_{1/2}$	time to damp to one-half amplitude, seconds
T	thrust, pounds (newtons)
u,v,w	components of airplane velocity with respect to inertial space projected along X, Y, and Z body axes, respectively, feet/second (meters/second)
$u_a, v_a, w_a$	components of airplane resultant velocity $V_A$ along X, Y, and Z body axes, respectively, feet/second (meters/second)
$u_g, v_g, w_g$	incremental linear velocity components along X, Y, and Z body axes, respectively, due to turbulence, feet/second (meters/second)
$u_g', v_g', w_g'$	velocity components of turbulence referenced to X, Y, and Z earth axes, respectively, feet/second (meters/second)
$V_A$	resultant aerodynamic velocity of airplane, feet/second (meters/second)
$V_{MO}$	maximum operational velocity, knots
$\alpha$	angle of attack, degrees
$\beta$	angle of sideslip, degrees

$\delta_a$  aileron deflection, positive for right roll command, degrees

$\delta_e$  elevator deflection, positive trailing edge down, degrees

$\delta_s$  stabilizer deflection, positive trailing edge down, degrees

$\delta_r$  rudder deflection, positive trailing edge left, degrees

$\zeta$  damping ratio

$\theta$  pitch attitude, degrees

$\rho$  air density, slugs/foot<sup>3</sup> (kilograms/meter<sup>3</sup>)

$\phi$  angle of bank, degrees

$\psi$  angle of yaw, degrees

$\omega_n$  undamped natural frequency, radians/second

$$C_{l\beta} = \frac{\partial C_l}{\partial \beta} \quad C_{n\beta} = \frac{\partial C_n}{\partial \beta} \quad C_{Y\beta} = \frac{\partial C_Y}{\partial \beta}$$

$$C_{l\delta_a} = \frac{\partial C_l}{\partial \delta_a} \quad C_{n\delta_a} = \frac{\partial C_n}{\partial \delta_a} \quad C_{Y\delta_a} = \frac{\partial C_Y}{\partial \delta_a}$$

$$C_{l\delta_r} = \frac{\partial C_l}{\partial \delta_r} \quad C_{n\delta_r} = \frac{\partial C_n}{\partial \delta_r} \quad C_{Y\delta_r} = \frac{\partial C_Y}{\partial \delta_r}$$

$$C_{lp} = \frac{\partial C_l}{\partial \frac{pb}{2V_A}} \quad C_{np} = \frac{\partial C_n}{\partial \frac{pb}{2V_A}} \quad C_{Yp} = \frac{\partial C_Y}{\partial \frac{pb}{2V_A}}$$

$$C_{lr} = \frac{\partial C_l}{\partial \frac{rb}{2V_A}} \quad C_{nr} = \frac{\partial C_n}{\partial \frac{rb}{2V_A}} \quad C_{Yr} = \frac{\partial C_Y}{\partial \frac{rb}{2V_A}}$$

$$C_{m\delta_e} = \frac{\partial C_m}{\partial \delta_e} \quad C_{X\delta_e} = \frac{\partial C_X}{\partial \delta_e} \quad C_{Z\delta_e} = \frac{\partial C_Z}{\partial \delta_e}$$

$$C_{m\delta_s} = \frac{\partial C_m}{\partial \delta_s} \quad C_{X\delta_s} = \frac{\partial C_X}{\partial \delta_s} \quad C_{Z\delta_s} = \frac{\partial C_Z}{\partial \delta_s}$$

$$C_{m\dot{q}} = \frac{\partial C_m}{\partial \frac{q\bar{c}}{2V_A}} \quad C_{m\dot{\alpha}} = \frac{\partial C_m}{\partial \dot{\alpha}} \quad C_{l\dot{\phi}} = \frac{\partial C_l}{\partial \dot{\phi}}$$

A dot over a symbol represents a derivative with respect to time.

## DESCRIPTION OF AIRPLANE

The configuration used in this investigation is considered to be representative of current subsonic jet-transport airplanes and to be flying at a weight of 175 000 pounds (778 435 newtons). The aerodynamic characteristics of the configuration are presented in table I. In general, the static aerodynamic derivatives were obtained from reference 4, and the dynamic derivatives from unpublished data, with the exception of  $C_{m\dot{q}}$  which was obtained from reference 5. The longitudinal- and lateral-directional dynamic-stability characteristics of the airplane, without stability augmentation, are presented in table II. These data presented in table II are based upon classical linearized, three degree-of-freedom equations of motion, and the characteristics presented were derived from root solutions of the characteristic equations. The low-speed and high-speed buffet boundaries of this airplane, as presented in reference 3, for a gross weight of 175 000 pounds force (778 435 newtons) and load factors of 1.00g units (9.8 meters/second<sup>2</sup>) and 1.50g units (14.7 meters/second<sup>2</sup>), are presented in figure 1.

## PROCEDURES AND CALCULATIONS

Time histories of the flight motions of the representative subsonic jet-transport airplane flying in severe turbulence were calculated by a high-speed digital computer which solved the equations of motion and associated formulas listed in the appendix. The equations of motion are Euler's equations representing six degrees of freedom along and about the airplane body-axes system. (See fig. 2 for illustration of body axes.)

The initial flight conditions used for the calculations were the efficiency cruise conditions for this subsonic jet-transport airplane; that is, an altitude of 40 000 feet (12.19 kilometers) and a true airspeed of approximately 470 knots ( $M \approx 0.82$ ). The variations of atmospheric properties with altitude were included in the calculations. The longitudinal- and lateral-directional static aerodynamic data were used as a function of angle of attack and Mach number. The effects of a Mach trim compensator were included in the calculations to trim the airplane at the desired Mach number.

The turbulence used in the present study was measured during severe storm penetrations that were made in conjunction with the National Severe Storms Project (refs. 6 and 7). The data used consisted of the vertical component  $w_g'$  and lateral component  $v_g'$  of the atmospheric turbulence encountered during four flights through two separate



storms. The longitudinal component  $u_g'$  was not measured during the storm traverses because of instrument failure. However, some longitudinal gusts were arbitrarily used in the early stages of the present investigation and it was determined that  $u_g'$  had little or no effect as to whether the aircraft was upset. (The magnitudes of the longitudinal gusts  $u_g'$  were similar to those presented in fig. 3(a) for the lateral gusts  $v_g'$ .) The effects of arbitrary variations in the vertical and lateral gusts were also studied. The gusts disturbed the airplane through changes in angles of attack and sideslip.

The measured turbulence samples used for the computations in this study are presented in figure 3 as plots of  $w_g'$  and  $v_g'$  against time. These gust velocities are presented in relation to an earth-axes system, and the equations used to transfer these gust components to the airplane body axes are presented in the appendix. (See fig. 2 for relationship of airplane body axes to earth axes.) In addition, the gusts were assumed to be acting through the center of gravity of the airplane; that is, the airplane was considered to be adequately represented by the point mass simulation technique.

Two control schemes were used briefly during the present investigation in an effort to control the motions of the airplane with the aerodynamic control surfaces – a loose-attitude or on-off control technique and the more conventional proportional control technique.

The effects of arbitrary variations in some of the more pertinent aerodynamic derivatives were also studied. For example, the damping derivatives in roll  $C_{l_p}$ , pitch  $C_{m_q}$ , and yaw  $C_{n_r}$ , as well as the effective-dihedral parameter  $C_{l_\beta}$  and the longitudinal static-stability parameter  $C_{m_\alpha}$ , were varied.

## CURRENT RECOMMENDED PILOTING PROCEDURES FOR FLYING IN TURBULENCE

Pilots are aware that when flying in severe turbulence it is possible to impose excessive structural loads on the airplane, and that the airplane attitude may reach undesirable extremes. The flexible sweptwing and high wing loading of current subsonic jet-transport airplanes make it probable that any structural damage which might occur in severe turbulence will be the result of airplane upset and recovery maneuvers in combination with the turbulence, rather than the effects of turbulence alone. Turbulence-penetration procedures have therefore been established to minimize airplane attitude excursions and thus maintain structural loads within acceptable limits.

In general, the piloting procedures for severe turbulence penetration are the same for all jet-transport airplanes; however, the following procedures are the ones recommended in reference 3 for the airplane used in the present study:

- (1) Do not operate above the specified normal cruise ceiling for the airplane weight.
- (2) Maintain indicated airspeed (IAS) of 280 knots or Mach number  $M$  of 0.80, whichever is lower. Maintain speed by maintaining attitude.
- (3) Maintain control of the airplane with the elevator. After establishing the stabilizer trim setting for penetration speed, do not change stabilizer trim.
- (4) Make an initial thrust setting for the target speed (IAS = 280 knots or  $M = 0.80$ ), and then do not change thrust unless required by extreme airspeed variation.
- (5) Set the flight director to the desired heading and zero the horizontal bar at the desired pitch attitude.
- (6) If the autopilot is not used, use the yaw damper in all cases.
- (7) If the autopilot is used, monitor stabilizer trim, attitude, airspeed, and altitude; be alert for an inadvertent autopilot disconnect. Also, if the autopilot is used, the altitude-hold mode must be left off for all penetrations of severe turbulence.

It was possible in the present study to confirm or validate several of these recommendations.

## RESULTS AND DISCUSSION

The calculated results are presented as time histories of pitch attitude angle  $\theta$ , angle of bank  $\phi$ , angle of yaw  $\psi$ , normal acceleration  $a_n$ , lateral acceleration  $a_y$ , Mach number  $M$ , altitude  $h$ , angle of attack  $\alpha$ , and angle of sideslip  $\beta$ . For the time histories of the motions in which various control techniques were used, the magnitudes and timing sequences of the control-surface deflections are indicated. Although only these more pertinent variables are presented, time histories of all the angles, velocities, and accelerations in the equations listed in the appendix were obtained. It should be mentioned that for these calculated time histories the Mach number had an artificial limit of 0.95 since this was the maximum value for which aerodynamic data were available for this configuration. Also, table III presents the range of variation and the root mean square of the normal and lateral accelerations experienced during the simulated flights discussed.

### Response of Airplane to Severe Turbulence

The time histories presented in figure 4 represent flights through four individual turbulence fields and use the turbulence components presented in figure 3. For each simulated flight, the airplane was trimmed at the cruise condition ( $h = 40\,000$  feet (12.19 kilometers);  $M = 0.82$ ) and flown through each set of turbulence. The investigation consisted of an open loop analysis; that is, no pilot control inputs were used. Examination of these time histories shows that the resulting motions in figures 4(a) and 4(b)

are appreciably different from the motions indicated in figures 4(c) and 4(d). The motions indicated in figures 4(a) and 4(b) would be termed upsets; however, the motions indicated in figures 4(c) and 4(d) could not be said to be normal flights. Therefore, the term upset must be defined. Reference 8 defines two types of upsets, moderate upsets and gross upsets, as follows: "A moderate upset is an excursion to a defined degree beyond any normal limit and the following would seem reasonable:

- (a) Too slow – not slower than the stall warning.
- (b) Too fast – not faster than  $V_{MO} + 30$  knots or  $M_{MO} + 0.03$  Mach number.
- (c) Excessive pitch – not beyond  $30^\circ$  noseup or  $20^\circ$  nosedown.
- (d) Excessive roll – not more than  $60^\circ$  bank.

A gross upset will then be anything beyond these limits." From these definitions, the motions indicated in figures 4(c) and 4(d) might be termed moderate upsets; whereas, the motions indicated in figures 4(a) and 4(b) would definitely be called gross upsets. The results of the present study are therefore discussed in relation to gross upsets, and the turbulence data presented in figure 3(a) are used unless specifically stated otherwise. The effects of variation of airplane stability and control characteristics and gust inputs from these conditions are examined.

#### Some Factors Affecting Flight Motions in Severe Turbulence

Effects of gust magnitudes.– The time history presented in figure 4(a) was calculated by using no pilot control inputs, no stability augmentation, and no autopilot, and is considered the basic flight. Examination of this time history shows that the airplane enters a steep spiral dive. The nose pitches down as much as  $35^\circ$  ( $\theta = -35^\circ$ ); the airplane rolls to the right as much as  $70^\circ$  ( $\phi = 70^\circ$ ); the heading is changing continuously ( $\psi$  approaches  $500^\circ$ ); the Mach number reaches its upper limit ( $M = 0.95$ ); the normal acceleration varies from  $-1.00$  to  $4.75g$  units ( $a_n = -2.00$  to  $3.75g$  units from normal  $1g$ -unit flight); and approximately 29 000 feet (8.84 kilometers) of altitude are lost ( $h$  varies from 40 000 feet (12.19 kilometers) to approximately 11 000 feet (3.35 kilometers)).

Several questions arise as to why atmospheric turbulence should cause such results. For example, why does the airplane enter a dive and why does the airplane roll to such large bank angles? In order to answer these questions, several additional calculations were made.

The time histories presented in figure 4 indicate that the spectrum content and/or the phasing of the atmospheric turbulence being considered can make a difference as to whether the airplane will be upset. In order to obtain some insight as to the peculiarities of the turbulence presented in figure 3(a) that caused the airplane to be upset, several calculations were made wherein these measured gusts were arbitrarily altered. The time

history presented in figure 5 was calculated with all conditions remaining the same as the basic flight (fig. 4(a)) except that only the vertical gusts  $w_g'$  were used; no lateral gusts  $v_g'$  were used. The resulting motion indicates that the airplane was not upset and only relatively small oscillations in pitch attitude, Mach number, and altitude were experienced. (The angles of bank and yaw remain zero throughout the time history because no lateral-directional disturbances were present.) These results indicate therefore that the vertical gusts were not the sole cause of the airplane entering a dive.

Another storm penetration was calculated wherein the inputs were the same as the basic flight except that only the lateral gusts  $v_g'$  were used;  $w_g'$  was set equal to zero. The resulting motion (fig. 6) shows that again only an oscillatory type of motion was experienced; the airplane did not enter a dive and did not achieve unusually large bank angles in any one direction. Therefore, the lateral gusts were not the sole cause of the airplane achieving bank angles on the order of  $50^\circ$  to  $70^\circ$ . Additional calculations were made by using the turbulence presented in figure 3(a), but by arbitrarily reducing  $w_g'$  and  $v_g'$ , one at a time, by 75 percent in an attempt to understand further the effects of the magnitudes of the vertical and lateral gusts. The resulting time histories, although not presented, showed that the airplane was upset in each instance. These results, when compared with those of figure 4(d), where there were large gust disturbances but the airplane was not upset, would indicate that the phasing between the vertical and lateral gusts may be more important than the magnitude of the atmospheric turbulence insofar as grossly upsetting the airplane is concerned.

Effects of variations in aerodynamic derivatives of airplane.- The question arises as to the effects of the inherent stability of the airplane on whether an upset will be experienced. From the time histories previously discussed, it appears that the tendency of the airplane to roll to unusually large bank angles and to enter a spiral dive could be a contributing factor to the jet upset in severe turbulence; that is, no upsets were calculated unless large bank angles were achieved.

Because the spiral mode of the basic airplane used in the present study was neutrally stable (see table II), it would not be expected to cause the airplane to diverge in roll after being disturbed. However, an examination of the various time histories, in which gross upsets were indicated, shows that the airplane is spirally unstable. This characteristic led to a detailed study of the aerodynamic derivatives which normally have a large influence on spiral stability.

Effective dihedral: Previous studies (for example, ref. 9) indicate that as Mach number increases to near maximum cruise, the effective dihedral of sweptwing airplanes decreases rapidly ( $C_{l_\beta}$  becomes less negative). This decrease in effective dihedral at high subsonic Mach numbers is a fundamental aerodynamic characteristic of aircraft of the general configuration under study and is caused by airflow separation on one wing; that is, during a sideslip at high speed, the leading wing is less swept than the trailing wing, and shock waves will form along the leading wing and cause flow separation and

reduce lift on the wing. This shock-wave induced-flow separation on the leading wing therefore causes a significant decrease in the effective dihedral. The measured values of  $C_{l\beta}$  for the airplane simulated in the present study (ref. 4) are presented in table I as a function of angle of attack and Mach number; at low angles of attack,  $C_{l\beta}$  changes from negative to positive values as the Mach number is increased from 0.80 to 0.90. For convenience,  $C_{l\beta}$  was also plotted against Mach number for the angle of attack at trim ( $\alpha = 0.84^\circ$  at  $h = 40\,000$  feet (12.19 kilometers)) and is presented in figure 7; trim Mach number for  $\alpha = 0.84^\circ$  and  $h = 40\,000$  feet (12.19 kilometers) is 0.82. Note that for the angle of attack at trim, the values of  $C_{l\beta}$  are positive for Mach numbers above about 0.86. As  $C_{l\beta}$  is reduced below about  $-0.003$  per degree, the spiral mode becomes unstable and this instability worsens as  $C_{l\beta}$  approaches positive values. If for any reason, including turbulence, the Mach number should be increased above approximately 0.86 and if any lateral disturbance such as turbulence should cause a wing to drop, the wing would have to be raised by the pilot or by some artificial means.

Calculations were made to determine the effects of the magnitude of  $C_{l\beta}$  on the tendency of an airplane to become upset in severe turbulence; again, no pilot control inputs were used. First,  $C_{l\beta}$  was used as a constant value of  $-0.0034$  per degree, which is approximately the measured value for the cruise trim condition ( $\alpha = 0.84^\circ$  and  $M = 0.82$ ). The resulting time history is presented in figure 8 and shows that the airplane was not upset;  $\theta$  never exceeded  $\pm 7^\circ$ , the maximum values of  $\phi$  were  $-14^\circ$  to  $25^\circ$ , the Mach number was not above 0.84 or below 0.78, and a maximum of 500 feet (0.15 kilometer) of altitude were lost. Additional calculations were made in which various other constant values of  $C_{l\beta}$  were used and the resulting time histories indicated that as the effective dihedral was decreased, the degree of disturbance of the airplane from level flight was progressively worsened while the airplane was flown through the turbulence shown in figure 3(a). It is of interest to note the results obtained when  $C_{l\beta}$  was held constant at  $-0.0034$  per degree (value used for the calculations presented in fig. 8) and the magnitude of the gusts arbitrarily doubled. The resulting time history is presented in figure 9, and although large changes in attitude were experienced, this motion would not be termed a gross upset.

These results indicate that the magnitude of  $C_{l\beta}$  can have an appreciable effect on whether an airplane will become upset in severe turbulence, and could be the sole cause of an upset if the pilot does not keep the wings reasonably level with the lateral control. Although in actual operations an obvious part of the piloting task is to maintain a wings-level attitude, the effect of marked changes in basic airplane characteristics can be an insidious factor. Thus, a rather sudden deterioration of  $C_{l\beta}$ , given a Mach number increase above  $M \approx 0.82$  in turbulence, can seriously degrade an already difficult control task, partly because such a change is unexpected. It is possible that very few

airline pilots are aware or prepared for such a change in handling qualities because they are rarely, if ever, exposed to conditions outside of their normal operating envelope.

**Damping in roll:** Variations were also made in the magnitude of the damping-in-roll derivative  $C_{l_p}$ , with all other aerodynamic derivatives being the basic values; that is, the same values as were used for the basic calculation presented in figure 4(a). As shown in table I, the basic value of  $C_{l_p}$  was -0.250 per radian. The additional values of this derivative for which time histories were calculated were 2, 4, and 10 times this basic value ( $C_{l_p} = -0.500, -1.000, \text{ and } -2.500$ , respectively). The resulting time histories indicate that if the value of  $C_{l_p}$  were on the order of -1.000, which is four times the basic value, the airplane would not be upset. The time history for this condition ( $C_{l_p} = -1.000$ ) is presented in figure 10.

**Damping in yaw:** The damping-in-yaw derivative  $C_{n_r}$  was arbitrarily varied in the same manner as was  $C_{l_p}$ ; that is, 2, 4, and 10 times the basic value, which was -0.190 per radian. The resulting time histories showed that when  $C_{n_r}$  was as much as -0.760 per radian, which is 4 times the basic value, the airplane was not upset. (See fig. 11.) Also, as was the case for the variations of  $C_{l_p}$ , further increases in the damping did not improve the resulting motion.

**Other derivatives:** Several other aerodynamic derivatives, such as  $C_{n_p}$ ,  $C_{l_r}$ ,  $C_{m_q}$ , and  $C_{m_{\dot{\alpha}}}$ , were also varied from the basic values, and none of these had any effect as to whether the airplane became upset.

Summary of factors affecting the calculated motions.- Although the factors determined during the present open-loop study are not to be taken as the only factors, or even the main factors, contributing to the jet upset problem, the following remarks indicate several factors regarding the inherent stability and response characteristics that might influence the motions of the aircraft in severe turbulence:

(1) The magnitude of the atmospheric turbulence does not necessarily cause the upset; instead the results of this study indicate that the phasing between the vertical and lateral gusts is more important.

(2) The inherent loss of positive effective dihedral as Mach number is increased above approximately 0.80 apparently can cause the airplane to enter a spiral dive and thus initiate the upset. The apparent sequence of events was that turbulence would sometimes cause a minor upset, generally lateral, which caused the Mach number to increase to the point that the effective dihedral decreased sufficiently so that the airplane would not raise its low wing (this is the condition of neutral, or negative, spiral stability). Since the airplane remained in a banked attitude and the longitudinal controls were still set for the original lift coefficient, it did not have enough vertical component of lift to support its

weight and continued to lose altitude. The airplane would be, technically, in a spiral dive; but the term spiral might give the wrong impressions since it would probably not have time to make a full 360° turn during the descent. As the speed increased and air density increased, the aircraft would gradually develop more lift and would finally pull out, as was the case in figure 4(a), if the bank angle did not continue to increase.

(3) The results of the present investigation indicate that the lack of sufficient amounts of damping in roll and/or yaw can contribute to the jet upset, probably in that provision of adequate damping reduced the magnitude of the lateral upset which initiated the major loss in altitude.

(4) It is apparent that the foregoing factors become significant only when there is a lack of attention to control, for whatever reason, on the part of the pilot.

#### Prevention of Upsets in Severe Turbulence

Variations in effective aerodynamics.- Obviously, the best way to determine how to prevent an upset in severe turbulence is to first determine what factor or factors cause the upset, and as discussed in the previous section, three factors have been noted as possible contributors to the upset.

The effect of Mach number on effective dihedral is apparently something that will have to be accepted for sweptwing airplanes. However, several possible methods can be used to keep  $C_{l\beta}$  from initiating or contributing to upsets in turbulence. The most obvious method is for the pilot not to allow the Mach number to exceed approximately 0.80. Owing to buffet-boundary considerations, this method is one of the present recommended piloting procedures for turbulent flight and is discussed subsequently herein. The next most obvious method of keeping the variation of  $C_{l\beta}$  with Mach number from contributing to the jet upset is for the pilot to combat the loss of effective dihedral by flying roll attitude; that is, by keeping the wings relatively level ( $\phi < \pm 20^\circ$ ) with the ailerons. The third alternative is to use a  $C_{l\beta}$  augmenter. This method would require the development of a sophisticated sideslip sensing device that could be used on operational airplanes in turbulent flight to alleviate the negative dihedral effect at transonic Mach numbers.

Another aid towards preventing jet upsets in severe turbulence is to have an effective yaw damper. As discussed previously, if the damping-in-yaw derivative  $C_{nr}$  is of sufficient magnitude, not less than about -0.800 per radian, the upset is less likely to occur. For the particular airplane represented in the present study, the desired value of  $C_{nr}$  could be obtained by using about 20 percent of the rudder authority. One of the present recommended piloting procedures is for the yaw damper to be on during turbulent flight.

An effective roll damper  $C_{l_p}$  which would aid in the prevention of upsets in severe turbulence was also determined during the present study. A comparison of the time histories presented in figures 11 and 10, wherein a yaw damper and a roll damper were used respectively, indicates that the roll damper was, in general, as effective in preventing the upset as was the yaw damper. In order to achieve the amount of  $C_{l_p}$  used in this case ( $C_{l_p} = -1.000$ ), approximately 100 percent of the aileron authority would be required.

A time history was also obtained wherein the yaw damper and roll damper ( $C_{n_r}$  and  $C_{l_p}$  increased to four times the basic values) were used simultaneously. The resulting motion indicated that when both dampers were used, the motion was similar to that obtained when the roll and yaw dampers were used separately.

Autopilot in turbulence.- Whether the autopilot is used or not, the aircraft and airline industries are in agreement with the fact that the yaw damper should be on for turbulence penetrations to improve the Dutch roll damping and thus reduce the pilot workload. Also, it is generally agreed, as stated previously under Current Recommended Piloting Procedures for Flying in Turbulence, that, if the autopilot is used, the altitude-hold mode should be off for turbulence penetrations. However, industry apparently has not definitely decided whether the autopilot should be used in turbulence penetration. Some factors favor having the autopilot off; others favor having it on. Some arguments for and against the use of the autopilot in turbulence are presented in reference 3. Reference 3 also states that it is neither necessary nor desirable to require that the autopilot be off in turbulence in that loss of control which might occur without the autopilot might well be prevented if the autopilot were used; also, use of the autopilot leaves the pilot free to monitor, which in itself is an important safety factor.

Although no attempt was made to incorporate an autopilot in the calculations made during the present study, as mentioned previously, attempts were made to control the attitude of the airplane by using either a loose-attitude control technique or a proportional control technique.

Loose-attitude control: Time histories were calculated wherein attempts were made to control pitch and bank angles within  $\pm 5^\circ$ , both singularly and in combination, with the use of the elevator and aileron, respectively. (Again, the turbulence data of fig. 3(a) were used.) These calculations were made with the aforementioned yaw damper ( $C_{n_r} = 4 \times \text{Basic value}$ ) on and off.

With the yaw damper off, a time history was calculated by using the same inputs as were used for the basic calculations (fig. 4(a)) except that an attempt was made to control the pitch attitude  $\theta$  within  $\pm 5^\circ$  with the elevator being deflected  $\pm 5^\circ$  whenever  $\theta$  exceeded these limits. The resulting motion showed that  $\theta$  was held within  $5^\circ$  and  $-10^\circ$ ;



however, the bank angle was as large as  $70^\circ$ ,  $\Delta\psi$  was greater than  $400^\circ$ , the Mach number varied from 0.69 to 0.89, and the airplane lost approximately 10 000 feet (3.05 kilometers) of altitude. From these results, it might be said that the loose-attitude technique of controlling pitch is better than flying the airplane hands off (fig. 4(a)); however, this technique would not be said to be an effective system for keeping the airplane from becoming upset. Actually, such a system would not be expected to be effective if the airplane is allowed to achieve large bank angles. This case was not repeated with the yaw damper on because the results presented in figure 11 (computed for yaw damper on and no control inputs) show that the bank and pitch angles experienced never exceeded approximately  $\pm 15^\circ$  and  $\pm 6^\circ$ , respectively; therefore, if an effective yaw damper is used, the use of a pitch-attitude autopilot would not be required.

The time history presented in figure 12 shows that when an attempt was made to control the bank angle within  $\pm 5^\circ$  (with aileron deflections of  $\pm 4^\circ$  when these limits were exceeded),  $\phi$  was essentially held within  $\pm 10^\circ$ ,  $\theta$  was never larger than  $\pm 7^\circ$ , the Mach number varied from 0.79 to 0.84, and the altitude did not vary more than approximately 700 feet (0.21 kilometer) from the trim altitude. Figure 12 also shows that the normal and lateral accelerations were approximately  $\pm 1.00$  g unit and  $\pm 0.50$  g unit, respectively ( $a_n = -0.20$  g unit to 1.90 g units and  $a_y = -0.45$  g unit to 0.50 g unit); thus, loose-attitude control of the bank angle would not be expected to induce excessive structural loads on the airplane. When the aforementioned yaw damper was used in conjunction with this loose-attitude control of  $\phi$ , the resulting motion was similar to that obtained without the yaw damper.

The time history presented in figure 13 was computed by using the pitch and roll loose-attitude control technique, and the results are very similar to those presented in figure 12 where only bank angle was controlled. Figure 13 shows that the elevator was required only twice during the simulated flight. Again, when the yaw damper was used in conjunction with the pitch and roll attitude control, no apparent effect on the resulting motion was obtained.

The results obtained when the loose-attitude control technique is used are summarized as follows:

- (1) When the wings were kept relatively level, no gross upsets were experienced.
- (2) Controlling pitch attitude alone was better than flying the airplane hands off but was not considered an adequate control procedure.
- (3) When the wings were kept relatively level with the ailerons, the addition of the pitch control and/or the use of the yaw damper showed little improvement in the resulting motions.

Proportional control: Because all results discussed thus far have shown that no gross upsets were obtained when the wings were kept relatively level, the only proportional-control scheme investigated was directed toward the control of bank angle and was accomplished by simply adding a term  $C_{l\phi}$  in the equations of motion. Effectively, the term  $C_{l\phi}$  is determined from  $C_{l\phi} = C_{l\delta_a} \frac{\delta_a}{\phi}$  where the magnitude of  $C_{l\phi}$  depends on the gain assigned to  $\delta_a/\phi$ . Various time histories were calculated wherein  $\delta_a/\phi$  was varied, and the results showed that the airplane was controlled very well as long as the gain was of sufficient magnitude. Figure 14 presents the motion obtained where  $\delta_a/\phi$  was as low as -0.10, and shows that the gross upset was prevented when the airplane was flown through the turbulence presented in figure 3(a). If the proportional-control technique can be said to represent a roll-control autopilot, then these calculated results would indicate the advantage of using the roll mode of the autopilot when severe turbulence is encountered.

Use of proper piloting procedures.- The general piloting procedures for severe turbulence penetration have been listed previously herein. These procedures, which were based on buffet-boundary considerations, were taken from reference 3, and the results of the present study do not contradict any of them. In regard to these recommended procedures, reference 3 also stated that, "Moderate turbulence will usually require operation one cruise level (4000 feet) below the normal cruise ceiling. Protection against greater than moderate turbulence will usually require operation two cruise levels (8000 feet) below this ceiling." A time history was calculated wherein the inputs were the same as the basic case (fig. 4(a)), except that the initial conditions were changed to correspond to the aforementioned piloting procedures; that is, the altitude was decreased from 40 000 feet (12.19 kilometers) to 32 000 feet (9.75 kilometers) (two cruise levels), and the true airspeed was decreased from 793 feet per second (241.71 meters per second) (which corresponds to  $M = 0.82$  at 40 000 feet (12.19 kilometers)) to 772 feet per second (235.31 meters per second) (which corresponds to  $IAS \approx 280$  knots and  $M \approx 0.78$  at 32 000 feet (9.75 kilometers)). The resulting motion is presented in figure 15, and as can be seen, the airplane was not grossly upset. The pitch attitude was no greater than  $-9^\circ$  to  $5^\circ$ ; the bank angle was no larger than approximately  $\pm 25^\circ$ ; the Mach number varied from approximately 0.76 to 0.83; and less than 2000 feet (0.61 kilometer) of altitude were lost.

This large effect of airspeed with altitude was unexpected because the dynamic characteristics of the airplane would not be expected to change considerably for such relatively small changes in altitude and airspeed. However, because a decrease in altitude tends to increase the aerodynamic damping of the airplane, and because the present study has shown that no gross upsets were experienced unless large roll angles were achieved,

calculations were made to determine the effects of altitude on the dynamic lateral-directional stability characteristics of the airplane. The change in the dynamic stability between 40 000 feet (12.19 kilometers) and 32 000 feet (9.75 kilometers) was such a small amount (table II) that this change would not be the reason the airplane was not upset when flying through the same storm (fig. 3(a)) two cruise levels (8000 feet (2.44 kilometers)) below the normal cruise altitude.

The most logical explanation as to why the airplane did not experience an upset when flown through turbulence at an altitude of 32 000 feet (9.75 kilometers) (fig. 15) is the variation of  $C_{l\beta}$  with Mach number. As stated previously, at 32 000 feet (9.75 kilometers) the initial Mach number was approximately 0.78, as compared to approximately 0.82 at an altitude of 40 000 feet (12.19 kilometers). As shown in table I, at low angles of attack the effective-dihedral parameter decreases rapidly for Mach numbers greater than 0.80.

Several time histories were calculated wherein the variation of  $C_{l\beta}$  with Mach number was arbitrarily varied to validate the hypothesis that the variation  $C_{l\beta}$  with Mach number, rather than increases in aerodynamic damping or variations of  $C_{l\beta}$  with angle of attack, was the factor that kept the airplane from entering a spiral dive when flown at an altitude of 32 000 feet (9.75 kilometers) (fig. 15). The following table summarizes the general conditions and results:

Figure	Initial altitude		Initial Mach number	$C_{l\beta}/M$ relationship	Result
	ft	km			
4(a)	40 000	12.19	0.82	Basic <sup>1</sup>	Upset
15	32 000	9.75	.78	Basic <sup>1</sup>	No upset
17	40 000	12.19	.82	Curve A <sup>2</sup>	Upset
18	32 000	9.75	.78	Curve B <sup>2</sup>	No upset
19	40 000	12.19	.82	Curve C <sup>2</sup>	No upset
20	32 000	9.75	.78	Curve D <sup>2</sup>	Upset

<sup>1</sup>  $C_{l\beta}$  used as function of  $M$  and  $\alpha$ .

<sup>2</sup>  $C_{l\beta}$  used as function of  $M$  only, but altered to desired break in  $C_{l\beta}/M$  curve.

Calculations were made to determine whether the variation of  $C_{l\beta}$  with Mach number or the variation with angle of attack was the primary cause of the results presented in figures 4(a) and 15; and to accomplish this, time histories were calculated wherein  $C_{l\beta}$  was solely a function of Mach number. The variations of  $C_{l\beta}$  presented in figure 16 as curves A and B, which correspond to the measured values at the trim angles of attack used for the calculation of the motions indicated in figures 4(a) and 15, respectively, were

used as inputs. The resulting time histories are presented in figures 17 and 18, respectively, and indicate that the variation of  $C_{l\beta}$  with Mach number was the principal factor that brought about the aforementioned results (figs. 4(a) and 15). Actually, examination of the time histories of figures 17 and 18 reveals that the resulting motions were similar to the original results obtained when  $C_{l\beta}$  was used as a function of angle of attack and Mach number (figs. 4(a) and 15, respectively).

The arbitrary variations of  $C_{l\beta}$  with Mach number, indicated in figure 16 as curves C and D, were used as inputs to validate further the implications of these results. Curve C was constructed so that the trim Mach number used for the initial conditions, where  $h = 40\,000$  feet (12.19 kilometers) and  $M = 0.82$ , would fall approximately 0.02 Mach number before the break in the curve for  $C_{l\beta}$ . A time history was calculated that corresponds to the basic condition (fig. 4(a)), except that the values of  $C_{l\beta}$  indicated as curve C were used; the results are presented in figure 19. The resulting motion indicated that the upset was not experienced. Similarly, the values of  $C_{l\beta}$  presented in figure 16 as curve D were arbitrarily chosen so that the trim Mach number used for the initial conditions at the lower altitude ( $h = 32\,000$  feet (9.75 kilometers) and  $M = 0.78$ ) would fall approximately 0.02 Mach number after the break in the curve for  $C_{l\beta}$ . A time history (fig. 20) was calculated that corresponds to the motion presented in figure 15, except that the values of  $C_{l\beta}$  indicated as curve D were used. Again, the airplane was grossly upset, and a spiral dive was experienced.

The results of the preceding calculations (figs. 17 to 20) indicate that the variation of  $C_{l\beta}$  with Mach number can be a contributing factor in jet upsets when severe turbulence is encountered and that by following the current recommended piloting procedure of decreasing the altitude two cruise levels and flying the airplane at the suggested airspeeds, the probability of turbulence increasing the Mach number to such an extent that  $C_{l\beta}$  will be reduced to the point of causing spiral divergence will be more remote. This recommended piloting procedure should always be followed, if practical, when severe turbulence is expected.

## CONCLUSIONS

An analytical investigation has been made to determine whether the inherent rigid-body, uncontrolled stability and response characteristics of subsonic jet-transport airplanes could result in a gross upset when the airplane was flying in severe turbulence; and, if so, what techniques might aid in the prevention of possible upsets from this cause. The investigation consisted mainly of calculations of the motions of an airplane when flown through a number of different samples of severe turbulence. The results of this study indicate the following conclusions:

1. When the airplane was trimmed at the cruise condition and flown through severe turbulence with no pilot inputs, the airplane could become grossly upset.

2. The cause of the gross upset was the spiral instability of the airplane at speeds only slightly above the efficiency cruise Mach number. The spiral instability resulted from the inherent decrease in effective dihedral with an increase in Mach number.

3. The apparent sequence of events was that turbulence would sometimes cause a minor upset, generally lateral, which caused the Mach number to increase to the point that the effective dihedral decreased sufficiently to cause a decided spiral instability which in turn resulted in the gross loss of altitude and a further increase in airspeed.

4. The lack of sufficient amounts of damping in roll and/or yaw can contribute to the jet upset.

5. The phasing between the vertical and lateral gusts may be more important than the magnitude of the atmospheric turbulence insofar as grossly upsetting the airplane is concerned.

6. By following the current recommended piloting procedure for turbulence penetration, that is, by decreasing the altitude two cruise levels and by flying the airplane at the suggested airspeeds (Indicated airspeed = 280 knots or Mach number = 0.80), the probability of turbulence increasing the Mach number to such an extent that the effective dihedral will be reduced to the point of causing spiral divergence will be more remote.

7. The results obtained when a loose-attitude control technique is used are summarized as follows:

(a) When the wings were kept relatively level, no gross upsets were experienced.

(b) Controlling pitch attitude alone was better than flying the airplane hands off, but was not considered an adequate control procedure.

(c) When the wings were kept relatively level with the ailerons, the addition of the pitch control and/or the use of the yaw damper showed little improvement in the resulting motions.

8. If the proportional-control technique can be said to represent a roll-control autopilot, these results would indicate the advantage of using the roll mode of the autopilot when severe turbulence is encountered.

Langley Research Center,  
National Aeronautics and Space Administration,  
Langley Station, Hampton, Va., July 26, 1968.

## APPENDIX

### EQUATIONS OF MOTION AND ASSOCIATED FORMULAS

The equations of motion used in calculating the motions experienced upon penetrating severe turbulence are

$$\dot{p} = \frac{I_Y - I_Z}{I_X} qr + \frac{\rho V_A^2 S b}{2 I_X} (C_{l\beta} \beta + C_{l\delta_a} \delta_a + C_{l\delta_r} \delta_r) + \frac{\rho V_A S b^2}{4 I_X} (C_{l_p} p + C_{l_r} r)$$

$$\dot{q} = \frac{I_Z - I_X}{I_Y} pr + \frac{\rho V_A^2 S \bar{c}}{2 I_Y} (C_m + C_{m\delta_e} \delta_e + C_{m\delta_s} \delta_s) + \frac{\rho V_A S \bar{c}^2}{4 I_Y} C_{m_q} q$$

$$\dot{r} = \frac{I_X - I_Y}{I_Z} pq + \frac{\rho V_A^2 S b}{2 I_Z} (C_{n\beta} \beta + C_{n\delta_a} \delta_a + C_{n\delta_r} \delta_r) + \frac{\rho V_A S b^2}{4 I_Z} (C_{n_p} p + C_{n_r} r)$$

$$\dot{u} = -g \sin \theta + vr - wq + \frac{\rho V_A^2 S}{2m} (C_X + C_{X\delta_e} \delta_e + C_{X\delta_s} \delta_s) + \frac{T}{m}$$

$$\dot{v} = g \cos \theta \sin \phi + wp - ur + \frac{\rho V_A^2 S}{2m} (C_{Y\beta} \beta + C_{Y\delta_a} \delta_a + C_{Y\delta_r} \delta_r) + \frac{\rho V_A S b}{4m} (C_{Y_p} p + C_{Y_r} r)$$

$$\dot{w} = g \cos \theta \cos \phi + uq - vp + \frac{\rho V_A^2 S}{2m} (C_Z + C_{Z\delta_e} \delta_e + C_{Z\delta_s} \delta_s)$$

The following formulas were also used:

$$V_A = (u_a^2 + v_a^2 + w_a^2)^{1/2}$$

$$u_a = u - u_g$$

$$v_a = v - v_g$$

$$w_a = w - w_g$$

$$u_g = -u_g' \cos \psi \cos \theta - v_g' \sin \psi \cos \theta + w_g' \sin \theta$$

## APPENDIX

$$v_g = -u_g'(\cos \psi \sin \phi \sin \theta - \sin \psi \cos \phi) \\ - v_g'(\cos \psi \cos \phi + \sin \psi \sin \phi \sin \theta) - w_g'(\sin \phi \cos \theta)$$

$$w_g = -u_g'(\cos \psi \cos \phi \sin \theta + \sin \psi \sin \phi) \\ - v_g'(\sin \psi \cos \phi \sin \theta - \cos \psi \sin \phi) - w_g'(\cos \phi \cos \theta)$$

$$\alpha = \tan^{-1} \frac{w_a}{u_a}$$

$$\beta = \sin^{-1} \frac{v_a}{V_A}$$

$$M = \frac{V_A}{K}$$

$$\dot{\theta} = q \cos \phi - r \sin \phi$$

$$\dot{\phi} = p + q \tan \theta \sin \phi + r \tan \theta \cos \phi$$

$$\dot{\psi} = \frac{r \cos \phi + q \sin \phi}{\cos \theta}$$

$$\dot{h} = u \sin \theta - v \cos \theta \sin \phi - w \cos \theta \cos \phi$$

$$a_n = -\left(\frac{\dot{w} - uq + vp - g \cos \theta \cos \phi}{g}\right)$$

$$g = 32.17 \left( \frac{3956.66}{3956.66 + \frac{h}{5280}} \right)^2$$

## REFERENCES

1. Bray, Richard S.; and Larsen, William E.: Simulator Investigations of the Problems of Flying a Swept-Wing Transport Aircraft in Heavy Turbulence. Conference on Aircraft Operating Problems, NASA SP-83, 1965, pp. 137-148.
2. Andrews, William H.; Butchart, Stanley P.; Sisk, Thomas R.; and Hughes, Donald L.: Flight Tests Related to Jet-Transport Upset and Turbulent-Air Penetration. Conference on Aircraft Operating Problems, NASA SP-83, 1965, pp. 123-135.
3. Soderlind, Paul A.: Jet Turbulence Penetration. Flight Stand. Bull. No. 8-63, Northwest Airlines, Inc., Nov. 12, 1963.
4. Brooks, Eugene N., Jr.; Decker, John P.; and Blackwell, James A., Jr.: Static Aerodynamic Characteristics of a Model of a Typical Subsonic Jet-Transport Airplane at Mach Numbers From 0.40 to 1.20. NASA TM X-1345, 1967.
5. Wright, Bruce R.; and Bower, Margaret L.: Aerodynamic Damping and Oscillatory Stability in Pitch for a Model of a Typical Subsonic Jet-Transport Airplane. NASA TN D-3159, 1966.
6. Staff, NSSP: National Severe Storms Project Objectives and Basic Design. Rep. No. 1, Nat. Severe Storms Project, Weather Bur., U.S. Dept. Commerce, Mar. 1961.
7. Goddard, Brent B.: The Development of Aircraft Investigations of Squall Lines From 1956-1960. Rep. No. 2, Nat. Severe Storms Project, Weather Bur., U.S. Dept. Commerce, Feb. 1962.
8. Davies, D. P.: Handling the Big Jets. ARB (Cheltenham, Engl.), 1967.
9. Magruder, William M.; and Fetty, R. L.: A Test Pilot's View of the Sub-Sonic Jet Upset Problem. Test Pilots' 1964 Report to the Aerospace Profession, Soc. Exp. Test Pilots, Sept. 1964, pp. 90-109.



TABLE I.- TABULATION OF AERODYNAMICS USED IN COMPUTATIONS

(a) Derivatives used as function of  $\alpha$  and M

$\alpha$	(a) Derivatives used as function of $\alpha$ and M														
	M = 0.40	M = 0.60	M = 0.80	M = 0.90	M = 0.95	M = 0.40	M = 0.60	M = 0.80	M = 0.90	M = 0.95	M = 0.40	M = 0.60	M = 0.80	M = 0.90	M = 0.95
	$C_m$					$C_x$					$C_z$				
-20	0.185	0.160	0.125	0.090	0.182	-0.034	-0.044	-0.059	-0.065	-0.073	0.60	0.60	0.59	0.58	0.67
-16	.090	.072	.045	.022	.095	-.034	-.044	-.061	-.061	-.072	.58	.55	.51	.50	.59
-12	.045	.025	.010	0	.067	-.034	-.044	-.061	-.056	-.071	.51	.47	.44	.42	.49
-8	.035	.020	0	-.022	.047	-.034	-.043	-.055	-.050	-.071	.38	.34	.34	.31	.39
-4	0	-.020	-.040	-.055	.015	-.032	-.037	-.043	-.043	-.071	.13	.11	.11	.10	.22
0	-.060	-.065	-.087	-.120	-.042	-.026	-.025	-.029	-.048	-.073	-.25	-.27	-.31	-.29	-.16
2	-.085	-.095	-.120	-.140	-.085	-.017	-.017	-.023	-.051	-.077	-.42	-.45	-.52	-.48	-.39
4	-.105	-.110	-.125	-.150	-.150	0	.001	-.020	-.053	-.077	-.60	-.63	-.70	-.75	-.60
6	-.110	-.105	-.130	-.158	-.168	.024	.020	-.024	-.052	-.071	-.75	-.79	-.79	-.75	-.79
8	-.110	-.110	-.140	-.172	-.188	.032	.012	-.032	-.052	-.072	-.88	-.90	-.85	-.84	-.93
10	-.120	-.145	-.170	-.170	-.190	.027	-.010	-.040	-.057	-.067	-.99	-.97	-.91	-.92	-1.01
12	-.135	-.182	-.220	-.175	-.202	.009	-.024	-.048	-.060	-.068	-1.08	-1.04	-.96	-.99	-1.07
14	-.170	-.230	-.250	-.205	-.235	-.008	-.030	-.055	-.064	-.070	-1.16	-1.09	-1.01	-1.07	-1.15
16	-.230	-.275	-.270	-.250	-.280	-.018	-.036	-.058	-.066	-.073	-1.22	-1.14	-1.08	-1.16	-1.26
18	-.330	-.335	-.350	-.315	-.345	-.024	-.041	-.061	-.067	-.074	-1.26	-1.18	-1.14	-1.22	-1.32
20	-.410	-.385	-.372	-.370	-.388	-.028	-.045	-.060	-.068	-.074	-1.29	-1.22	-1.22	-1.29	-1.38
	$C_{l\beta}$					$C_{n\beta}$					$C_{Y\beta}$				
-20	0.0034	0.0035	0.0033	0.0033	0.0031	0.0033	0.0038	0.0035	0.0037	0.0048	-0.0215	-0.0215	-0.0209	-0.0213	-0.0221
-16	.0033	.0032	.0033	.0024	.0025	.0033	.0038	.0035	.0037	.0048	-.0217	-.0219	-.0213	-.0215	-.0226
-12	.0024	.0020	.0020	.0007	.0006	.0033	.0038	.0034	.0037	.0048	-.0219	-.0223	-.0216	-.0217	-.0231
-8	.0002	0	-.0003	-.0016	-.0020	.0032	.0037	.0034	.0037	.0047	-.0220	-.0225	-.0218	-.0220	-.0234
-4	-.0020	-.0019	-.0028	-.0029	-.0010	.0032	.0036	.0034	.0037	.0046	-.0215	-.0221	-.0220	-.0221	-.0235
0	-.0031	-.0033	-.0044	.0005	.0005	.0029	.0033	.0032	.0037	.0039	-.0198	-.0200	-.0210	-.0210	-.0211
2	-.0033	-.0038	-.0043	.0013	.0003	.0026	.0028	.0030	.0036	.0031	-.0190	-.0186	-.0203	-.0200	-.0195
4	-.0036	-.0041	-.0022	.0008	-.0009	.0026	.0023	.0033	.0033	.0029	-.0187	-.0180	-.0200	-.0190	-.0200
6	-.0036	-.0041	-.0026	-.0029	-.0031	.0025	.0023	.0036	.0031	.0027	-.0188	-.0174	-.0210	-.0198	-.0208
8	-.0035	-.0033	-.0025	-.0022	-.0045	.0025	.0031	.0038	.0033	.0022	-.0190	-.0190	-.0210	-.0210	-.0213
10	-.0030	-.0023	-.0021	-.0015	-.0063	.0029	.0034	.0039	.0033	.0017	-.0190	-.0195	-.0213	-.0208	-.0198
12	-.0024	-.0020	-.0023	-.0032	-.0046	.0033	.0035	.0038	.0031	.0014	-.0195	-.0200	-.0215	-.0213	-.0189
14	-.0017	-.0015	-.0029	-.0035	-.0041	.0037	.0037	.0036	.0033	.0014	-.0201	-.0202	-.0213	-.0215	-.0180
16	-.0011	-.0012	-.0028	-.0029	-.0038	.0037	.0037	.0037	.0033	.0012	-.0190	-.0200	-.0208	-.0218	-.0185
18	-.0012	-.0014	-.0023	-.0033	-.0037	.0031	.0037	.0043	.0032	.0010	-.0187	-.0185	-.0210	-.0223	-.0190
20	-.0015	-.0017	-.0022	-.0035	-.0037	.0028	.0036	.0043	.0031	.0007	-.0186	-.0182	-.0212	-.0227	-.0194
	$C_{m_q}$					$C_{n_p}$									
-20	30	4	-20	-40	-38	0.172	0.182	0.174	0.168	0.169					
-16	8	-5	-3	-32	-33	.162	.172	.169	.162	.164					
-12	-7	-15	-3	-25	-29	.142	.152	.153	.146	.147					
-8	-11	-21	-19	-22	-27	.113	.122	.125	.120	.120					
-4	-12	-20	-19	-24	-19	.073	.080	.087	.083	.083					
0	-13	-16	-20	-22	-18	.020	.026	.032	.032	.032					
2	-14	-16	-21	-20	-20	-.013	-.008	-.002	0	0					
4	-16	-19	-23	-23	-28	-.042	-.041	-.034	-.033	-.035					
6	-17	-18	-13	-12	-18	-.059	-.058	-.053	-.050	-.056					
8	-17	-15	-15	-30	-13	-.073	-.072	-.070	-.067	-.070					
10	-14	-10	-7	-16	-38	-.088	-.087	-.082	-.080	-.084					
12	-11	-5	-3	-46	-8	-.103	-.101	-.096	-.096	-.100					
14	-6	-2	-10	-9	-20	-.113	-.110	-.105	-.105	-.104					
16	15	4	-10	-43	-29	-.121	-.118	-.110	-.110	-.108					
18	30	7	-50	-27	-35	-.129	-.125	-.113	-.114	-.110					
20	25	5	-17	-41	-37	-.136	-.131	-.116	-.116	-.112					

TABLE I.- TABULATION OF AERODYNAMICS USED IN COMPUTATIONS — Concluded

(b) Derivatives used as constants

$C_{l_{\delta a}}$	0.00093
$C_{l_{\delta r}}$	0.00030
$C_{l_p}$	-0.250
$C_{l_r}$	0.200
$C_{m_{\delta s}}$	-0.030
$C_{m_{\delta e}}$	-0.0125
$C_{n_{\delta a}}$	0
$C_{n_{\delta r}}$	-0.0020
$C_{n_r}$	-0.190
$C_{X_{\delta s}}$	0.0025
$C_{X_{\delta e}}$	0.0010
$C_{Y_{\delta a}}$	0
$C_{Y_{\delta r}}$	0.0048
$C_{Y_p}$	-0.110
$C_{Y_r}$	0.375
$C_{Z_{\delta s}}$	-0.010
$C_{Z_{\delta e}}$	-0.004

TABLE II.- DYNAMIC-STABILITY CHARACTERISTICS OF AIRPLANE

	h = 40 000 ft (12.19 km); M = 0.82	h = 32 000 ft (9.75 km); M = 0.78
Short period:		
$\omega_n$ , rad/sec . . . . .	1.62	1.63
P, sec . . . . .	4.2	4.3
$\zeta$ . . . . .	0.39	0.45
$2\zeta\omega_n$ , rad/sec . . . . .	1.27	1.48
Phugoid:		
P, sec . . . . .	>100	>100
Roll mode:		
$t_R$ , sec . . . . .	1.99	1.54
$t_{1/2}$ , sec . . . . .	1.38	1.07
Spiral mode:		
$t_{1/2}$ , sec . . . . .	2332	76
Dutch roll:		
$\omega_n$ , rad/sec . . . . .	1.40	1.59
P, sec . . . . .	4.51	3.99
$\zeta$ . . . . .	0.09	0.12
$C_{1/2}$ . . . . .	1.27	0.94
$\left  \frac{\phi}{\beta} \right $ . . . . .	2.22	2.84

**TABLE III.- RANGE OF VARIATION AND ROOT MEAN SQUARE OF NORMAL AND LATERAL ACCELERATIONS EXPERIENCED DURING SIMULATED FLIGHTS IN SEVERE TURBULENCE**

Figure	Maximum normal acceleration, $a_n$ , g units	Maximum lateral acceleration, $a_y$ , g units	Root mean square	
			$a_n$	$a_y$
4(a)	-1.00 to 4.75	-0.48 to 0.75	0.891	0.148
4(b)	0.20 to 3.00	-0.25 to 0.25	.723	.083
4(c)	-0.50 to 1.60	-0.35 to 0.30	.310	.106
4(d)	0 to 2.00	-0.30 to 0.40	.249	.078
5	-0.20 to 1.80		.293	0
6	0.57 to 1.10	-0.40 to 0.50	.065	.115
8	-0.20 to 1.90	-0.40 to 0.50	.298	.115
9	-0.90 to 2.50	-0.90 to 1.10	.606	.221
10	-0.20 to 1.90	-0.40 to 0.48	.296	.101
11	-0.20 to 1.80	-0.34 to 0.37	.297	.071
12	-0.20 to 1.90	-0.45 to 0.50	.298	.115
13	-0.20 to 1.80	-0.46 to 0.49	.291	.115
14	-0.20 to 1.90	-0.40 to 0.50	.296	.117
15	-0.40 to 2.40	-0.50 to 0.50	.379	.134
17	-0.20 to 4.00	-0.50 to 0.50	.779	.149
18	-0.60 to 2.30	-0.40 to 0.40	.382	.126
19	-0.20 to 1.90	-0.50 to 0.50	.304	.122
20	-0.50 to 3.60	-0.40 to 0.40	.722	.134

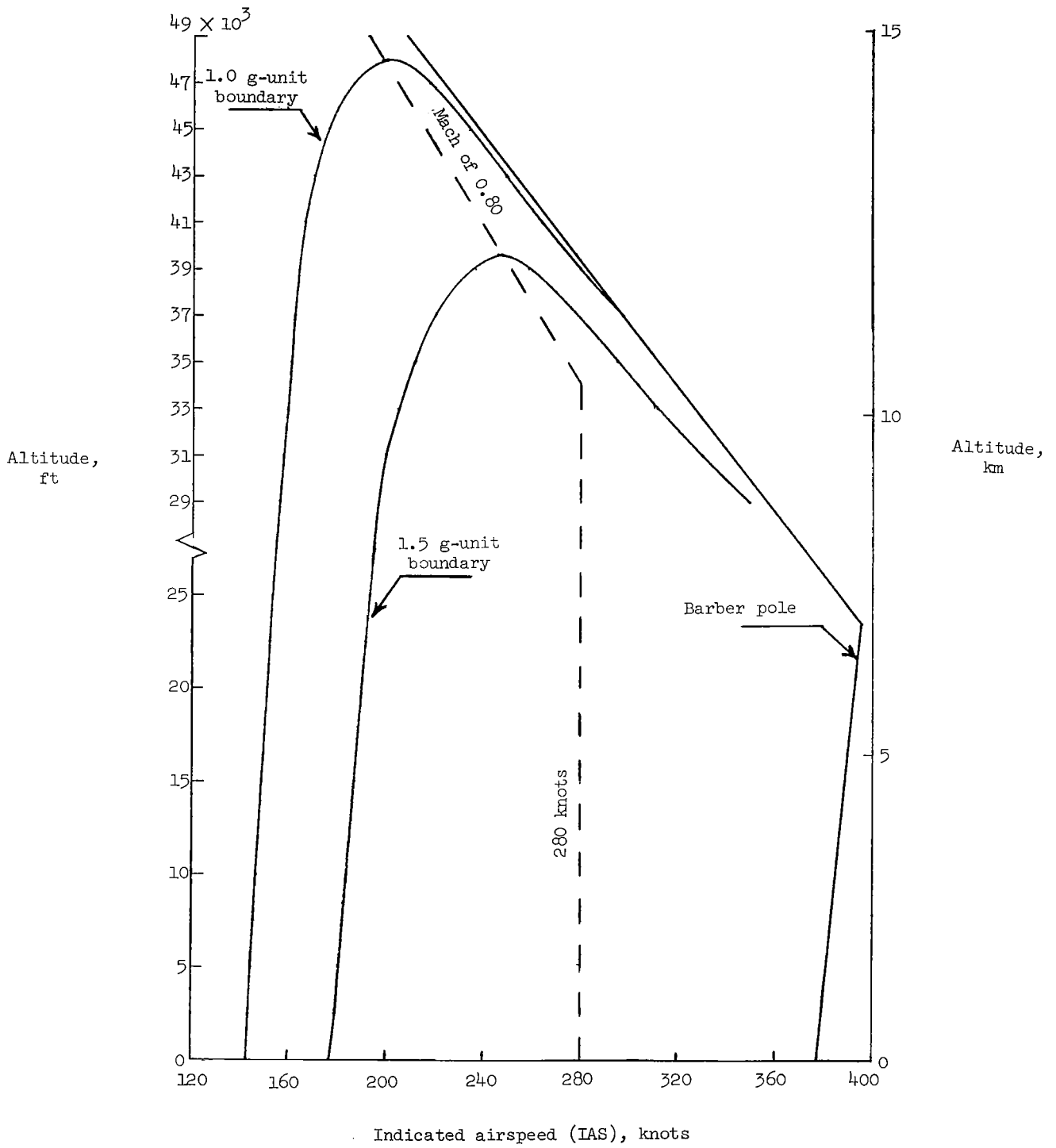


Figure 1.- Indication of low-speed and high-speed buffet boundaries of simulated airplane. Weight = 175 000 pounds force (778 435 newtons).

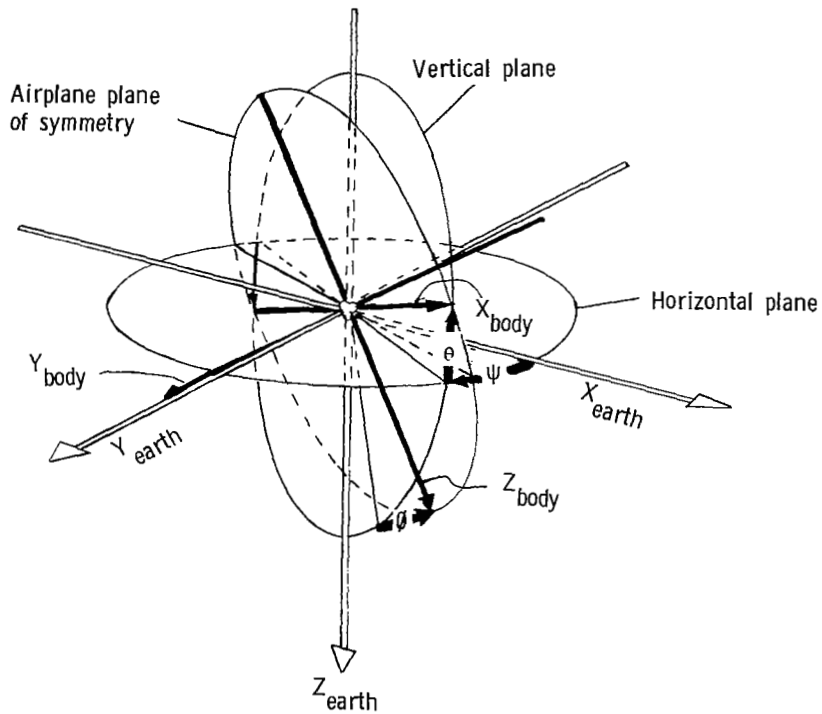
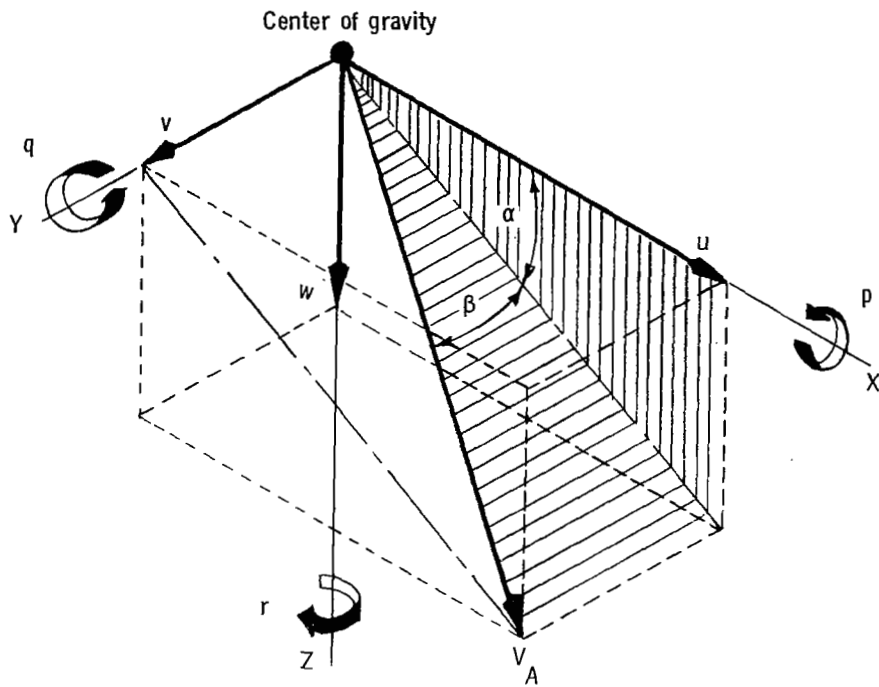
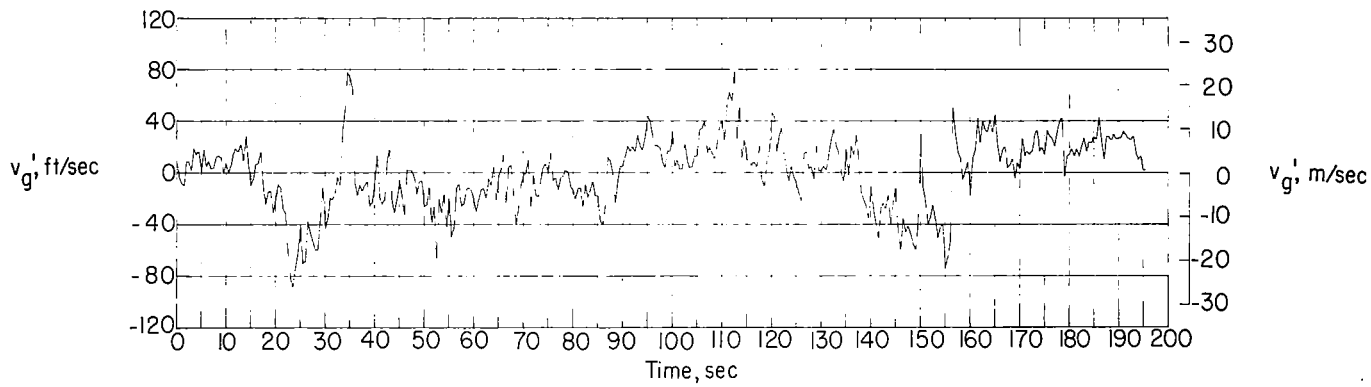
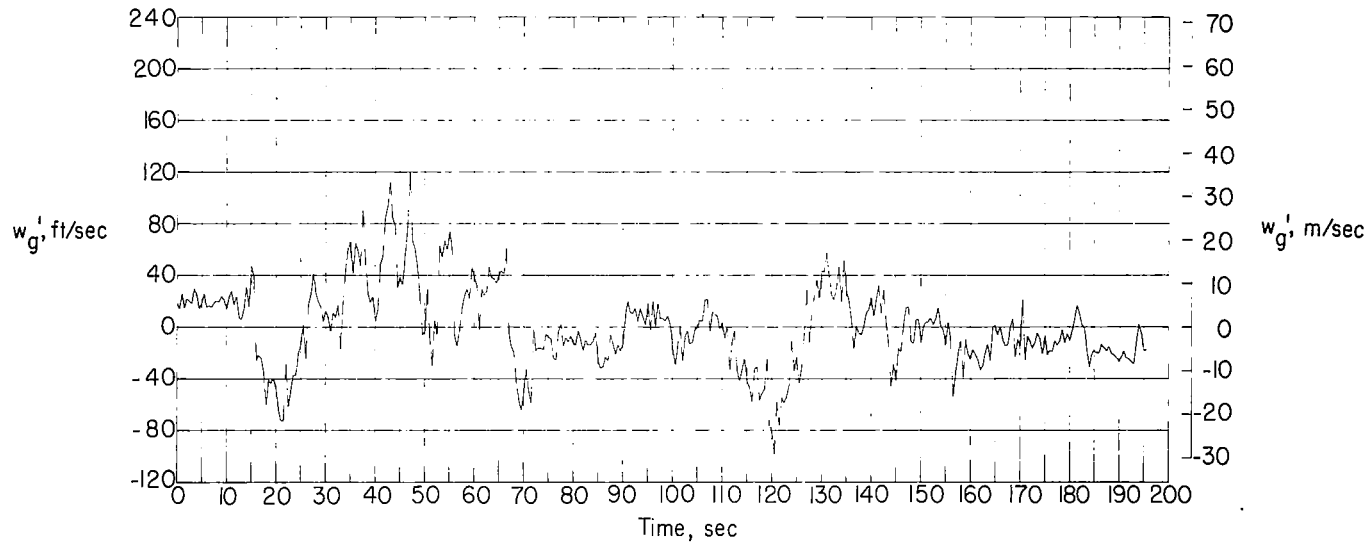
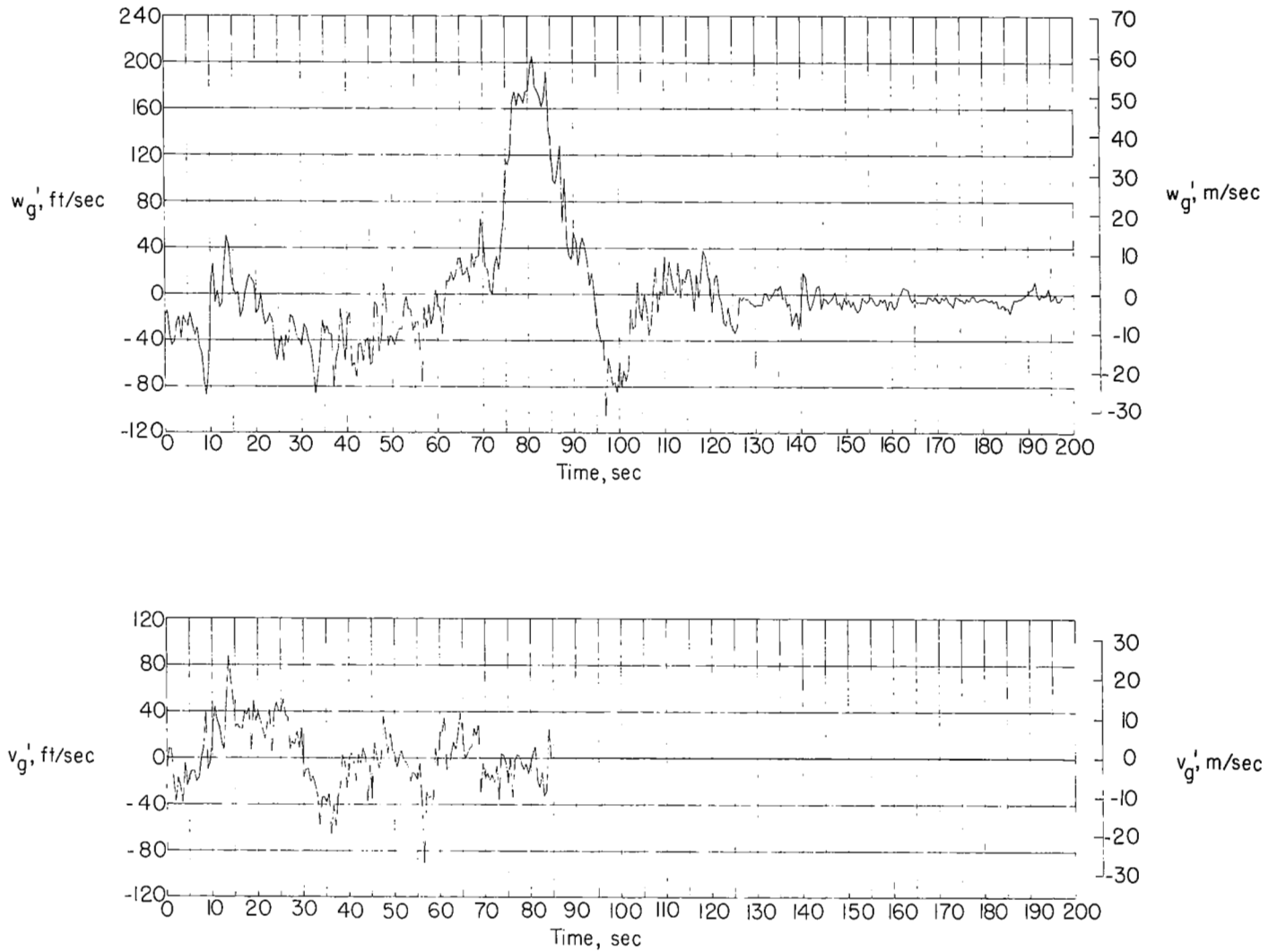


Figure 2.- Body system of axes and related angles. Arrows indicate positive directions.



(a) Basic set of gust samples.

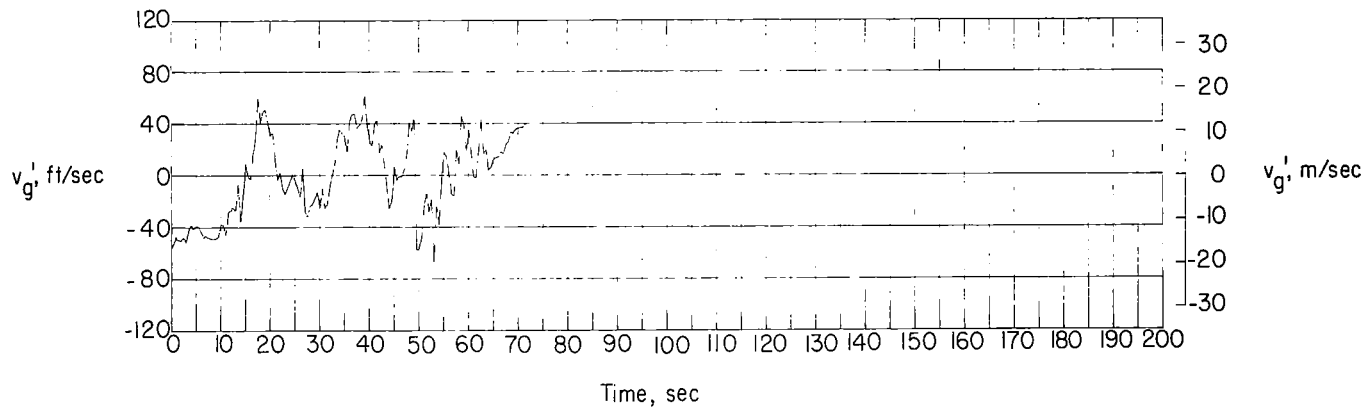
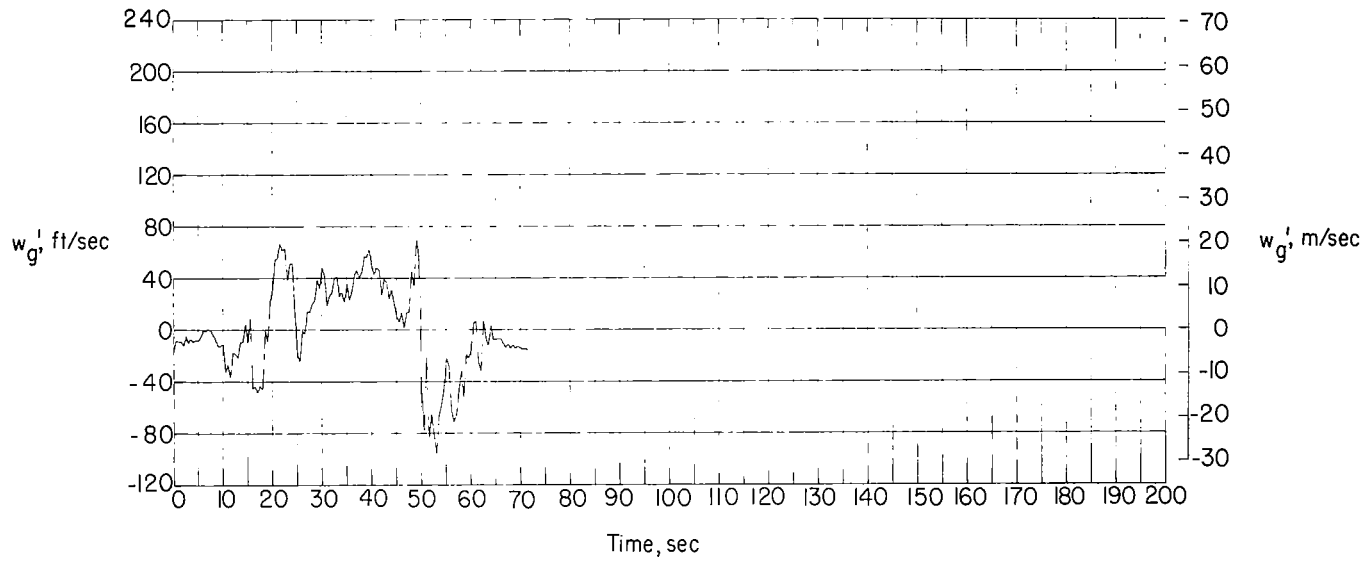
Figure 3.- Indication of magnitude and phasing of four sets of gust samples used in calculations.



(b) Second set of gust samples.

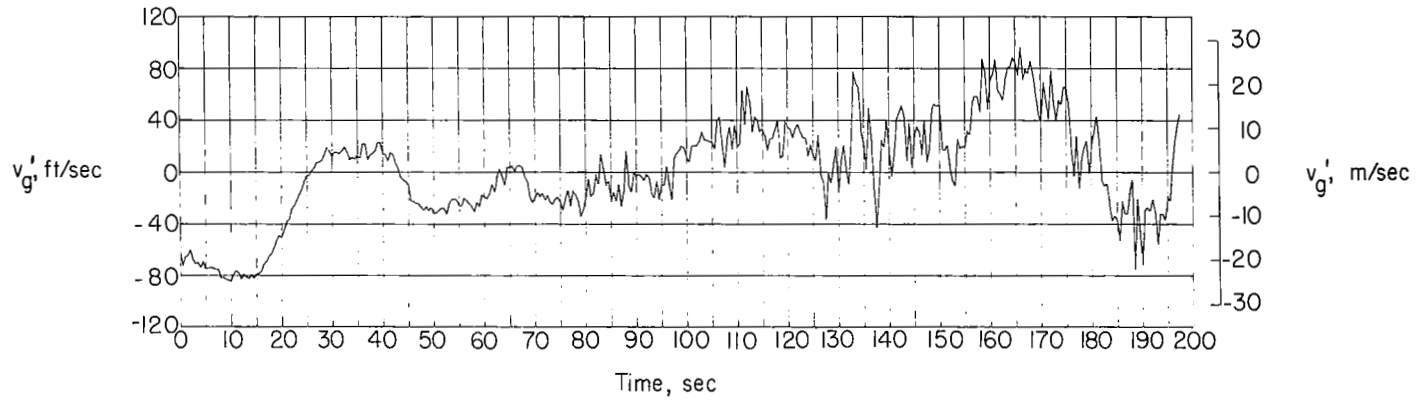
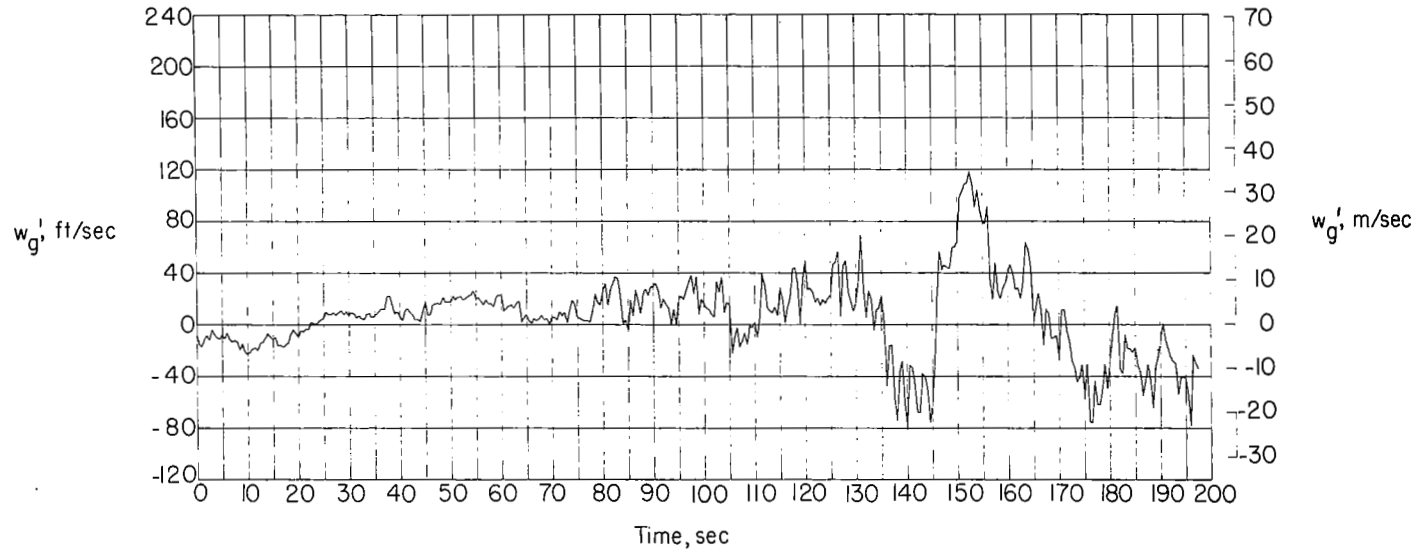
Figure 3.- Continued.





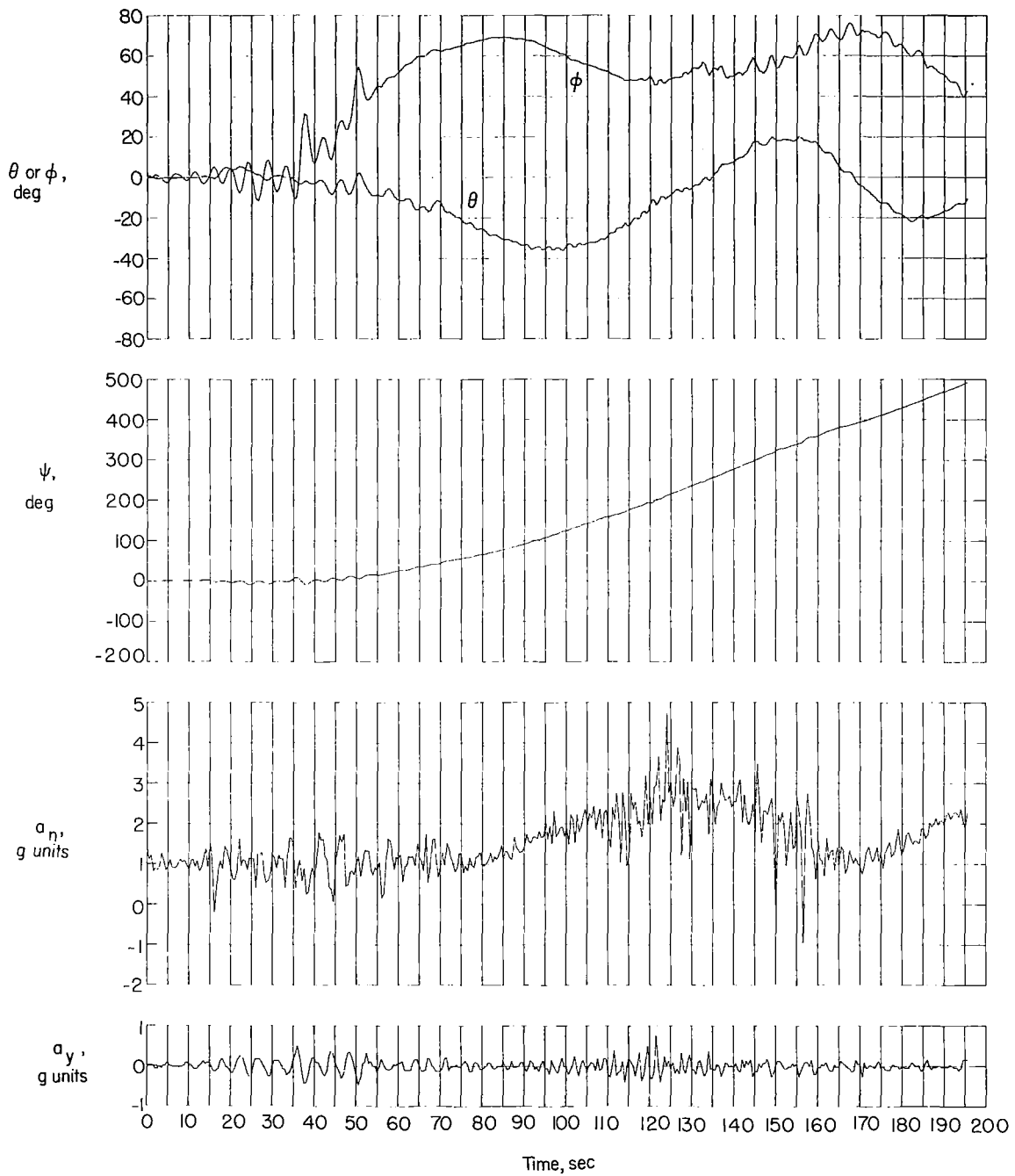
(c) Third set of gust samples.

Figure 3.- Continued.



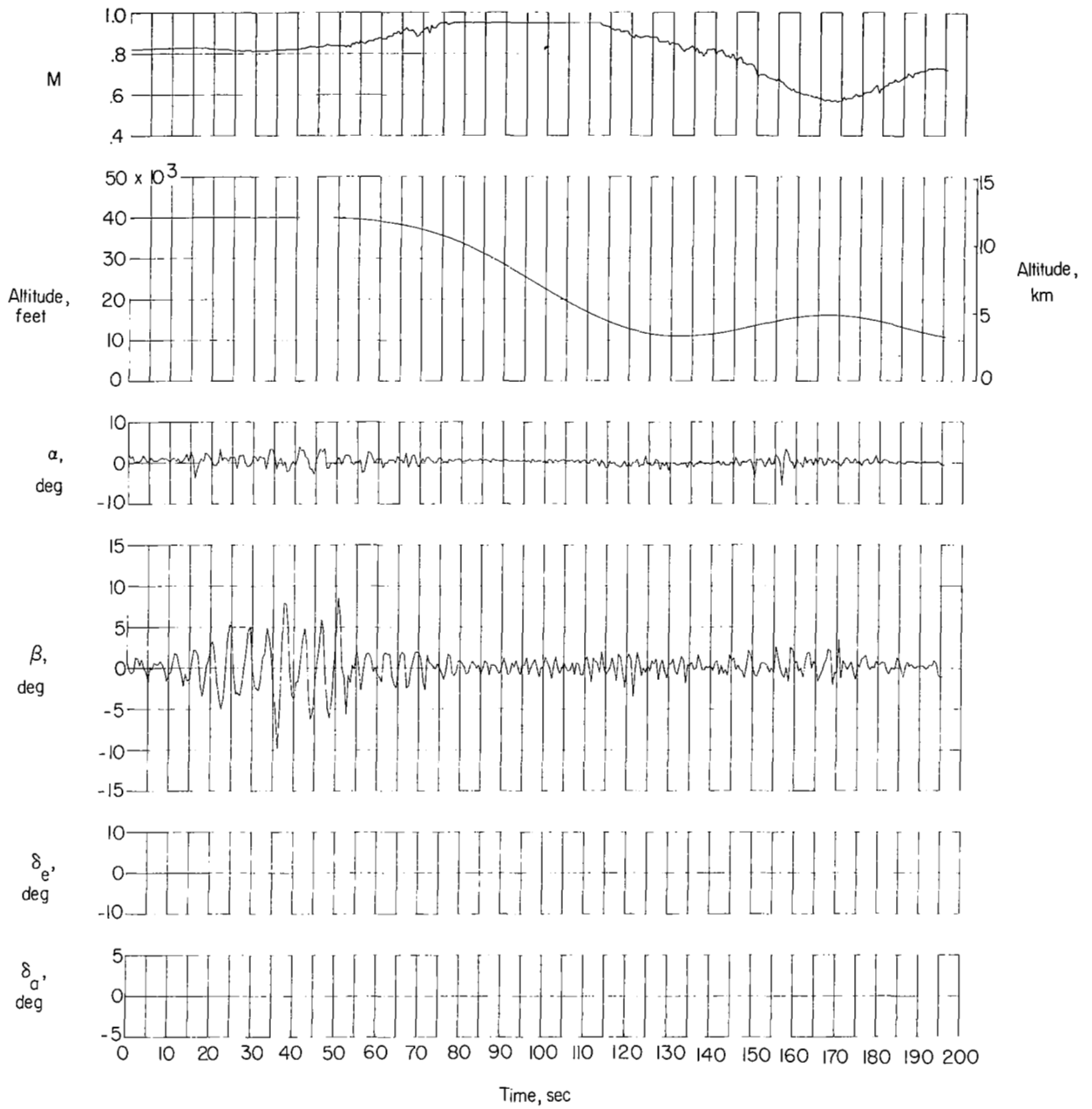
(d) Fourth set of gust samples.

Figure 3.- Concluded.



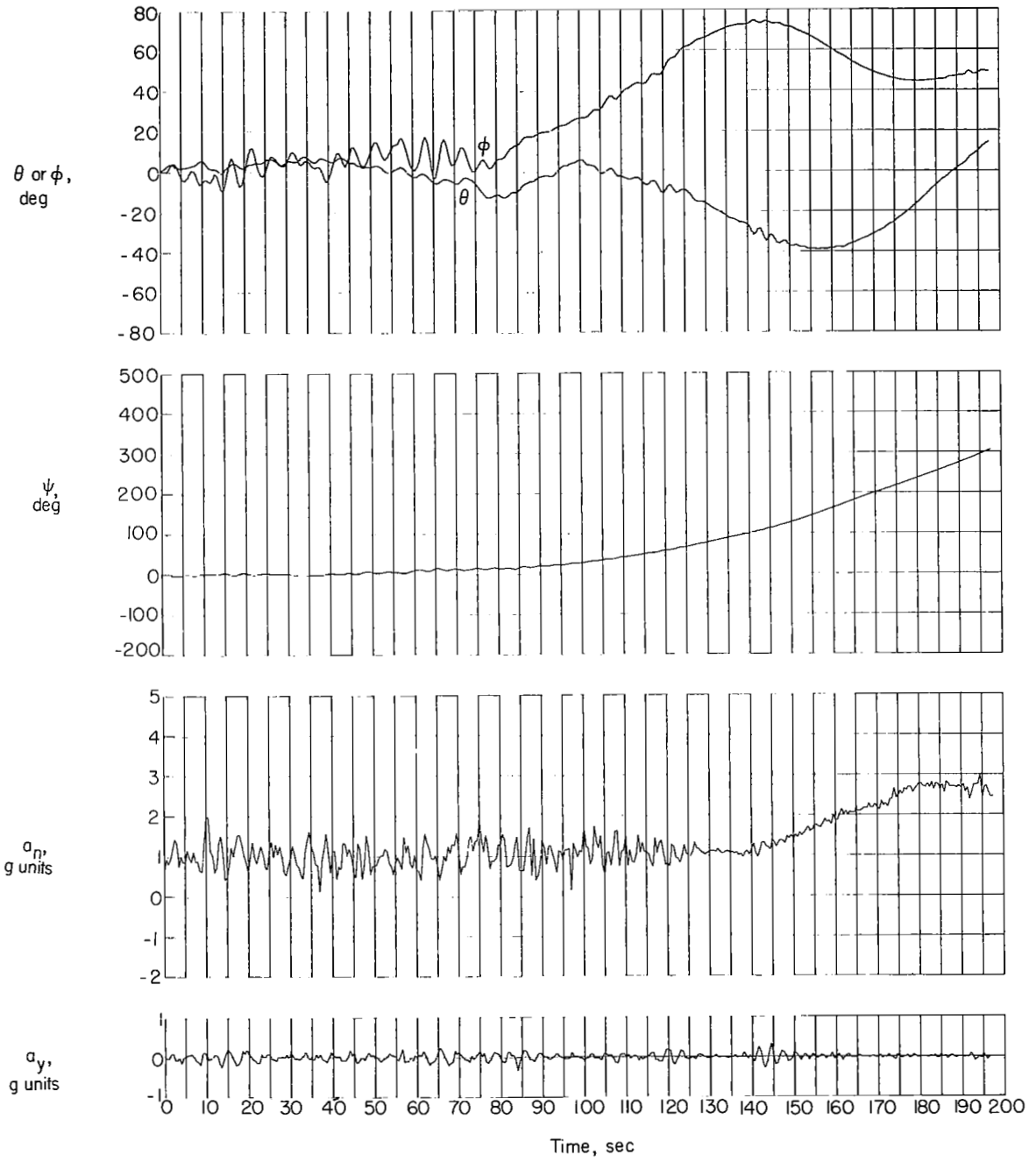
(a) Response to basic gust samples of figure 3(a).

Figure 4.- Time histories of motions obtained when measured gust samples of figure 3 were used.



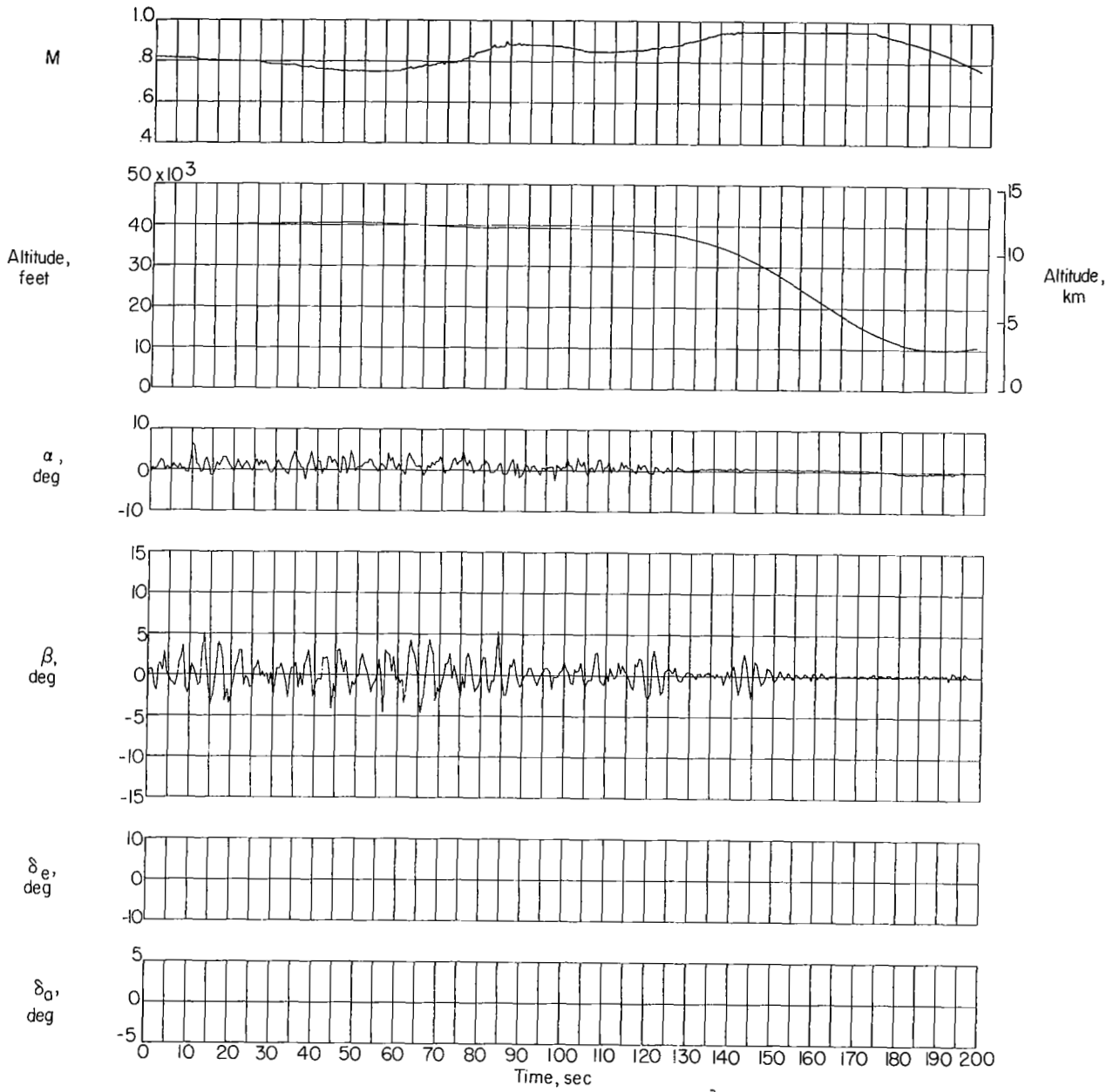
(a) Concluded.

Figure 4.- Continued.



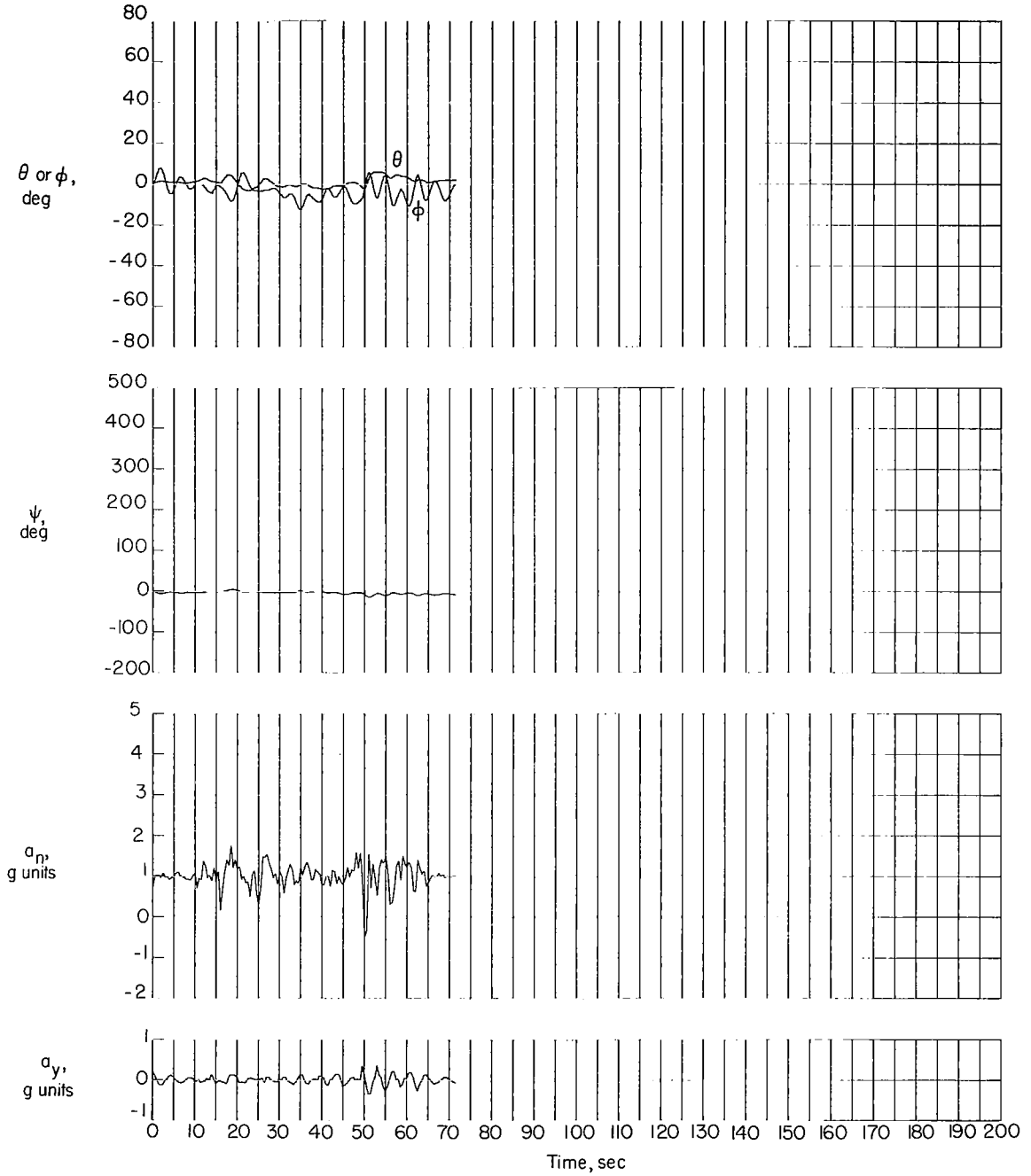
(b) Response to gust samples of figure 3(b).

Figure 4.- Continued.



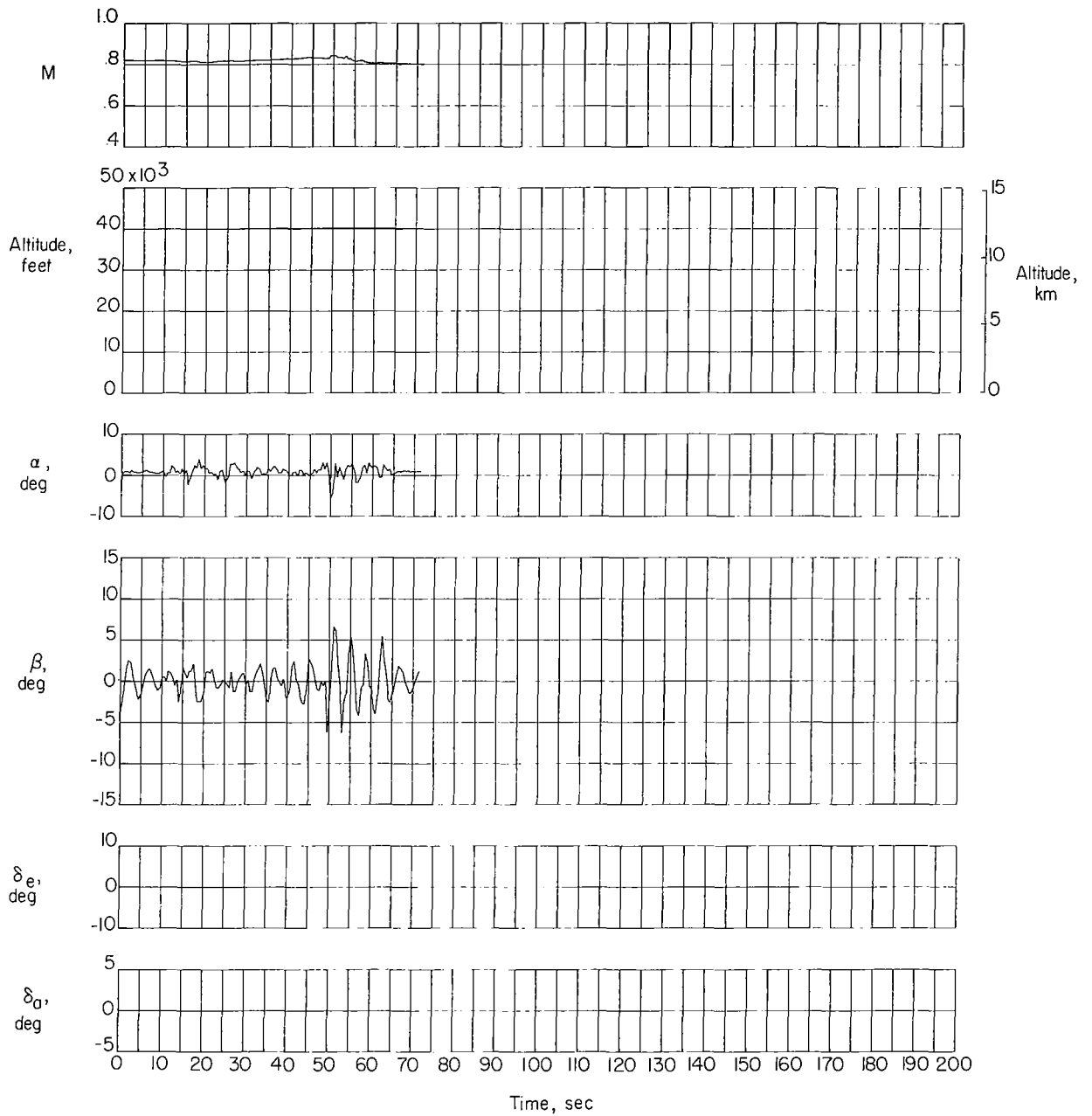
(b) Concluded.

Figure 4.- Continued.



(c) Response to gust samples of figure 3(c).

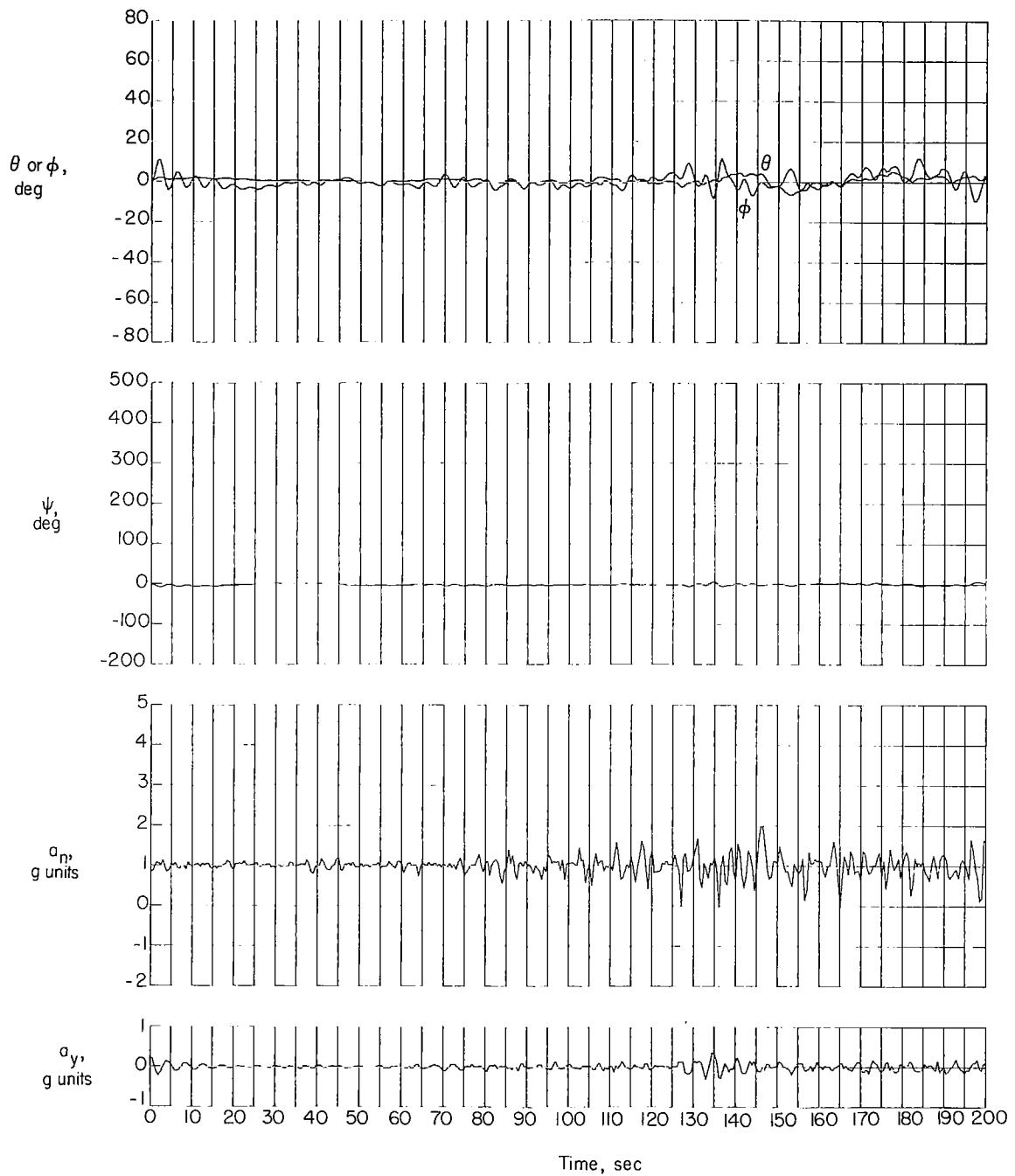
Figure 4.- Continued.



(c) Concluded.

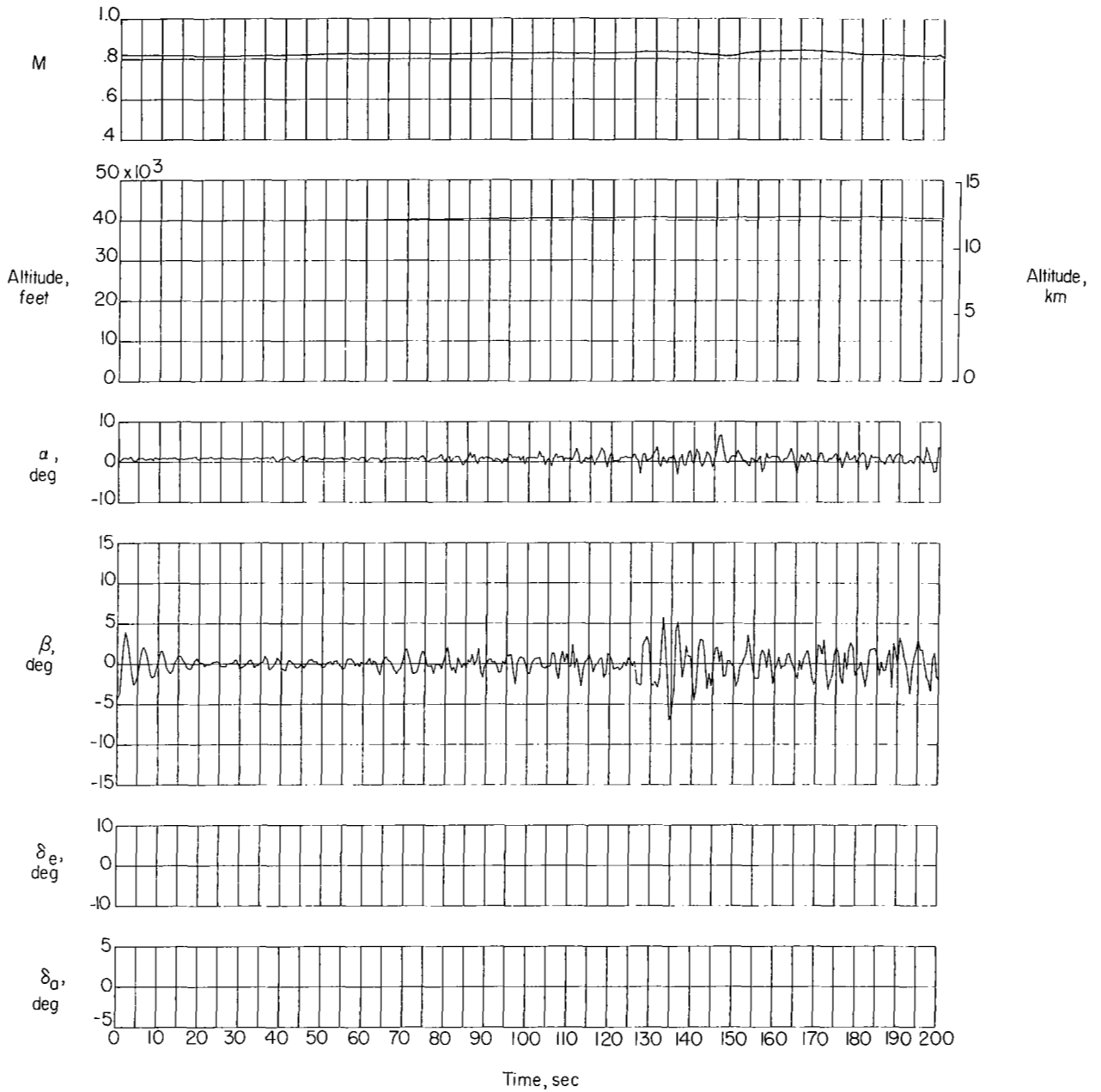
Figure 4.- Continued.





(d) Response to gust samples of figure 3(d).

Figure 4.- Continued.



(d) Concluded.

Figure 4.- Concluded.

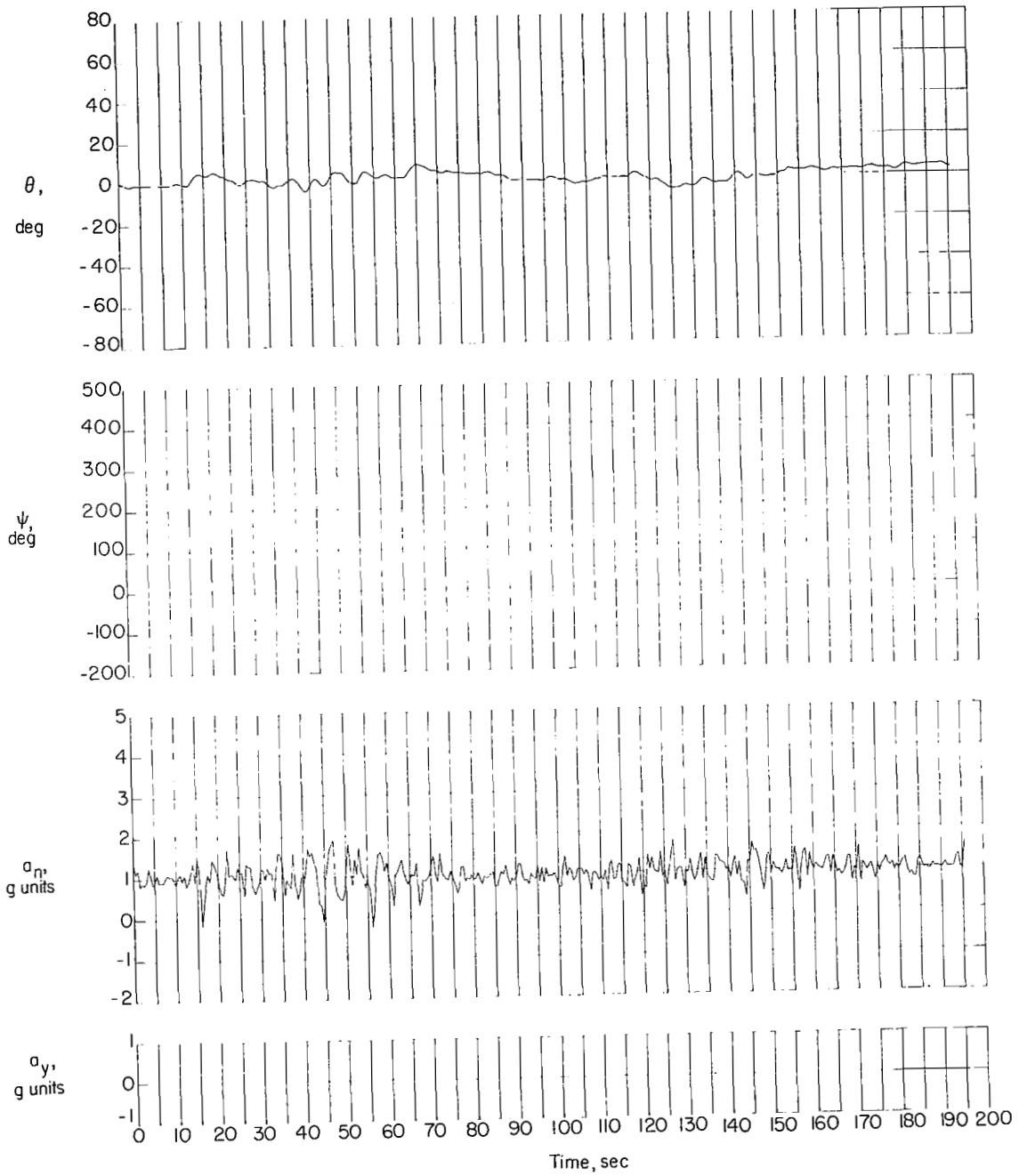


Figure 5.- Indication of motion obtained when only vertical gusts  $w_g'$  of figure 3(a) were used.

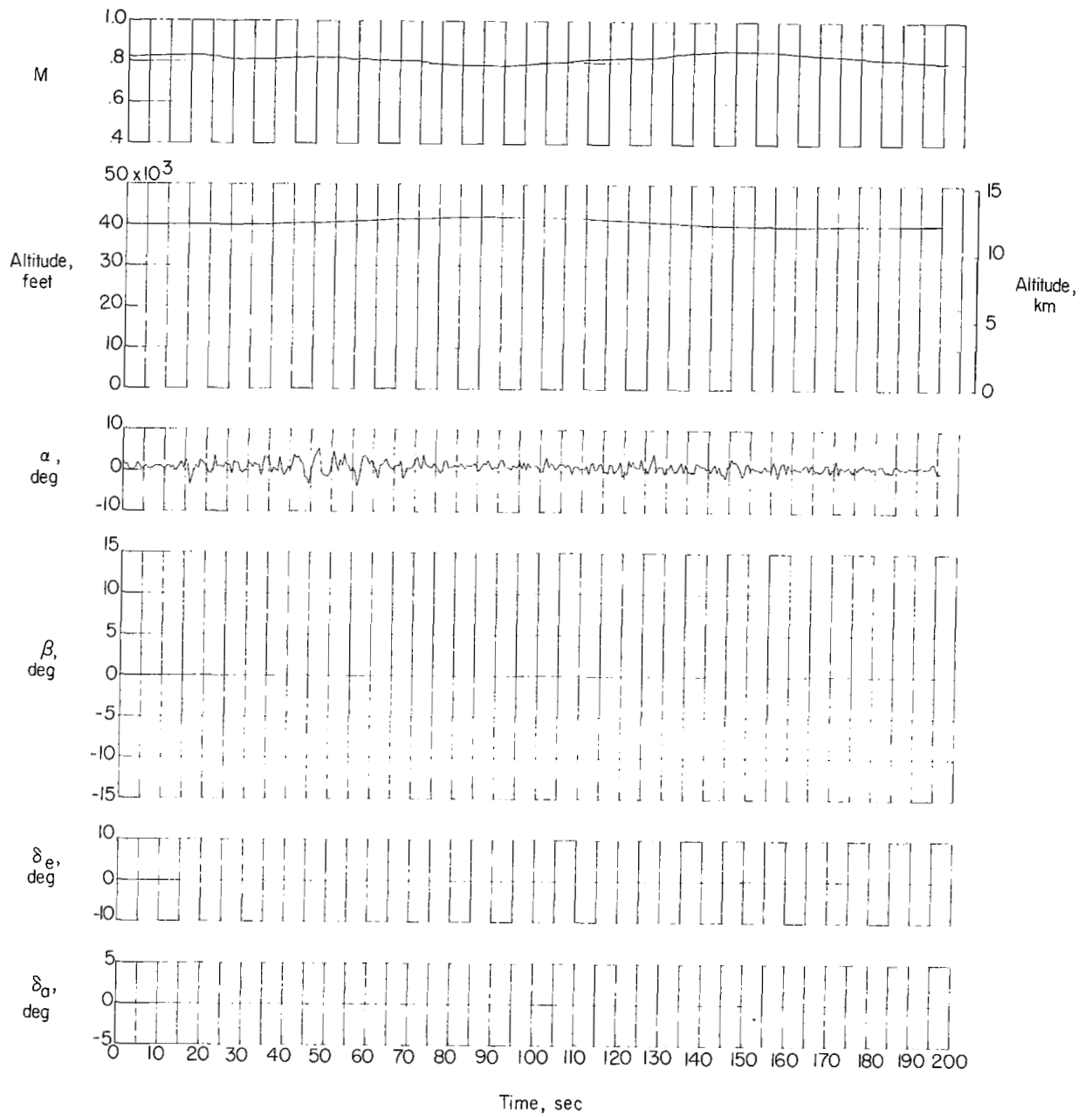


Figure 5.- Concluded.

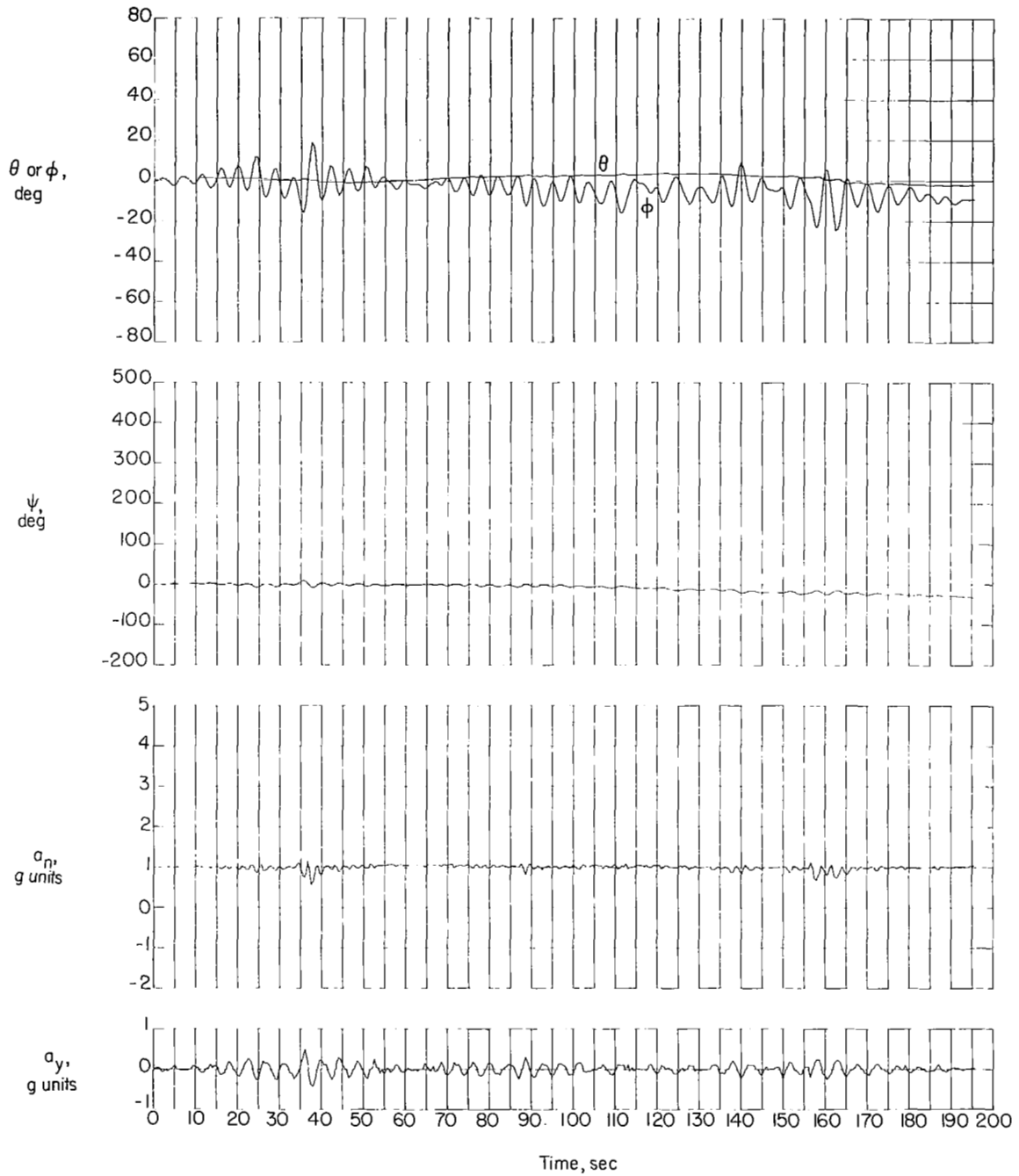


Figure 6.- Indication of motion obtained when only lateral gusts  $v_g'$  of figure 3(a) were used.

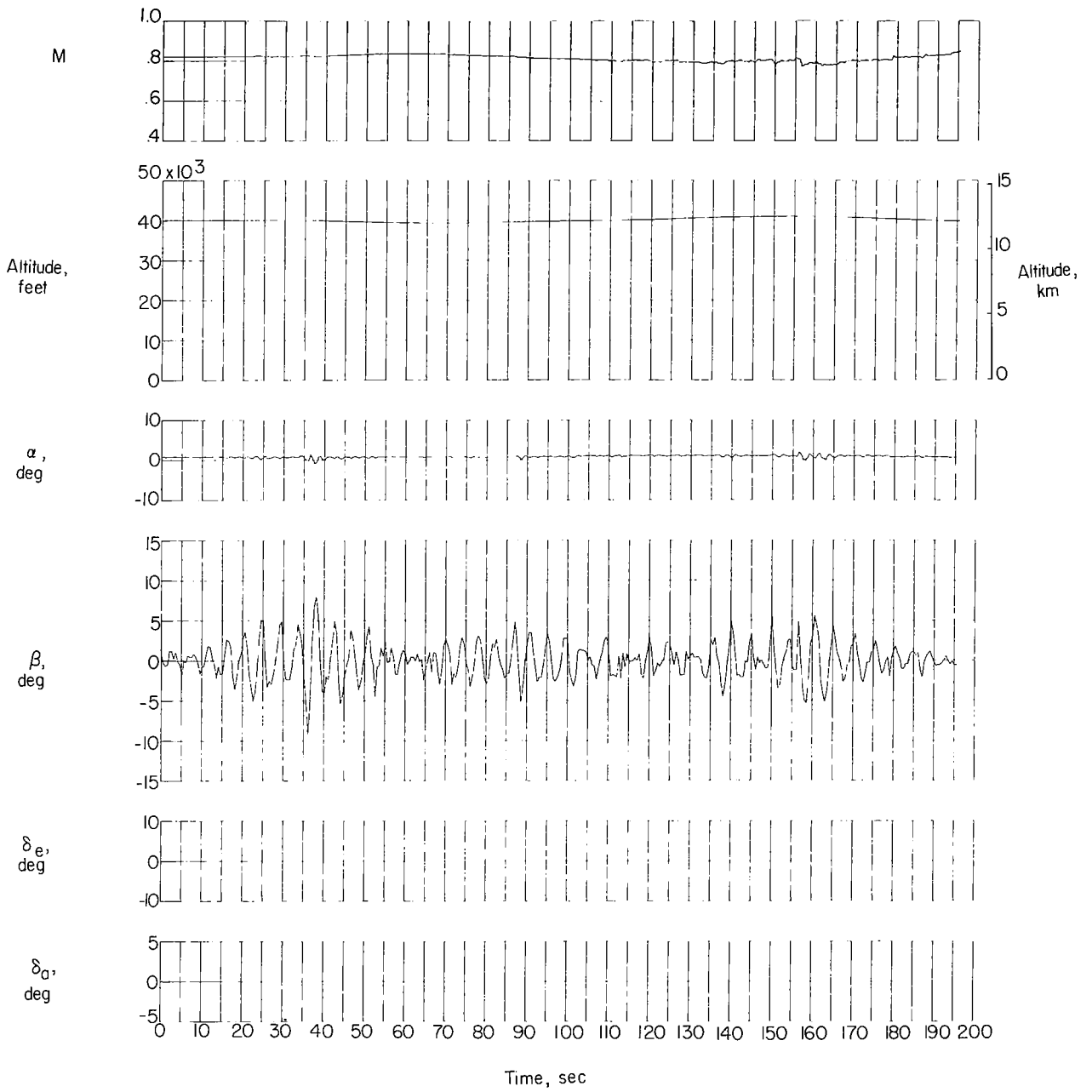


Figure 6.- Concluded.

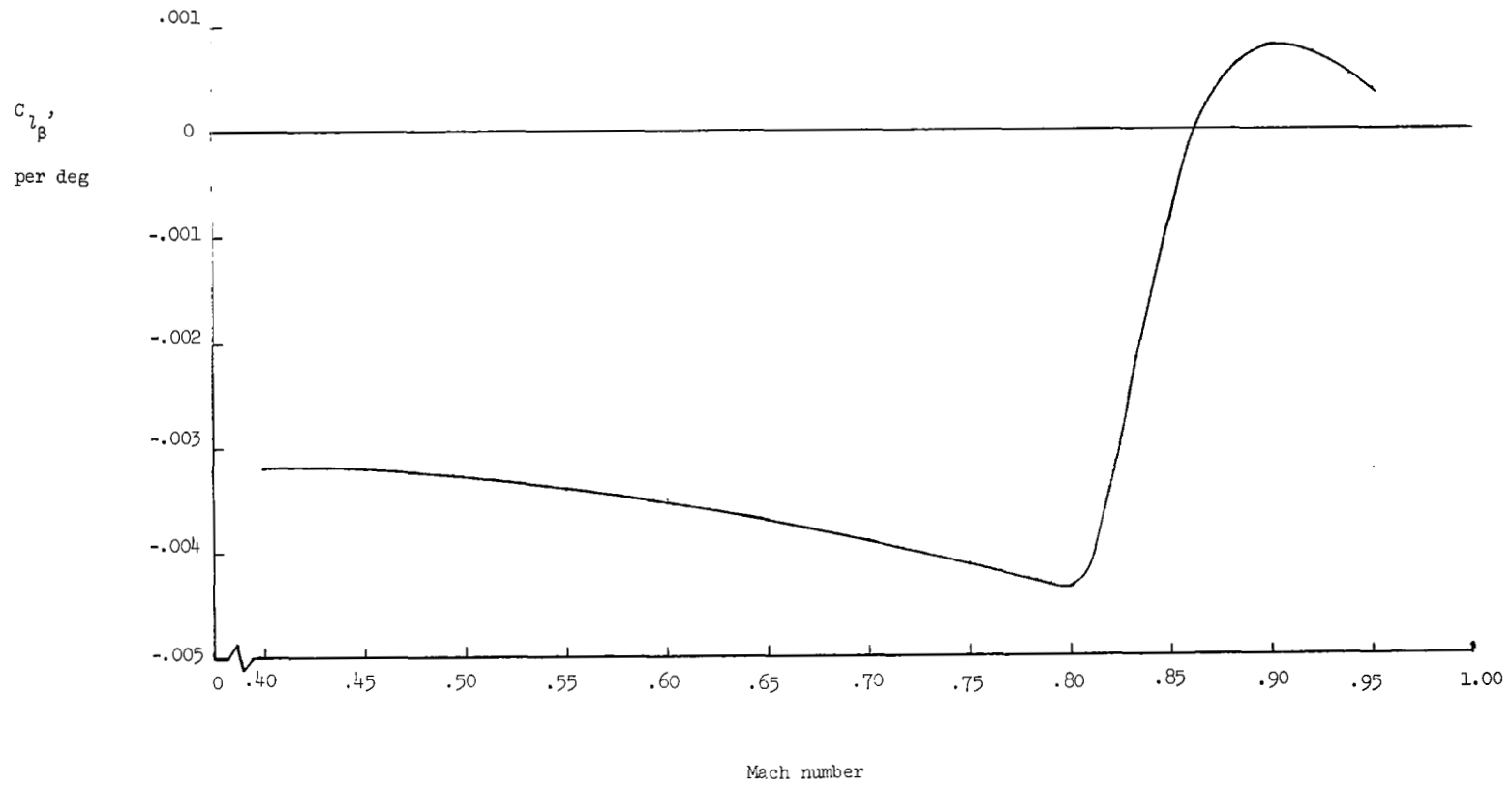


Figure 7.- Variation of effective dihedral with Mach number at trim for  $\alpha = 0.84^\circ$ .

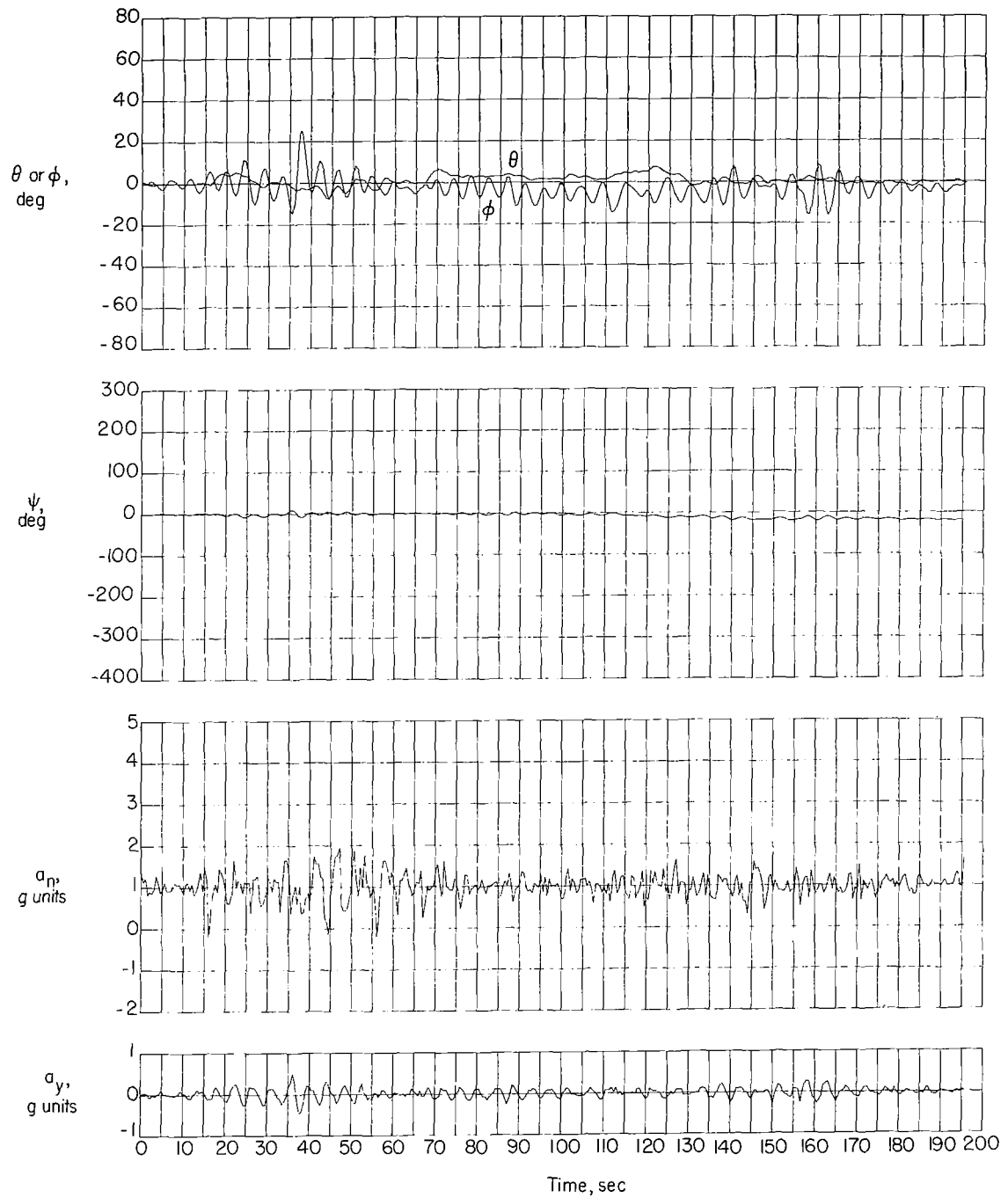


Figure 8.- Time history of motion obtained when  $C_{l\beta}$  was held constant at  $-0.0034$  per degree and gusts of figure 3(a) were used.



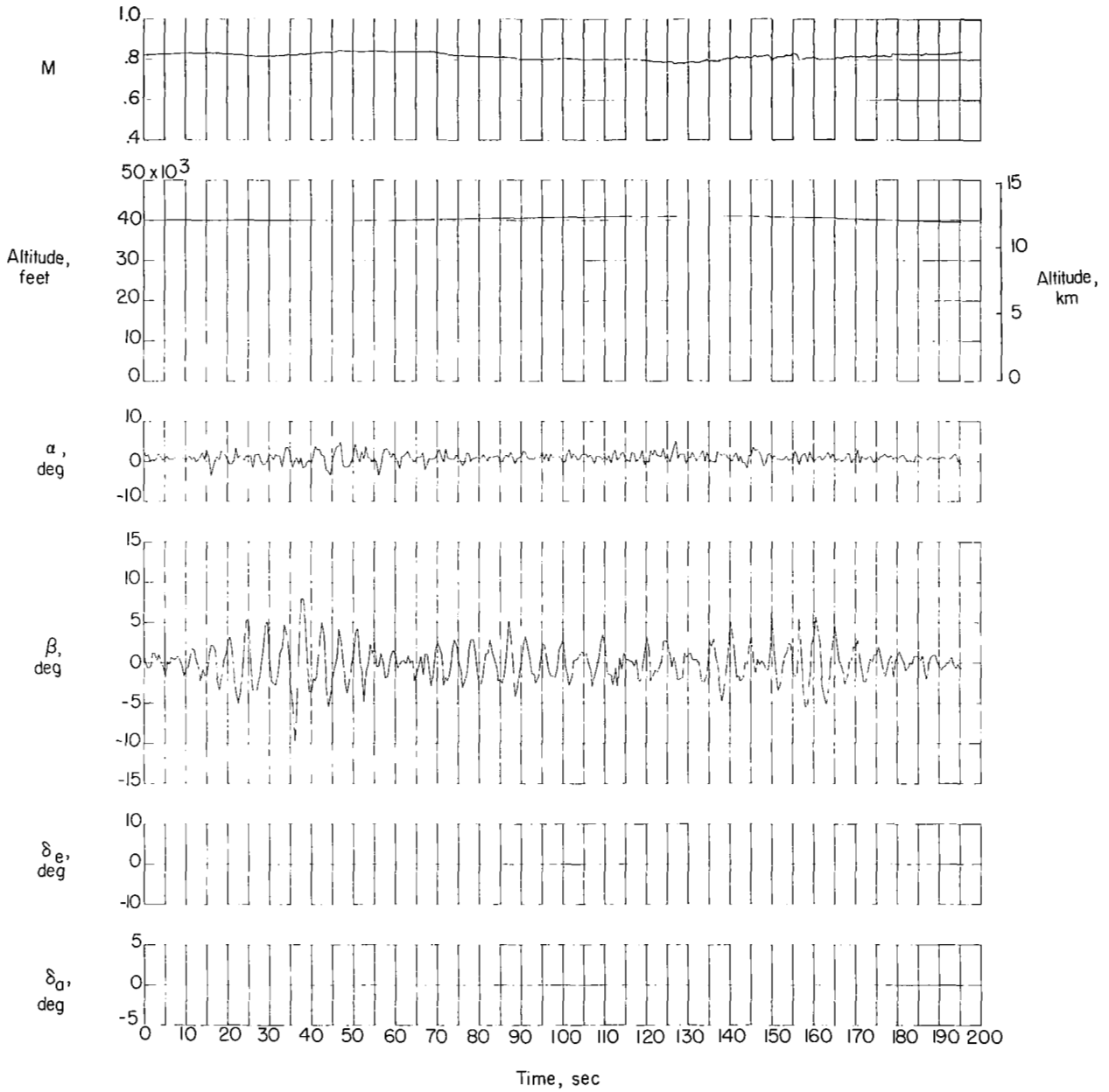


Figure 8.- Concluded.

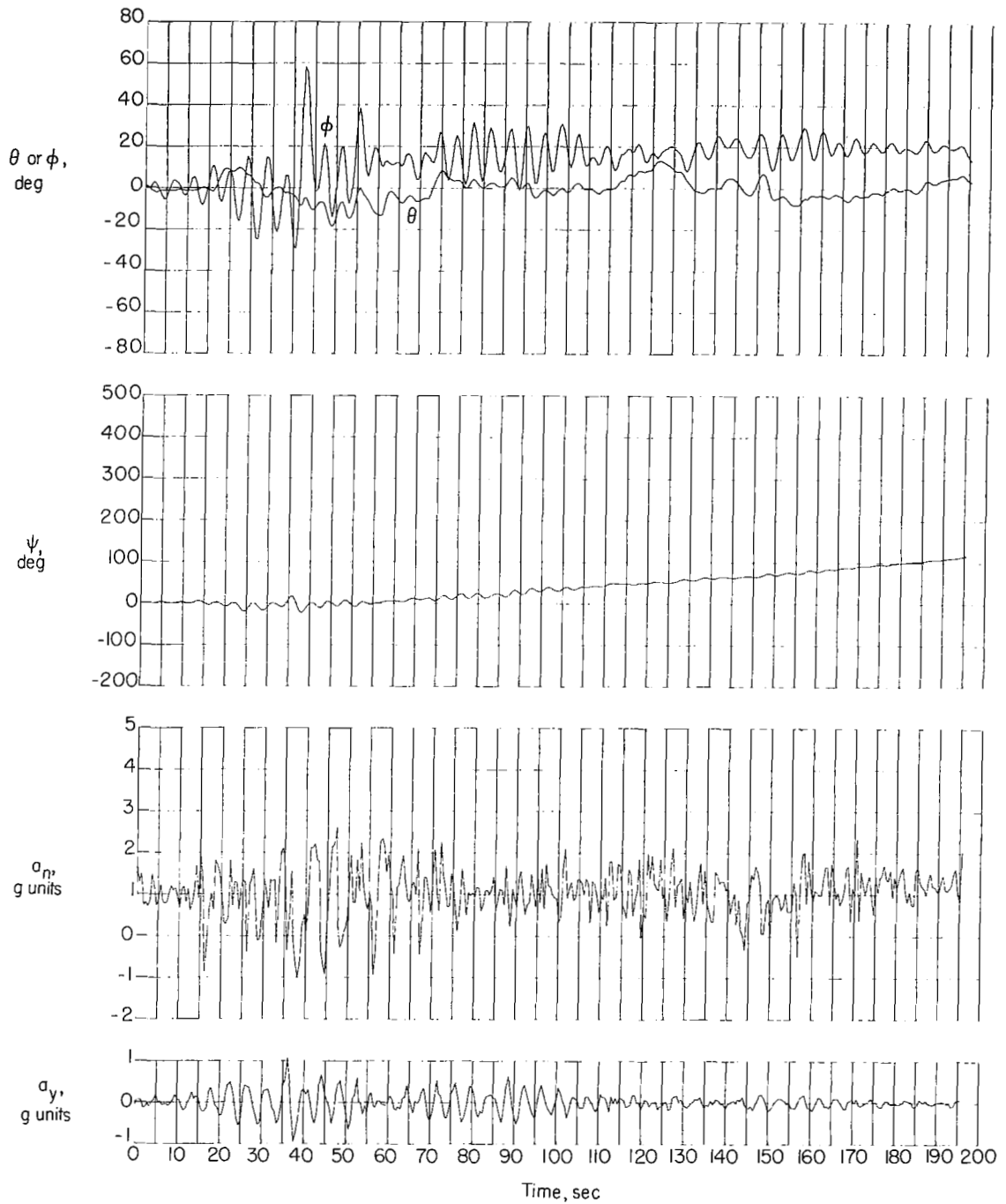


Figure 9.- Time history of motion obtained when  $C_{l\beta}$  was held constant at  $-0.0034$  per degree and gusts of figure 3(a) were arbitrarily doubled in magnitude.

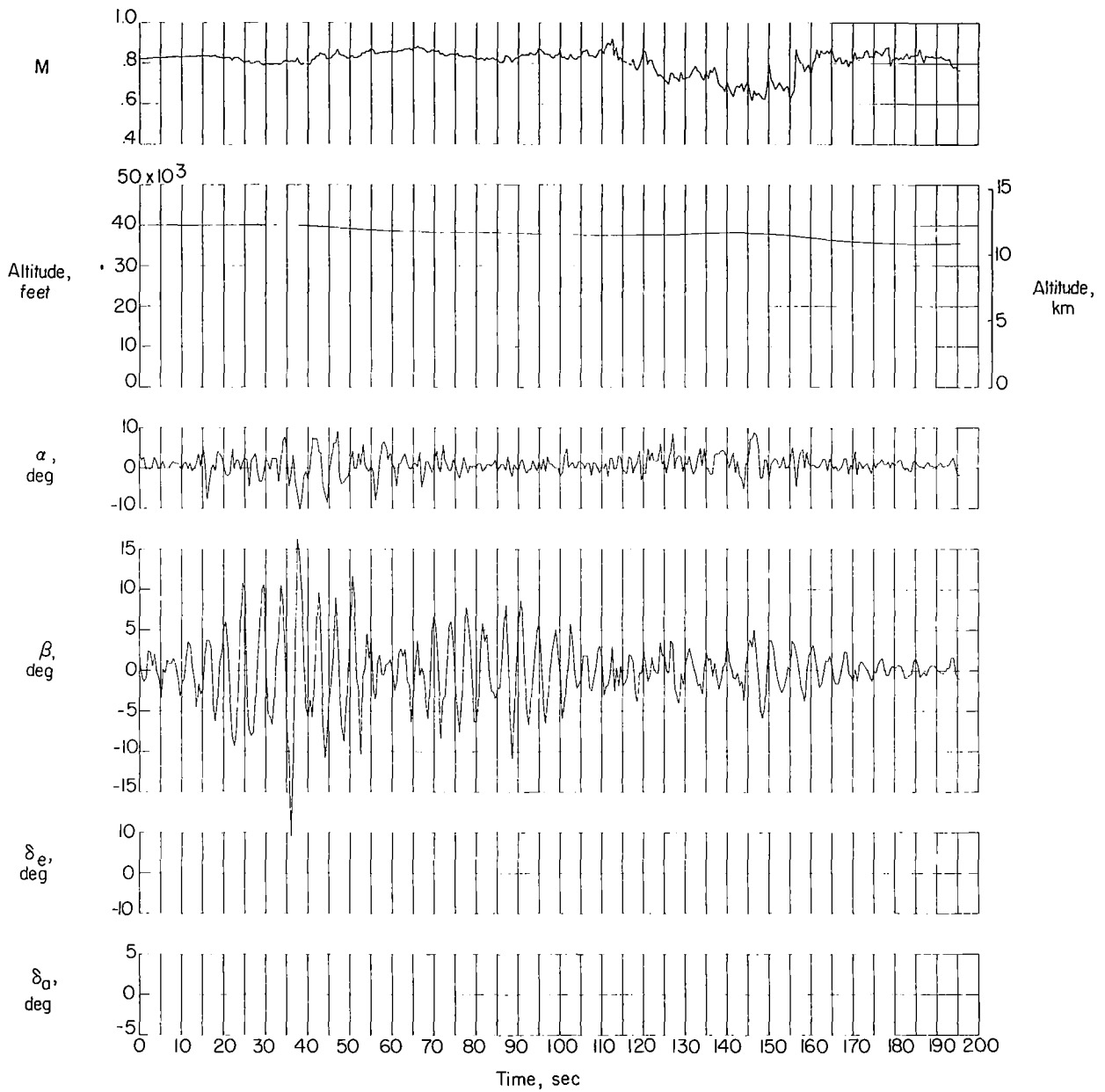


Figure 9.- Concluded.

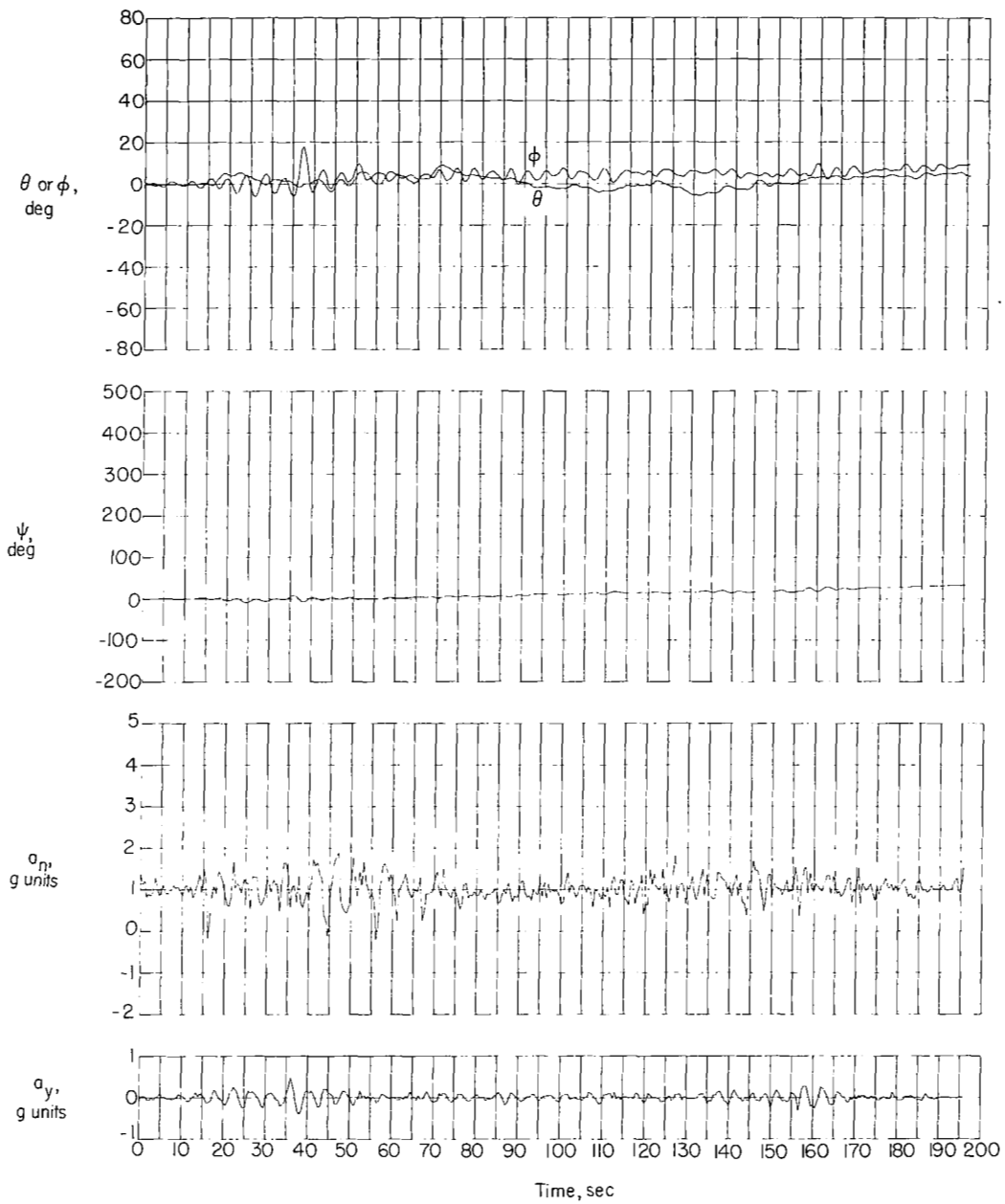


Figure 10.- Indication of motion obtained when  $C_{l_p}$  was set equal to -1.000 per radian and gusts of figure 3(a) were used.

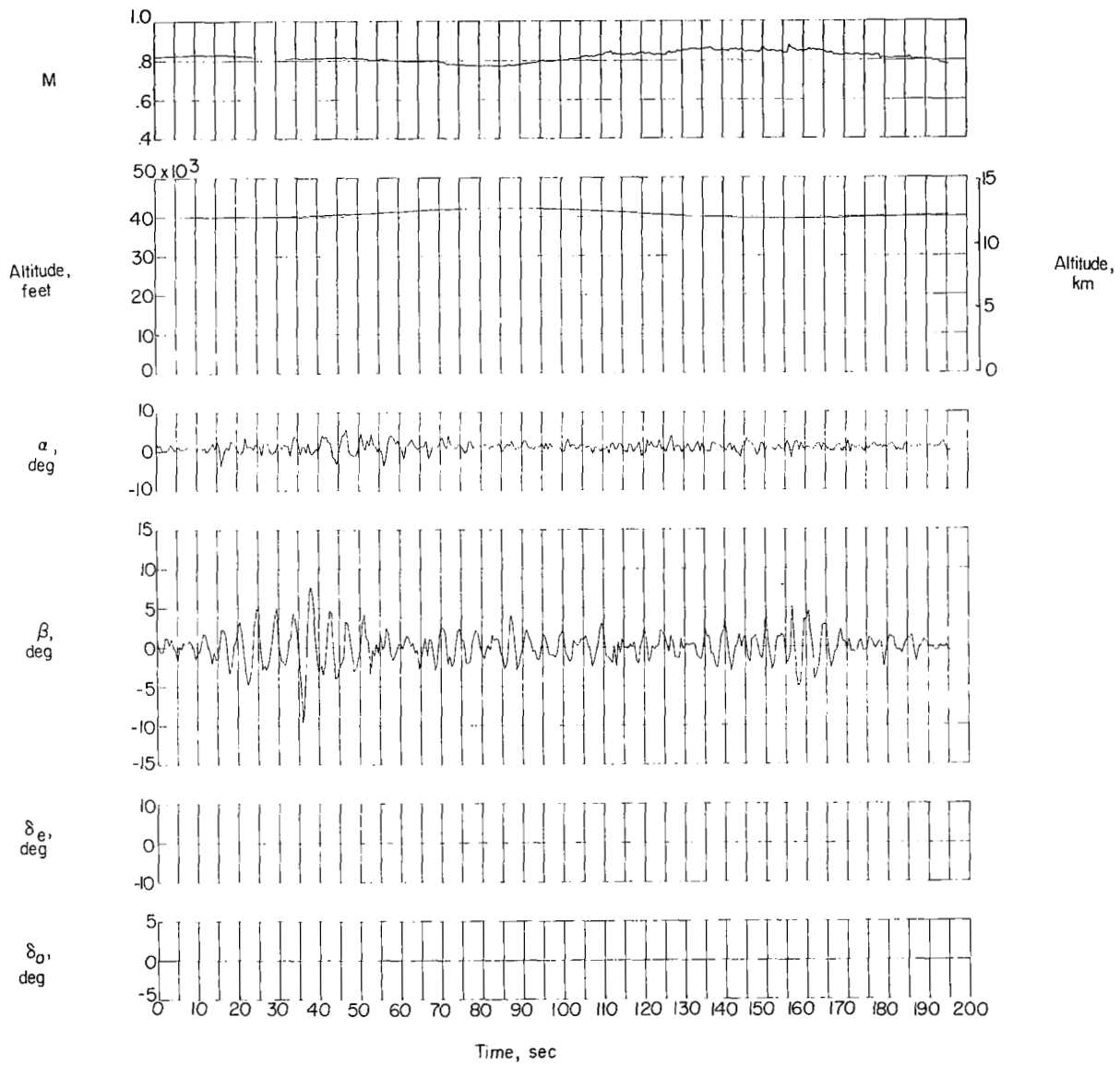


Figure 10.- Concluded.

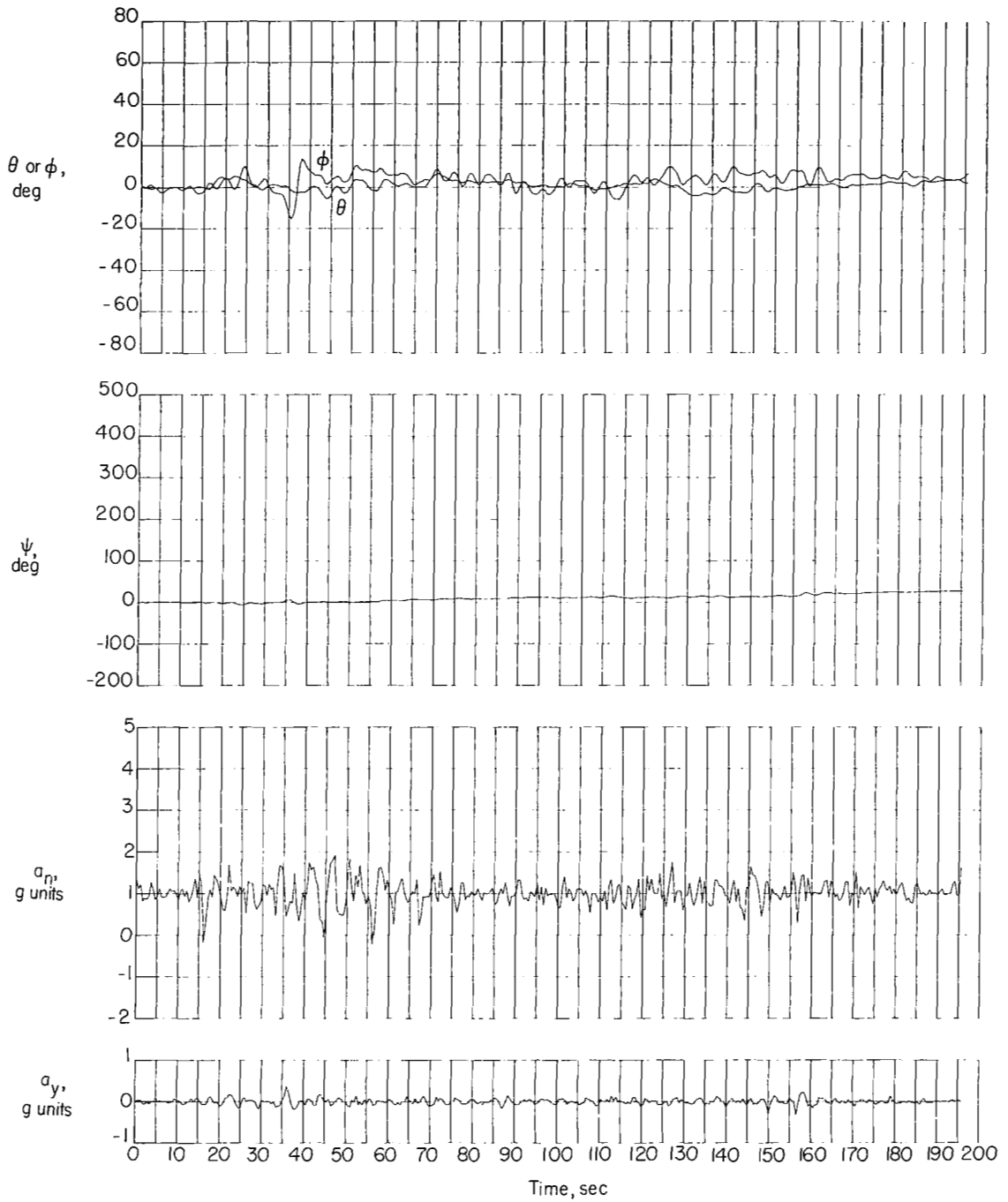


Figure 11.- Indication of motion obtained when  $C_{n_r}$  was set equal to -0.760 per radian and gusts of figure 3(a) were used.

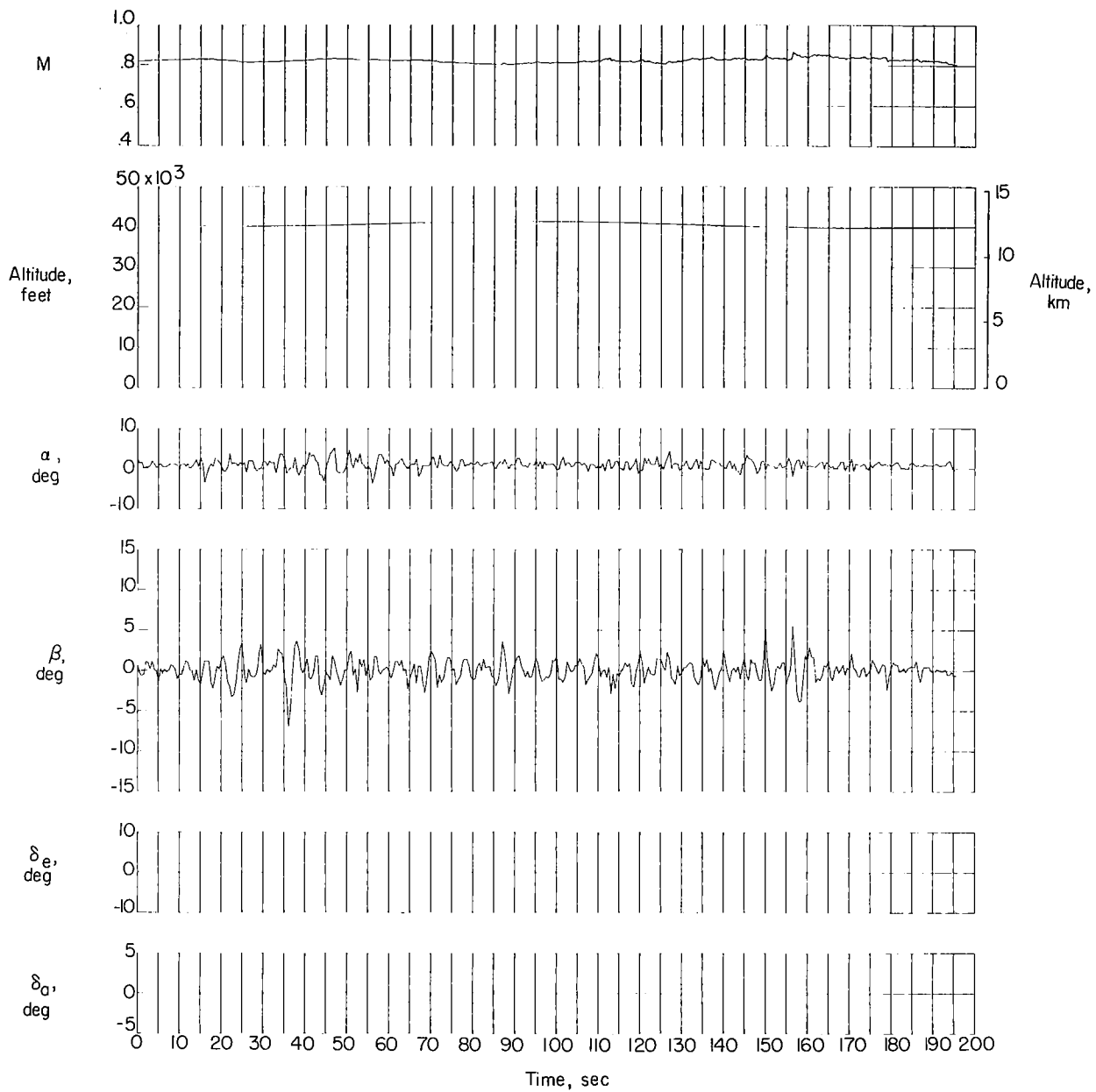


Figure 11.- Concluded.

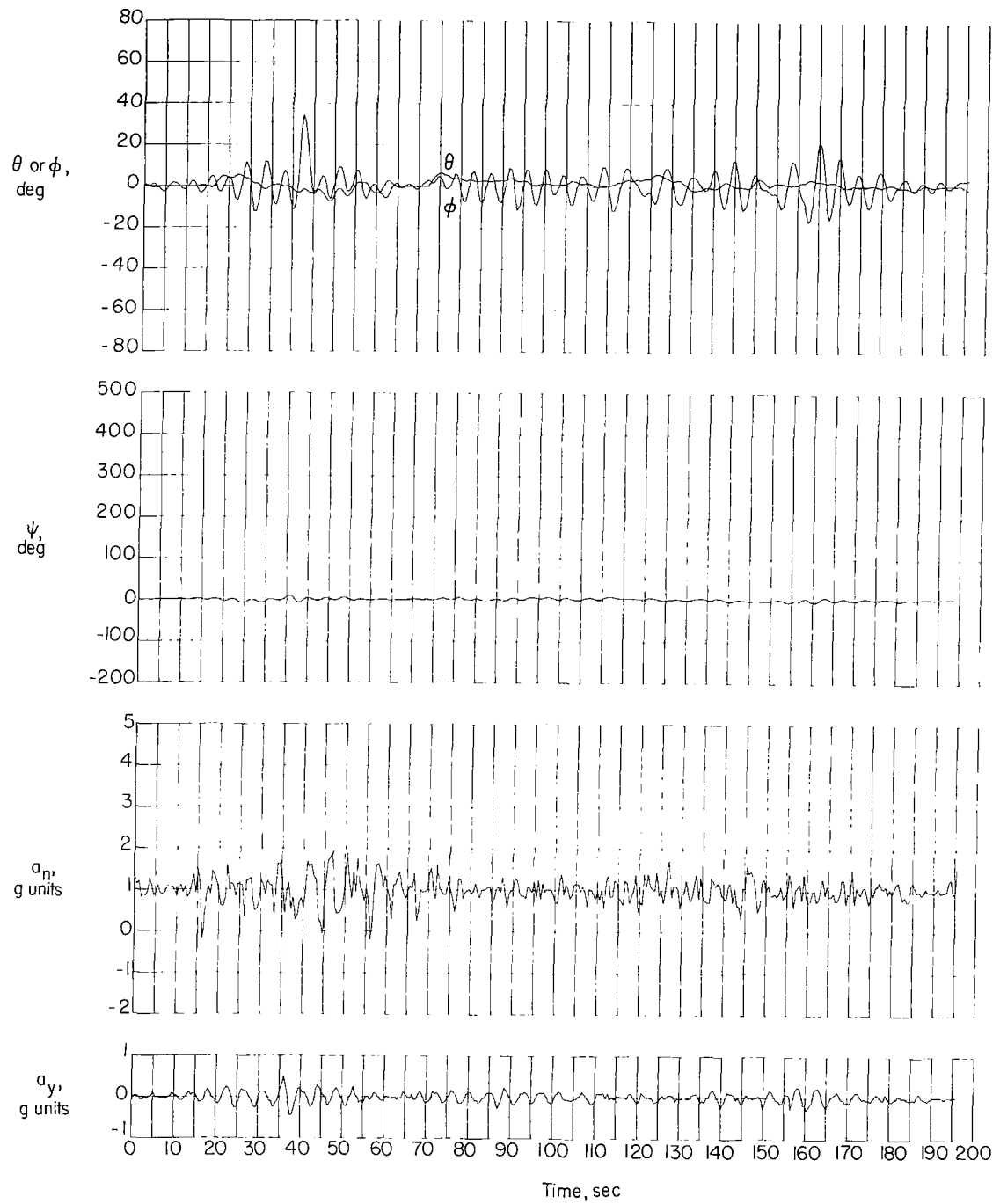


Figure 12.- Indication of motion obtained when bank angle was controlled loosely with ailerons.



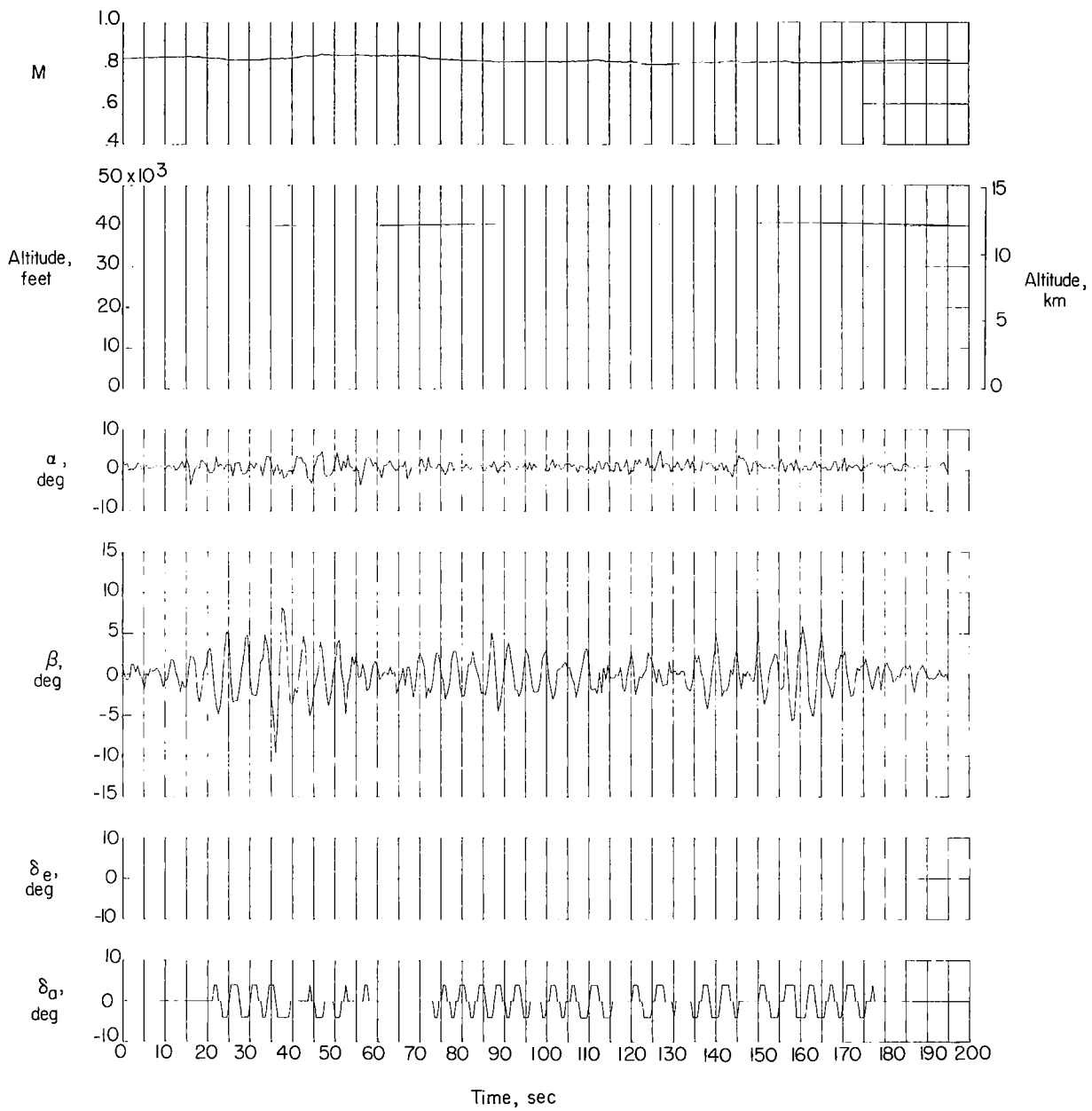


Figure 12.- Concluded.

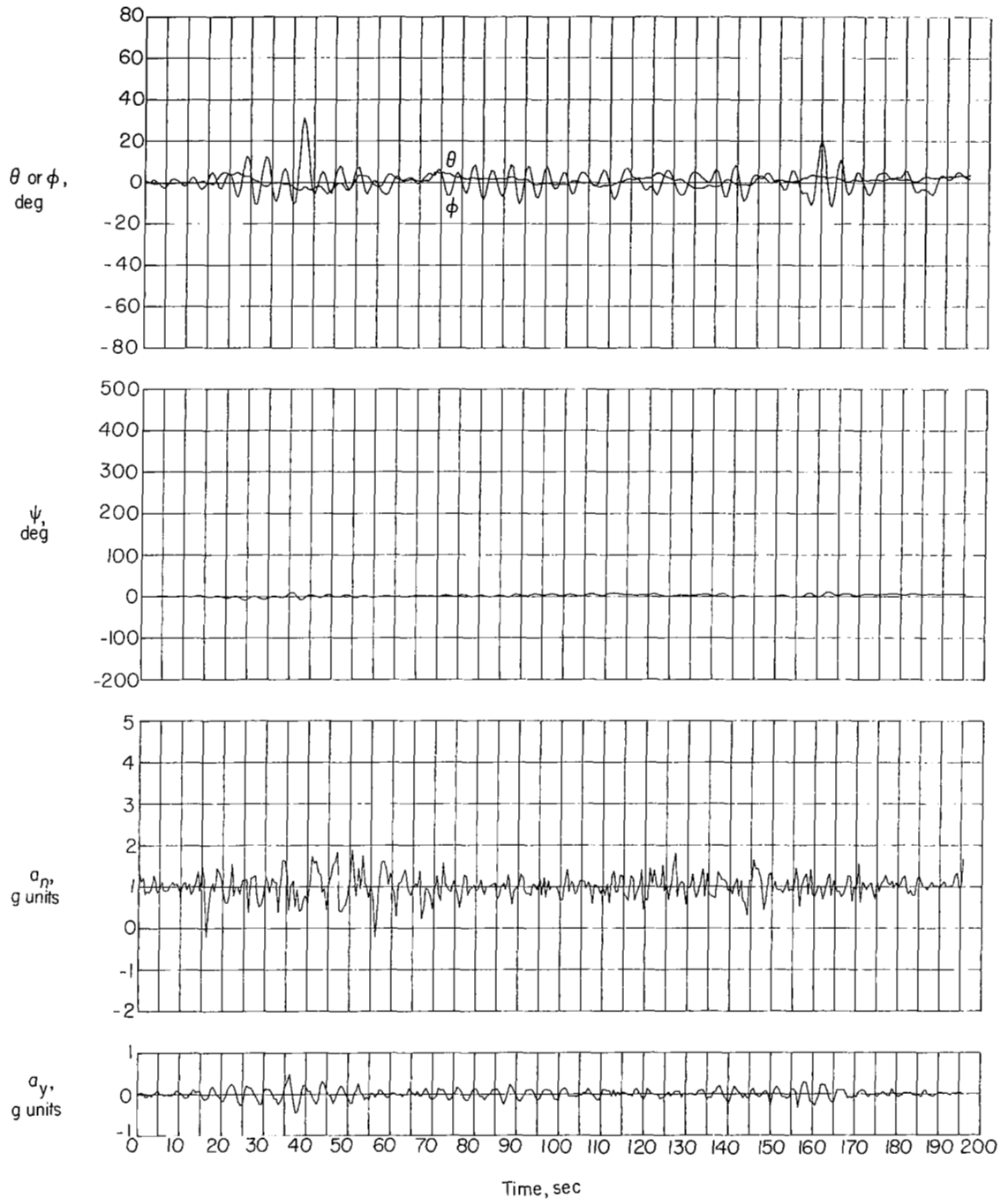


Figure 13.- Indication of motion obtained when bank angle and pitch angle were controlled loosely with ailerons and elevator, respectively.

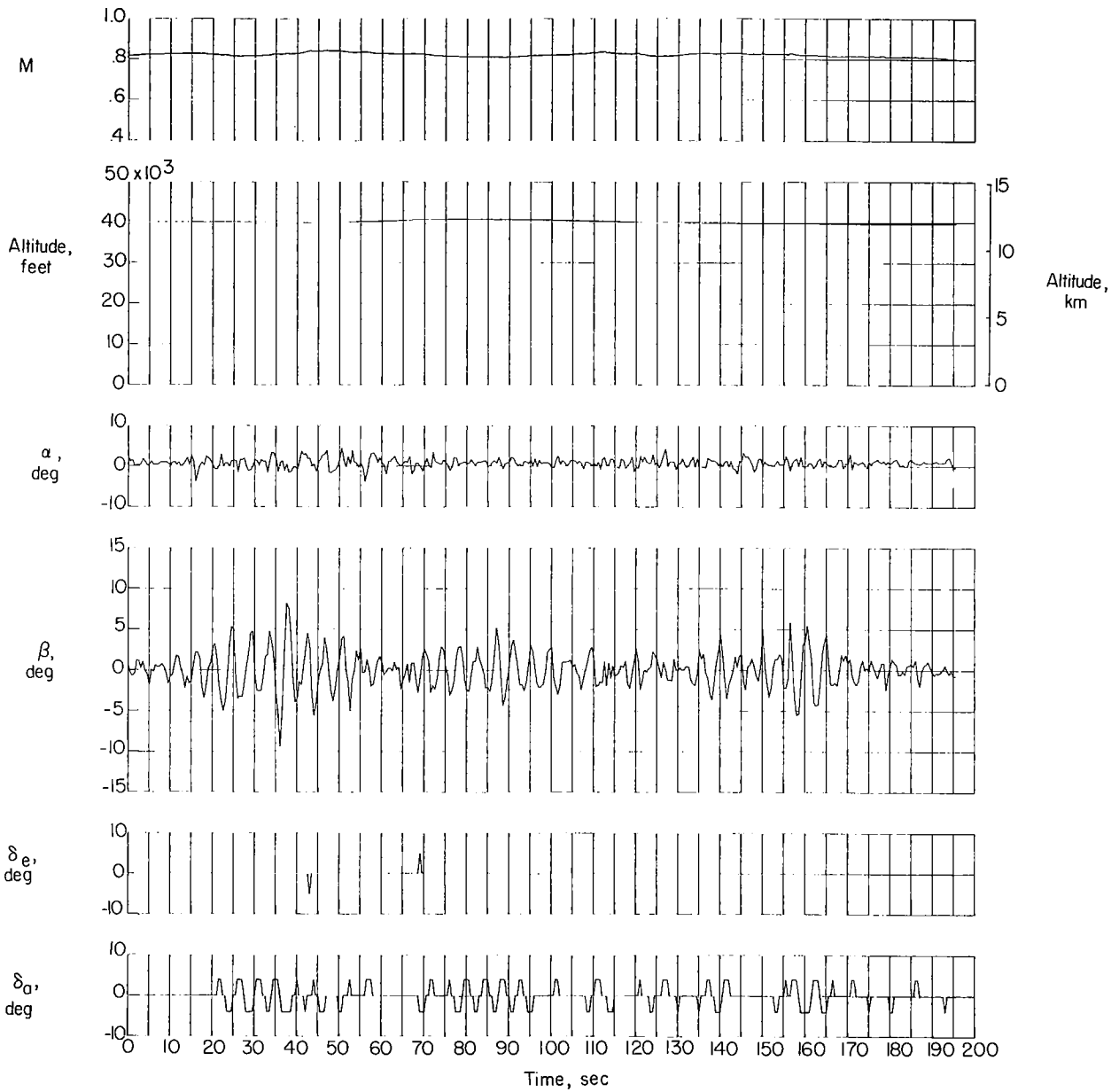


Figure 13.- Concluded.

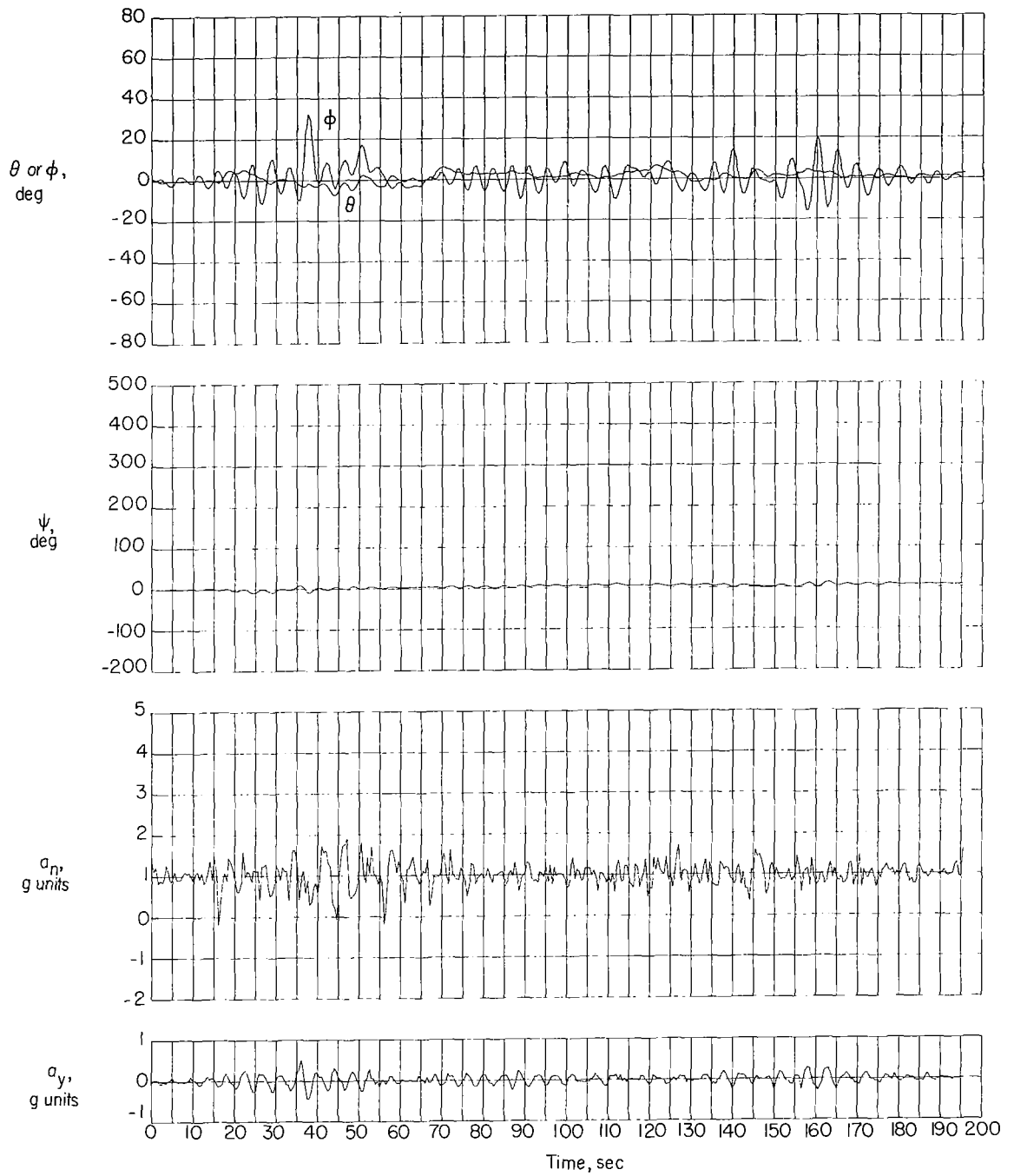


Figure 14.- Time history of motion obtained when  $\frac{\delta_a}{\phi} = -0.10$  and gusts of figure 3(a) were used.

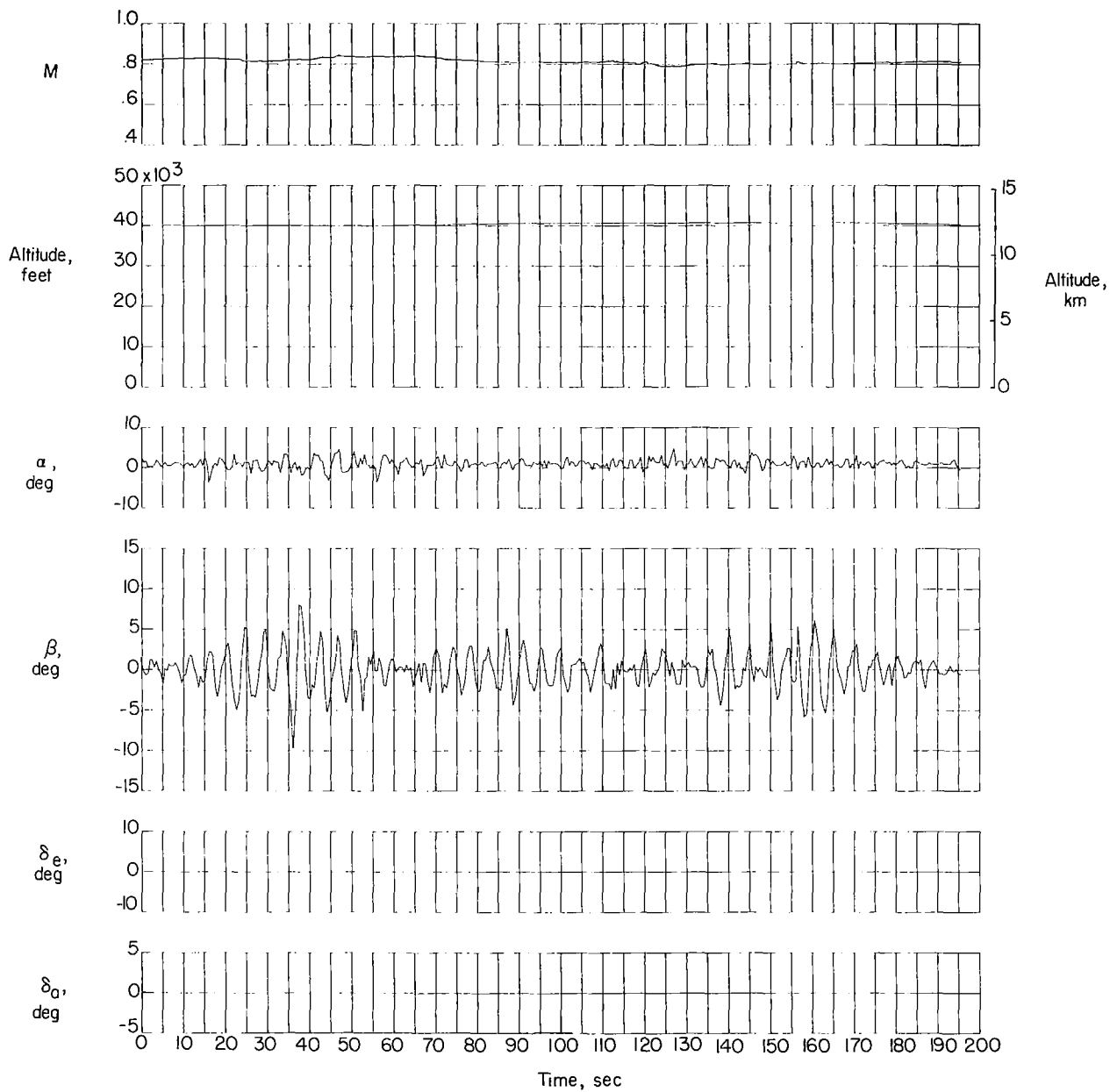


Figure 14.- Concluded.

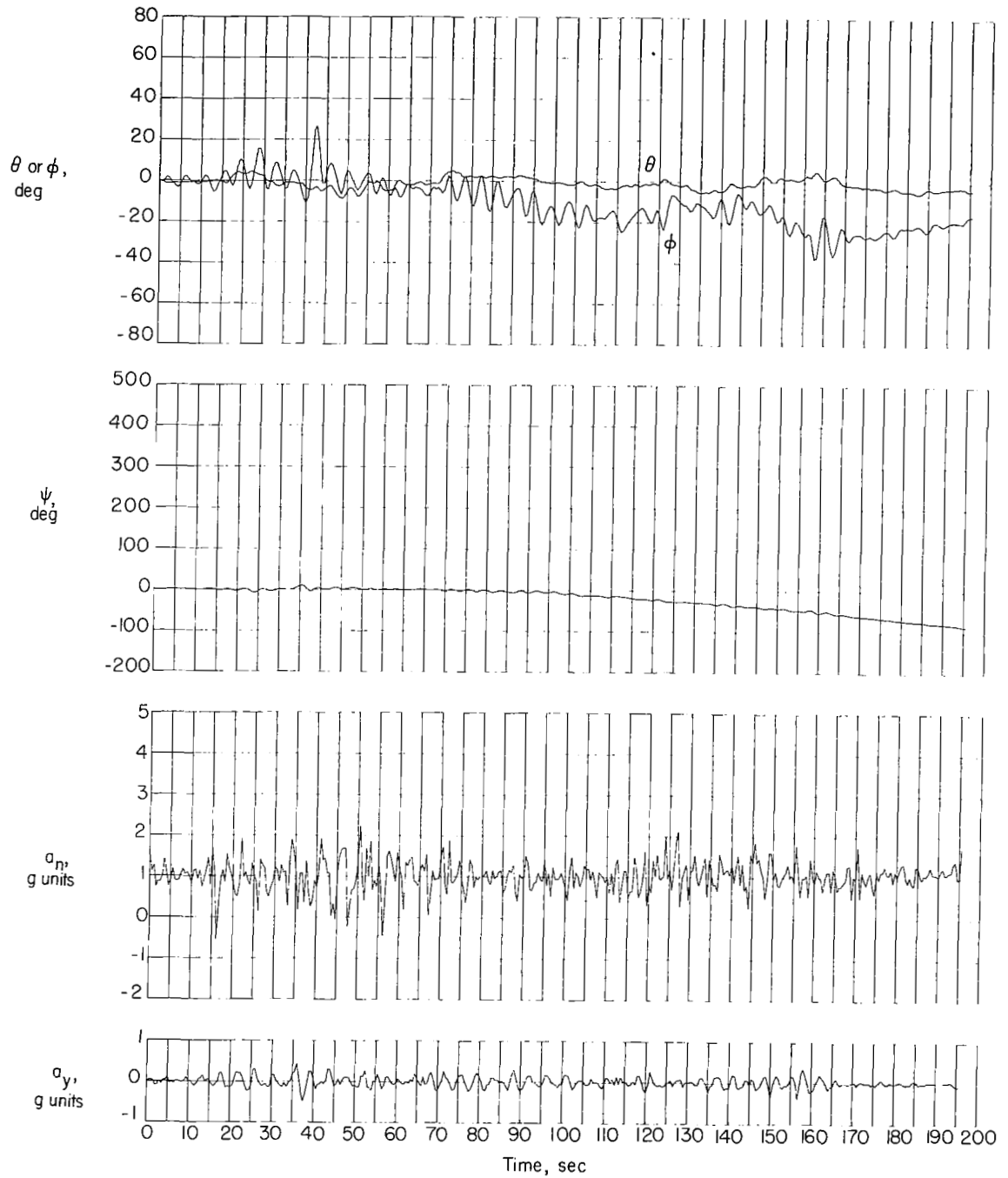


Figure 15.- Time history of motion obtained when initial altitude and airspeed were 32 000 feet (9.75 kilometers) and  $M = 0.78$ , respectively.

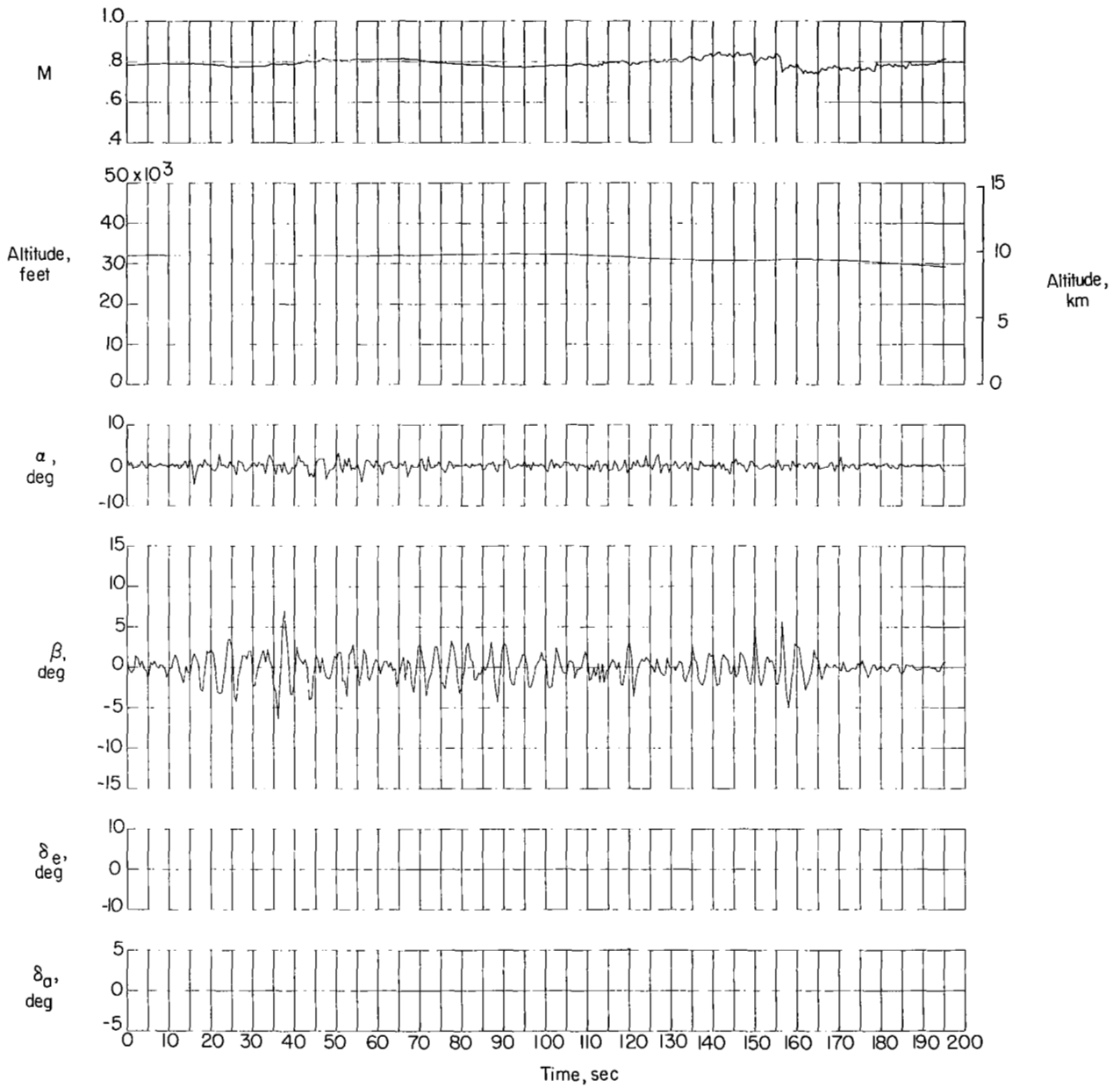


Figure 15.- Concluded.

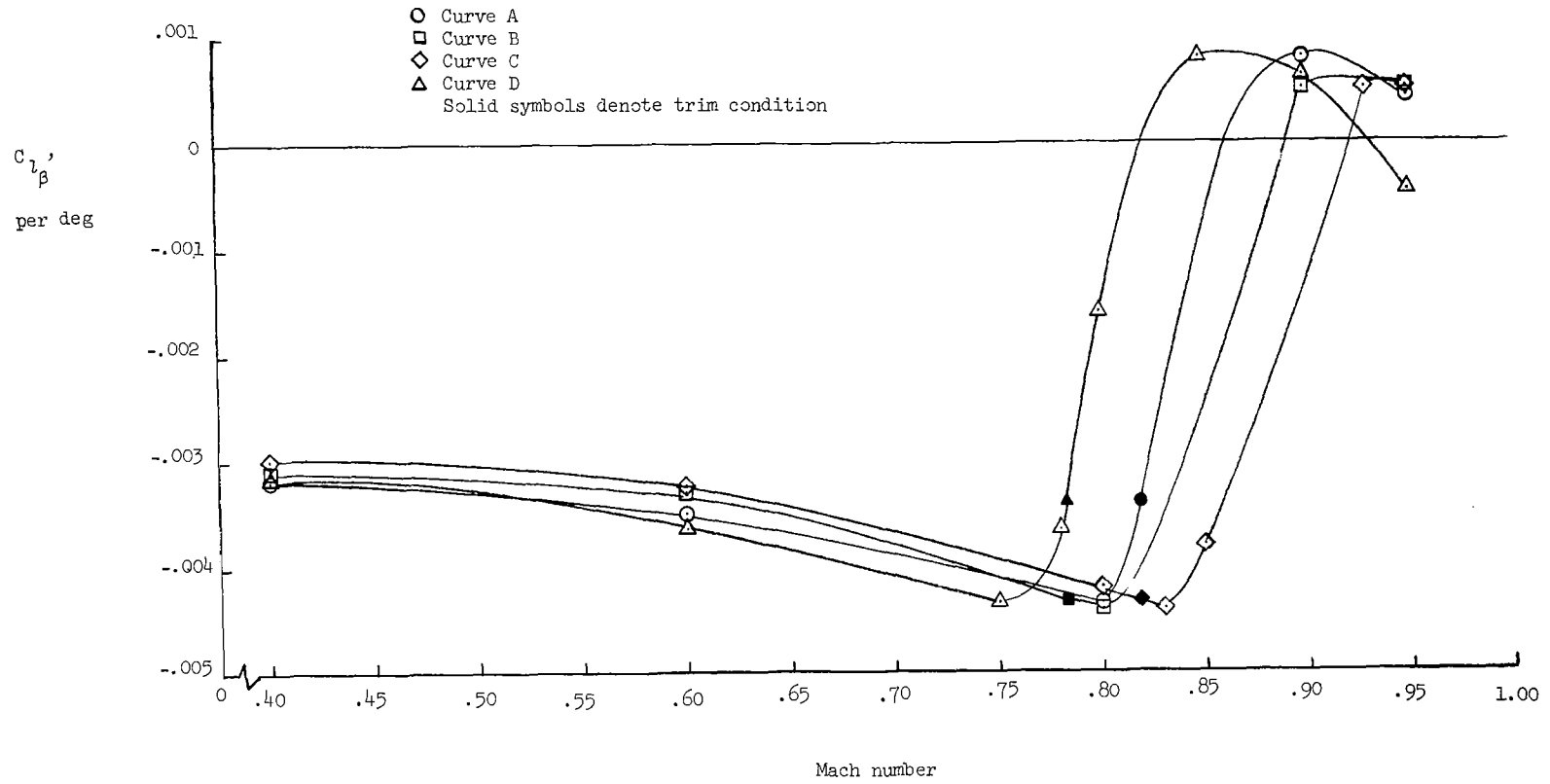


Figure 16.- Variations of effective dihedral with Mach number.



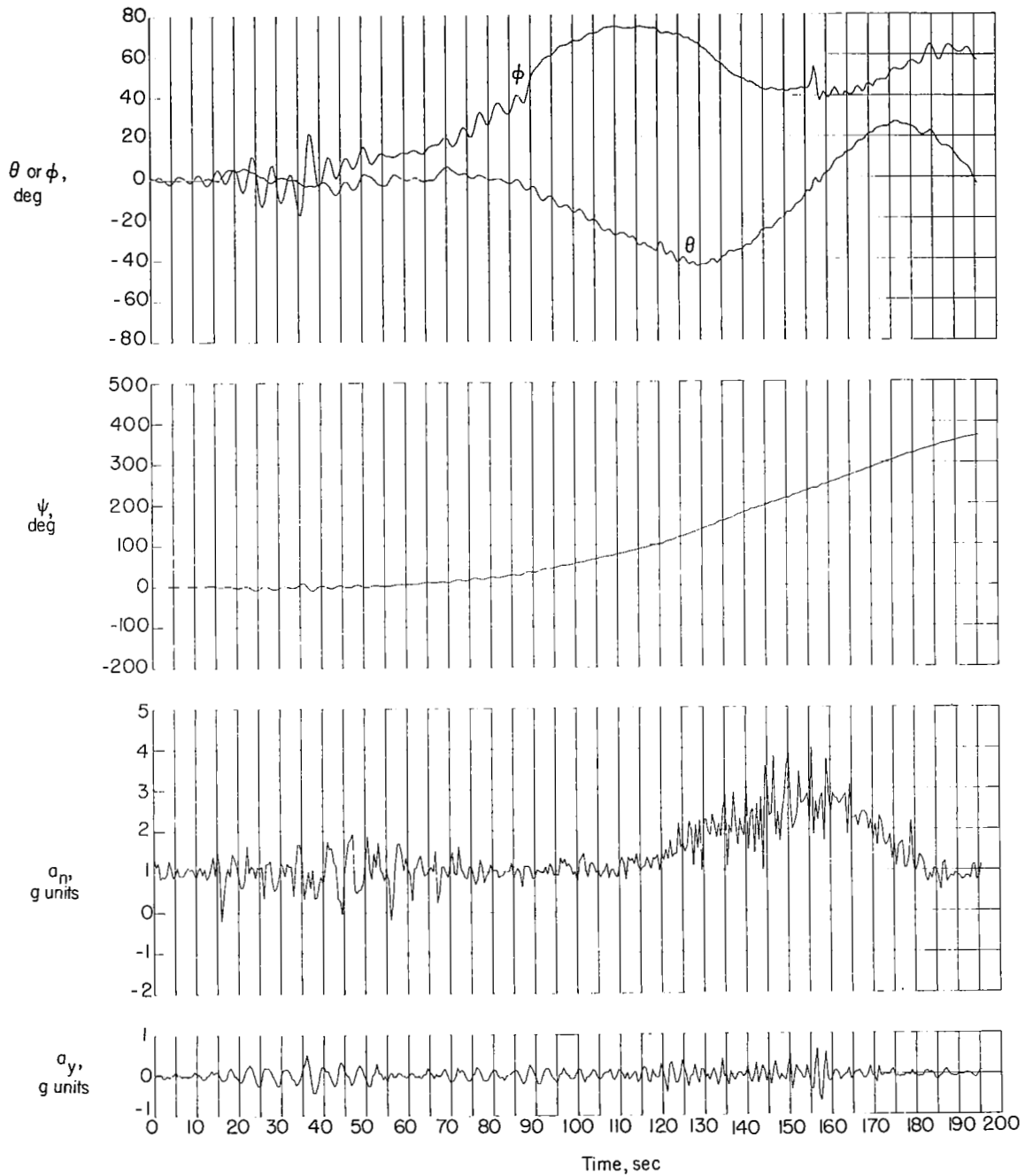


Figure 17.- Indication of motion obtained when curve A of figure 16 was used for  $C_{L\beta}$ . Initial conditions:  $h = 40\ 000$  feet (12.19 kilometers) and  $M = 0.82$ .

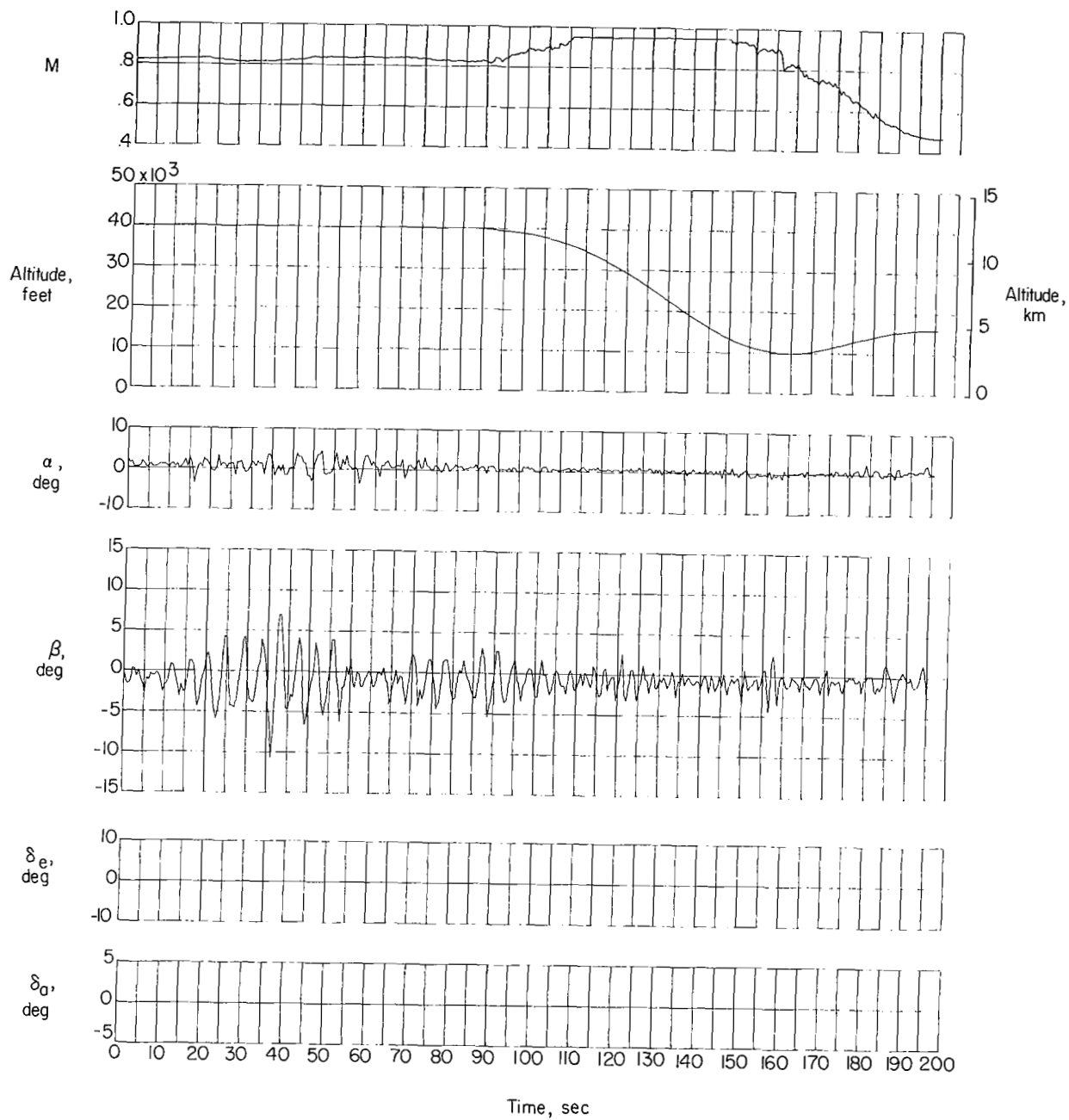


Figure 17.- Concluded.

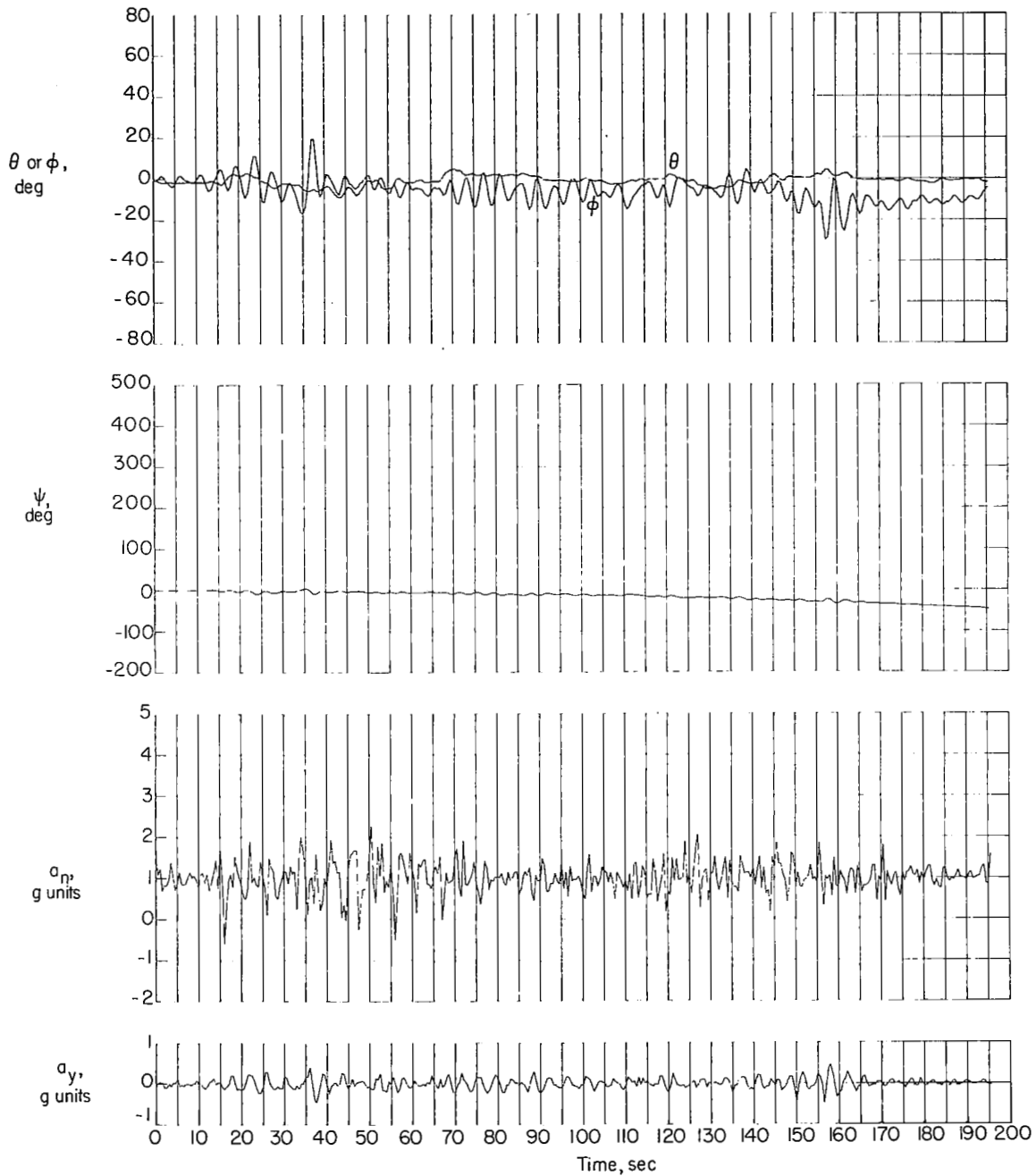


Figure 18.- Indication of motion obtained when curve B of figure 16 was used for  $C_{L\beta}$ . Initial conditions;  $h = 32\ 000$  feet (9.75 kilometers) and  $M = 0.78$ .

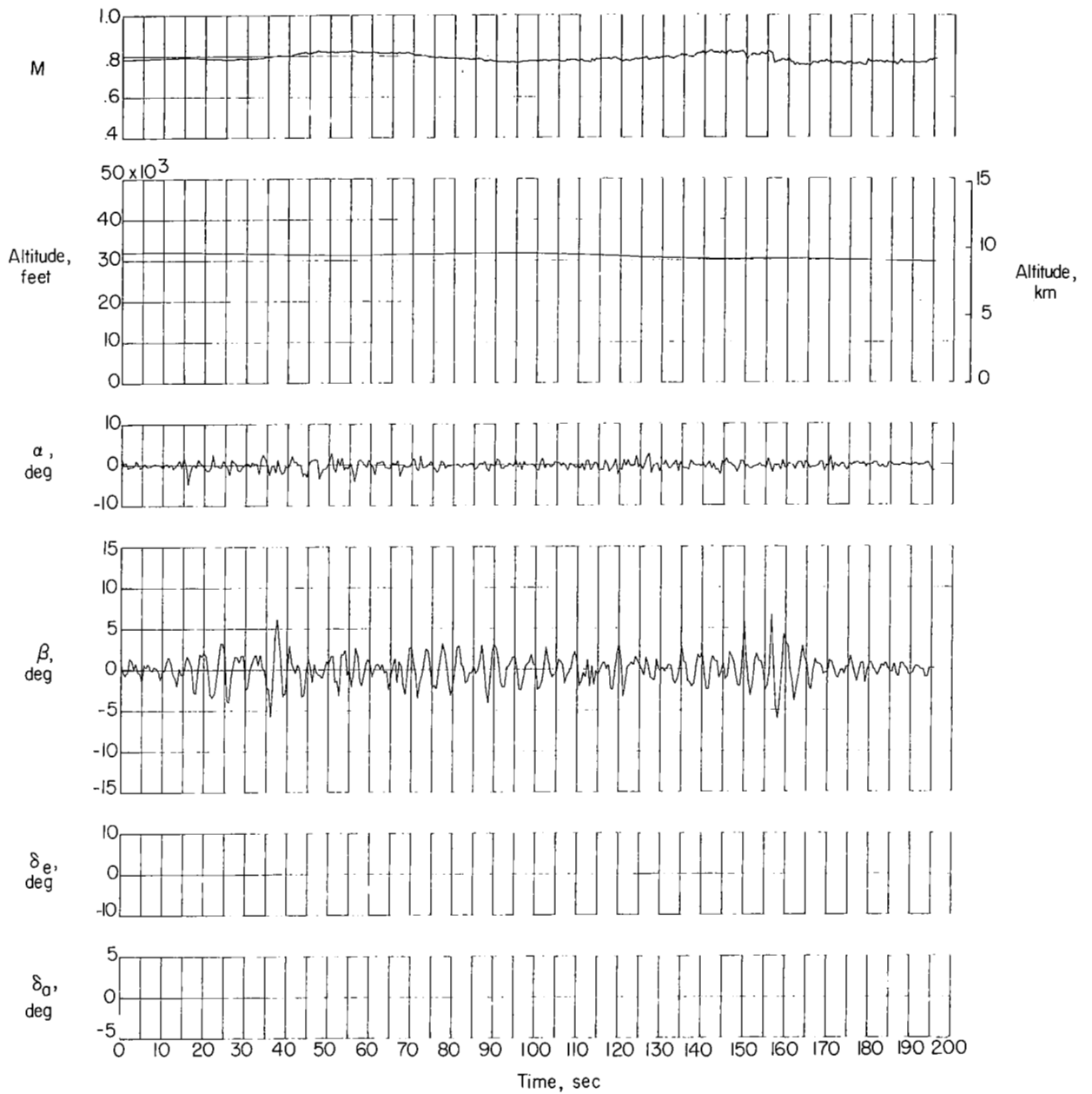


Figure 18.- Concluded.

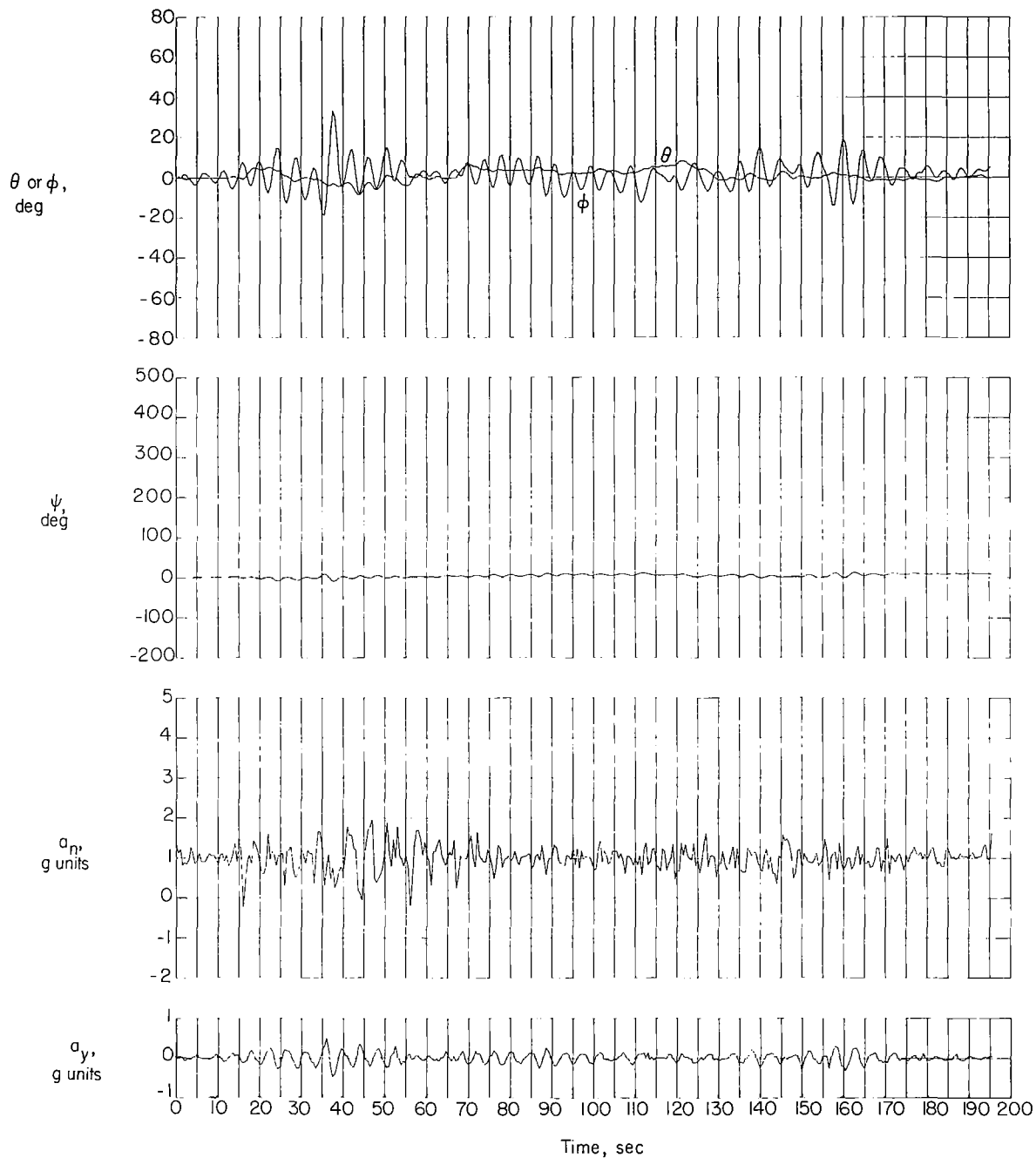


Figure 19.- Indication of motion obtained when curve C of figure 16 was used for  $C_{L\beta}$ . Initial conditions:  $h = 40\,000$  feet (12.19 kilometers) and  $M = 0.82$ .

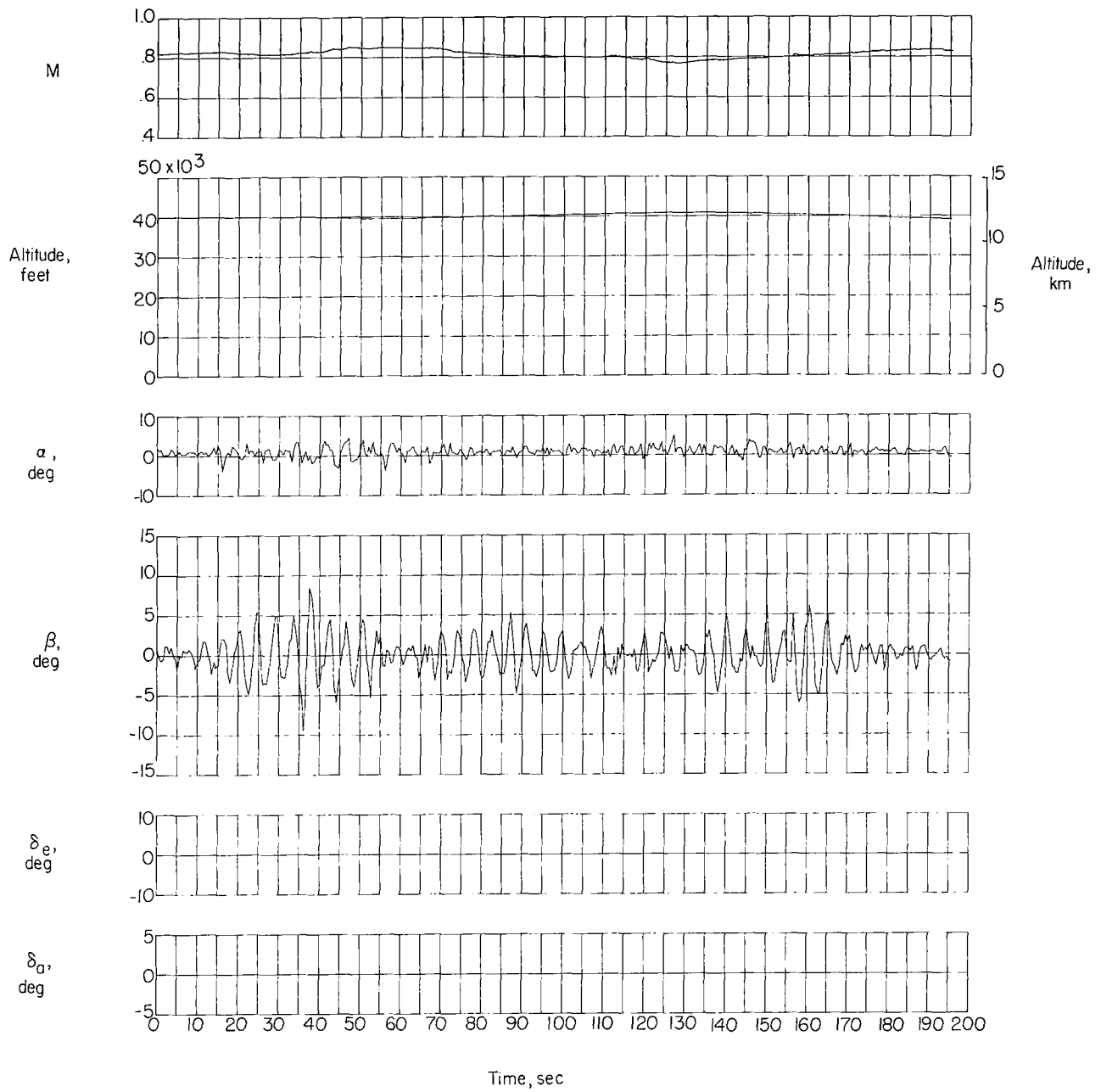


Figure 19.- Concluded.

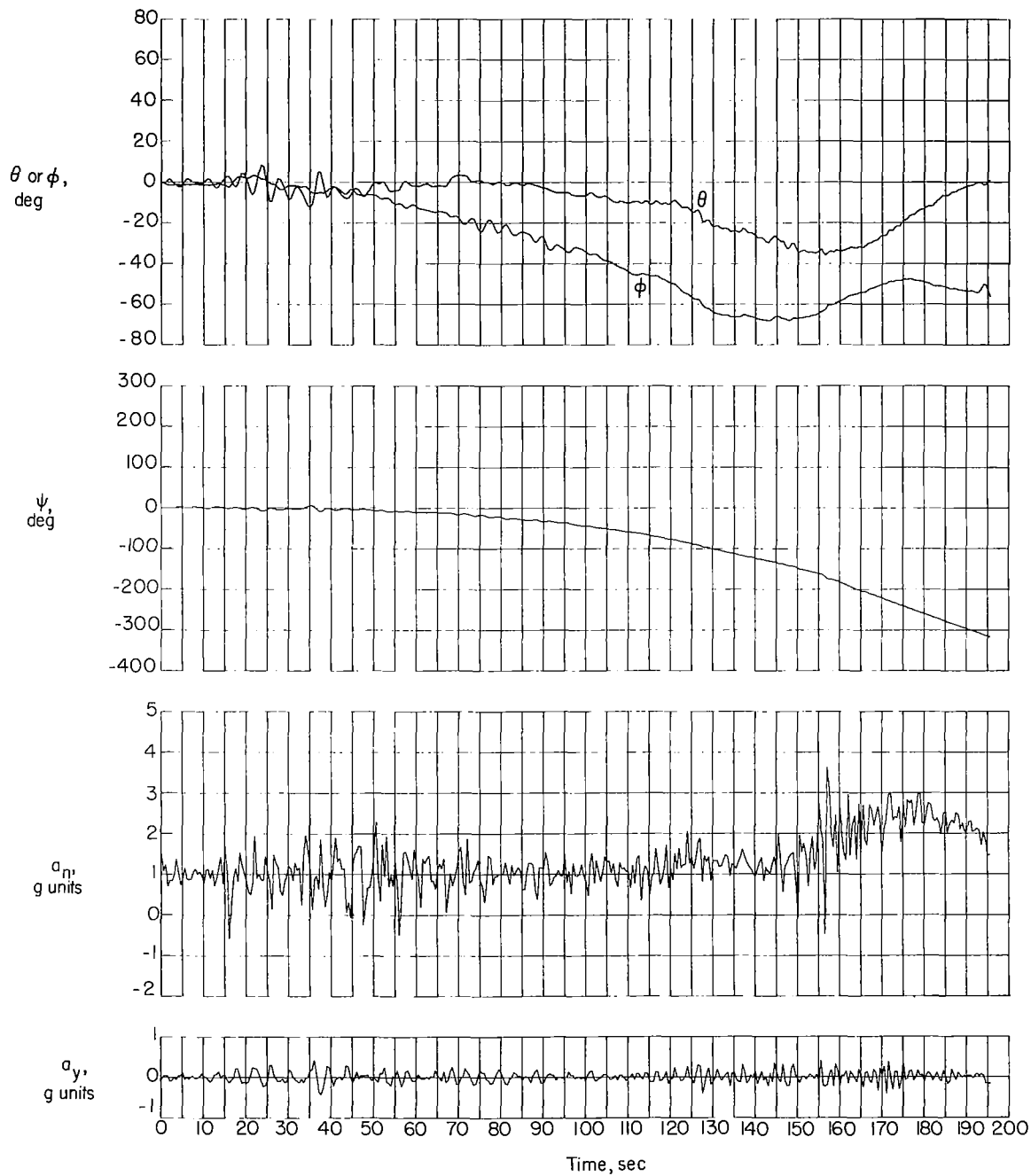


Figure 20.- Time history of motion obtained when curve D of figure 16 was used for  $C_{L\beta}$ . Initial conditions:  $h = 32\ 000$  feet (9.75 kilometers) and  $M = 0.78$ .

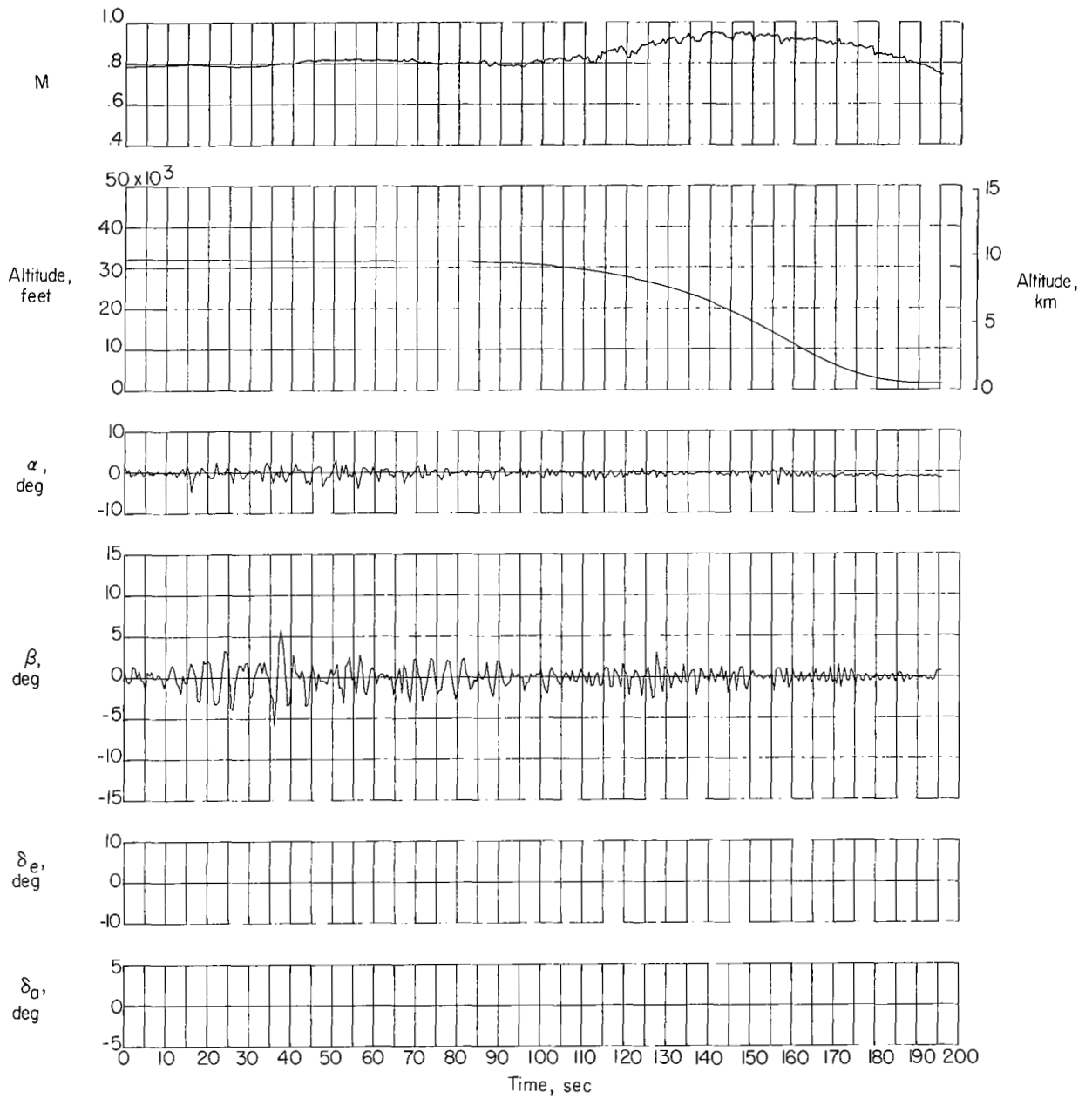


Figure 20.- Concluded.